PhD degree in Systems Medicine (curriculum in Molecular Oncology)

European School of Molecular Medicine (SEMM),

University of Milan and University of Naples “Federico II”

Settore disciplinare: bio/11

Polo-like kinase Cdc5 contributes to mitotic spindle elongation *via* the kinesin-5 motor protein Cin8

Cecilia Claudi

IEO, Milan

Matricola n. R11147

Supervisor: Dr. Rosella Visintin

IEO, Milan

Anno accademico 2017-2018

Table of contents

List of abbreviations

APC/C	Anaphase promoting complex or cyclosome
aMT	Astral microtubule
ATP	Adenosine triphosphate
bp	Base pair
CDK	Cyclin-dependent kinase
CEN	Centromere
CPC	Chromosomal passenger protein
DAPI	4',6-diamidino-2-phenylindole DNA Deoxyribonucleic acid
DNA	Deoxyribonucleic acid
FEAR	Cdc14 early anaphase release (network)
GAP	GTPase-activating protein
GEF	Guanine nucleotide exchange factor
GDP	Guanosine diphosphate
GFP	Green fluorescent protein
GTP	Guanosine triphosphate
IF	Indirect immunofluorescence
iMT	Interpolar microtubule
HU	Hydroxyurea
KT	Kinetochore
kMT	Kinetochore microtubule
MAP	Microtubules-associated protein
MEN	Mitotic exit network
MT	Microtubule
MTOC	Microtubule-organizing centre
PBD	Polo-box domain
Plk	Polo-like kinase
SAC	Spindle assembly checkpoint
SCS	Sister chromatid separation
SE	Spindle elongation
SPB	Spindle pole body
SPOC	Spindle position checkpoint
ts	termosensitive

Figures index

Introduction

Materials and methods

Results

Boxes index

Tables index

Abstract

Proper chromosome segregation requires an orderly sequence of events, whereby spindle elongation follows the dissolution of sister chromatid linkages. Chromosome segregation starts at the onset of anaphase when the separase triggers the cleavage of cohesin, a protein complex that holds sister chromatids together. Next, chromatids are segregated into the daughter cells by the pulling force of the mitotic spindle. The mitotic spindle is a sophisticated and complex machinery built of microtubules, microtubule associated proteins and motor proteins. Despite the fundamental role of the mitotic spindle, the molecular mechanisms underlying its regulation remain elusive. Proper spindle function requires that microtubule dynamics are stabilized at anaphase. This change in microtubule dynamics is perceived as dictated by a shift in the balance of kinase and phosphatase activities in favor of the phosphatases. The finding that cells simultaneously lacking the polo-like kinase Cdc5 and the phosphatase Cdc14 cannot progress through anaphase albeit having cleaved cohesin due to defects in spindle elongation, challenges the view of mitotic exit as a time for protein dephosphorylation.

The aim of my work is to understand the molecular mechanism by which the two proteins contribute to anaphase spindle elongation, with a particular focus on the role of Cdc5. We identified the kinesin 5 motor protein Cin8 as a key target of the "Cdc14-Cdc5" spindle elongation pathway. We show that besides being dephosphorylated by Cdc14, Cin8 is also phosphorylated by Cdc5 on residues S409 and S441, and that this phosphorylation is crucial for the function of the kinesin in anaphase spindle elongation, likely because of the impact it has on the interaction between Cin8 and microtubules. Since these residues, S409 and S441, are located within a highly conserved stretch of amino acids, it will be interesting to test whether this regulation is conserved in other vertebrates as well. The finding that Cin8 is simultaneously a substrate of a kinase and a phosphatase sheds light on the complexity of mitotic exit regulation and is in complete agreement with recent data

showing that approximately equal numbers of phosphosites are phosphorylated and dephosphorylated during mitotic progression and exit. Since it appears that phosphorylation and dephosphorylation events are equally important to the point that kinases and phosphatases cooperate to regulate the same substrates, the view of mitotic exit as the realm of phosphatases is dismantled and the continuous need for single molecule studies in addition to global analyses investigation is put forward.

1 Introduction

1.1 Mitosis

1.1.1 An historical perspective

The discovery that all living organisms are made of cells (Schleiden 1838, Schwann 1839) which proliferate by growth and division (Remak, 1850) was perhaps the most important biological discovery of the 19th century. Starting from Virchow's 1855 realization that "*Omnis cellula e cellula*", meaning that cells only arise from pre-existing cells, the cell cycle has been the subject of intense investigation. Microscopists and embryologists first described the cytology of cell division, but could only speculate about the underlying mechanisms. It was only later in the 70s and 80s, with the blossoming of molecular biology that geneticists, cell biologists and biochemists began illustrating the cell cycle in molecular terms. Their work uncovered that the basic processes and control mechanisms are universally conserved within the eukaryotic kingdom, and led to the view of the cell cycle as a highly regulate sequence of events that brings about the reproduction of the cell. These studies benefited from work coming from a wide range of organisms, each with its own particular biological and methodological advantages.

In parallel the will to knowledge drove the development of technology particularly for what concerns microscopes.

It was the 17th century when the first microscope prototypes were created independently by the work of Hans and Zacharias Janssen and Robert Hooke. History tells that in 1661 R. Hooke commissioned by King Charles II of England to create a series of microscopic studies on insects went beyond what requested and observed every possible thing. When

observing thin cork slices, he found empty spaces surrounded by walls organized in a structure that reminded him of the *cellulae* or small rooms inhabited by monks; hence the name cell. The term *cells* stuck and Hooke was credited with discovering the building blocks of all life in 1663.

Significant improvement for microscopy was later made by Antonie van Leeuwenhoek who let the microscope to achieve a magnification of 300x. This increased resolution brought visualization to a deeper depth and it propelled forward the knowledge of the time, leading to the elaboration of concepts that still stand true, including the cell theory. However, if scientists understood that cells derive from pre-existing cells and that the hereditary material was located in the nucleus, the nature of the hereditary information remained a mistery.

It was Walther Flemming that first observed and described the behaviour of chromosomes during a normal cell division. A pioneer in the study of stained preparations, he recognized within the nucleus that a certain class of dyes revealed a threadlike material, which he termed chromatin, or "stainable material." By looking at cells killed at different cell cycle stages he pictured the entire sequence of changes occurring in the nucleus during cell division. His work, collected and published in the form of a hand-drawn time-lapse movie, is the first detailed representation of chromosomal behavior during mitosis **(Figure 1.1)**.

Figure 1.1 Walther Flemming's drawings of mitosis
Walther Flemming portrait and hand drawn llustration from Zellsubstanz, Kern und Zelltheilung (Flemming 1882).

His attention to details allowed him to correctly hypothesize that mitosis ends with chromosome partition into the two daughter cells and, after Virchow "*Omnis cellula e cellula*", he described the phenomena as "*Omnis nucleo e nucleo"*, suggesting that every nucleus derives from a predecessor one.

At this point, the relationship between the thick (chromosomes) and thin (the spindle) fibers observed in the fixed specimen was still missing; both were thought to be a manifestation of nuclear structures as this organelle prepare to divide (Flemming, 1879). However, given that the visualization of the mitotic fibers was possible only on fixed specimen and strongly relied upon the fixative and staining conditions applied by cytologists at the time, it raised the concern that they maybe an artefact of sample preparation and opened a controversial debate between cytologists and microscopists about the validity of the fibers.

It was only thanks to polarized light microscopy and electron microscopy that the spindle fibers were visualized and legitimated. In the early 1950s Shinya Inoue used polarized

light microscopy to visualize the birefringence (BR) resulting from the presence of fibrous material within the living spindle, thereby conferming the presence of the spindle fibers. Conclusive evidence that spindles are made of filaments came from electron microscopy studies that also showed that microtubules attach specialized structures on chromosomes. The relationship between microtubule fibers and chromosomes was finally established and represented a key turning point in our understanding of chromosome segregation during mitosis.

1.1.2 The chromosome cycle

The process by which a single cell originates two identical daughter cells is known as mitotic cell cycle or mitosis (**Figure 1.2**). To ensure that each daughter cell receives a full complement of the hereditary material, the duplication and segregation of chromosomes must occur with great fidelity. The mitotic cell cycle is arbitrarily divided into four phases: M phase for the entire mitotic period, S for the period of chromosome duplication (synthesis), and G1 (Gap1) and G2 (Gap2) for the gaps between S and M phases. S, G1 and G2 phases are collectively identified as interphase. Sustained cell proliferation requires that cells duplicate all their constituents, a process known as cell growth, at the same rate as they duplicate and segregate their chromosomes into daughter cells, which is known as the chromosome cycle. For this reason, cells spend most of their lifetime in interphase preparing to divide.

Interphase is characterized by high metabolic activity and sustained cellular growth and results in the cell to approximately double its size. Indeed, interphase is characterized by cycles of growth and protein synthesis alternated with G1 and G2 phases, that provide additional time before transiting respectively into S phase and into mitosis.

During G1, the cell in response to intra- or extra-cellular signals decide if conditions are favourable for cell cycle commitment, and if so, it gets ready to support chromosome replication during S phase. If most of the macromolecules are continuously synthesized during the cell cycle, the genetic material and the centrosomes, or spindle pole bodies (SPBs) in yeast, are present in one copy per cell and therefore they are duplicated once per cell cycle typically in S phase (Andersen, 1998). Following replication each chromosome consists of two sister chromatids. During G2 the cell begins to reorganize its contents in preparation for the M phase that, albeit being the shortest, is also the most spectacular phase of the cell cycle. The M phase includes two segregation processes: 1) chromosome segregation (mitosis) and 2) the physical separation of the two daughter cells (cytokinesis). Based on chromosomal rearrangements and other events mitosis is arbitrarily divided in multiple subphases: prophase (P), prometaphase (PM) (not in yeast), metaphase (M), anaphase (A) and telophase (T) **(Figure 1.2).**

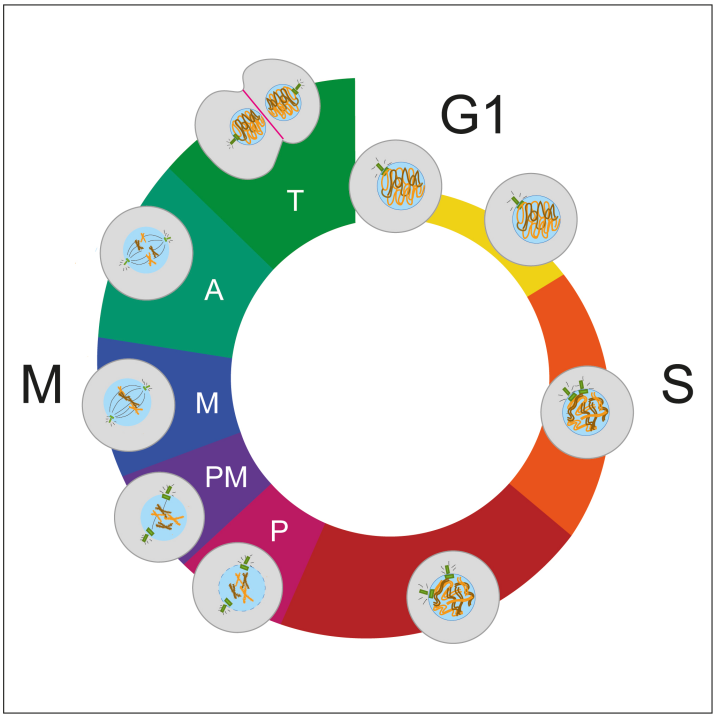

Figure 1.2 The cell cycle
Schematic representation of the cell cycle phases

During prophase, chromatin condenses into distinct chromosomes and the nuclear membrane starts to breakdown. Following completion of prophase, the cell enters prometaphase which is characterized by the disassembly of the nuclear envelope (only in vertebrates) and the assembly of the mitotic spindle. The spindle serves as tracks along which chromosomes move. It is composed by polymers of tubulin (microtubules MTs) extending from centrosomes, or SPBs in yeast, and it is arranged in bipolar arrays. During metaphase, the spindle captures chromosomes via a proteinaceous complex named kinetochore, that builds on centromeric DNA. Once all chromosomes are attached by microtubules emanated from the opposite centrosomes the cell can transit to anaphase. The metaphase to anaphase transition is triggered by the dissolution of the linkages that hold sister chromatids together from the time of their syntheisis. Separated sister chromatids are next equally segregated into the daughter cells by the pulling and the pushing forces of the mitotic spindle. Mitosis ends with telophase, during which the nucleus envelope re-forms, the chromosomes decondense into interphase chromatin, and the mitotic spindle is disassembled. The two individual daughters are finally formed with the separation of the cytoplasm, a process named cytokinesis.

1.2 The mitotic spindle

The delicate task of segregating the genetic material is performed by the microtubule fibers of the mitotic spindle which physically set apart the two sets of chromosome and equally segregate them between the daughter cells.

Central to the activity of this sophisticated machinery is its ability to quickly adopt different-transitory conformations that originate from dynamic cycles of shrinkage and growth of the microtubule fibers. Dynamicity is an inner property of microtubules. Each microtubule is a bundle of 13 protofilaments, polymers of α–β tubulin dimers that can add or loose subunits, thereby determining the length of the overall structure (**Figure 1.3**). Three kinds of microtubules are the building blocks of the mitotic spindle: (i) interpolar microtubules (iMTs), which control spindle elongation, (ii) kinetochore microtubules (kMTs), which link and guide chromosome movement to the poles and (iii) astral microtubules (aMTs), which contact the cellular cortex and guide spindle positioning along the polarity axis. Despite its fundamental role, the molecular mechanisms that regulate spindle microtubule dynamics remain elusive. Since the mitotic spindle is conserved from yeast to human, the very simple spindle of budding yeast became an attractive model for elucidating the molecular mechanisms at the bases of this molecular machinery.

1.2.1 Microtubule structure and function

Microtubules are composed of a globular protein called Tubulin. Tubulin consists of heterodimer of α and β tubulin encoded in yeast by *TUB1 TUB3* and *TUB2* genes, respectively. Each dimer has a polarity and, consequently, the longitudinal association of tubulin subunits results in a polar oligomer, named the protofilament.

In turn, 13 protofilaments are arranged in parallel strands in bundle, forming a hollow cylinder of 25 nm in diameter, the microtubule (**Figure 1.3**).

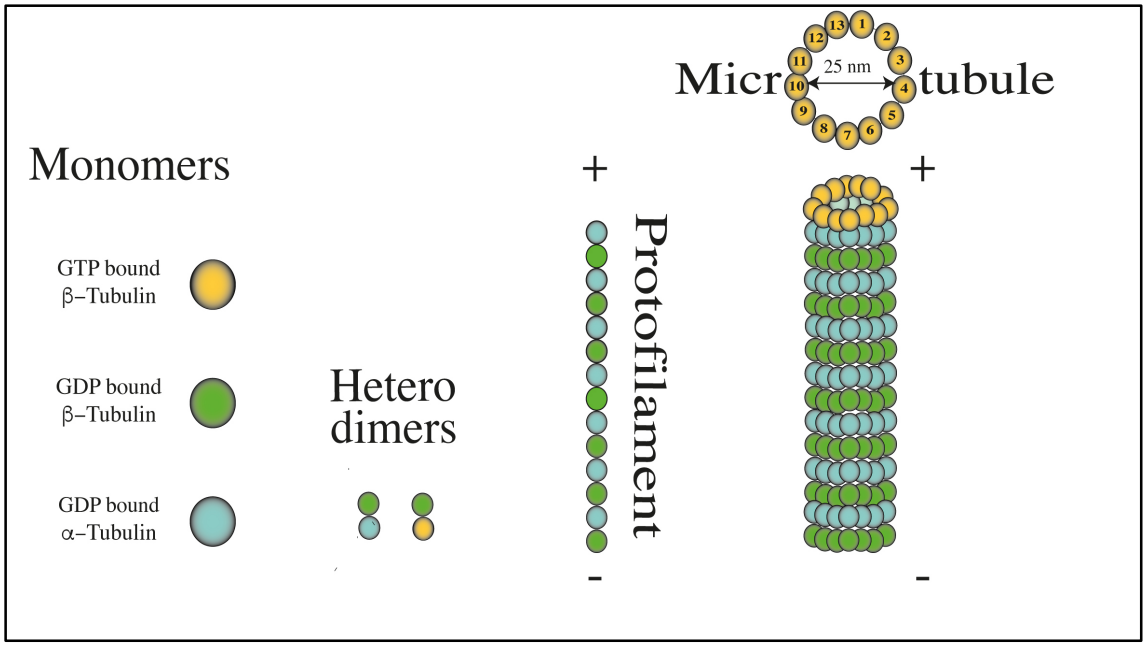

Figure 1.3 The states of Microtubule
Several levels of associations lead to microtubule: GDP bound to α and β Tubulin or GTP bound to β Tubulin represent the basic units in microtubule polymerization. Heterodimers of GDP-αTub/GDP-βTub and GDP-αTub/GTP-βTub associate in tandem to form polar protofilaments. The parallel association of 13 protofilaments is called Microtubule. Microtubules are rigid hollow rods approximately 25 nm in diameter.

Given to this design, the microtubule is a polar and dynamic structure with distinct ends: a plus end (+ end) that exposes β tubulin and a minus end (- end) that exposes α tubulin. Both α and β tubulin can bind guanosine triphosphate (GTP), the nucleotide that powers microtubules polymerization, while the dimeric complex hydrolyze it and convert it to

guanosine diphopshate (GDP). In their stable state microtubules are concave, cylindrical structures predominantely composed of GDP-bound tubulin protofilaments (**Figure 1.4**).

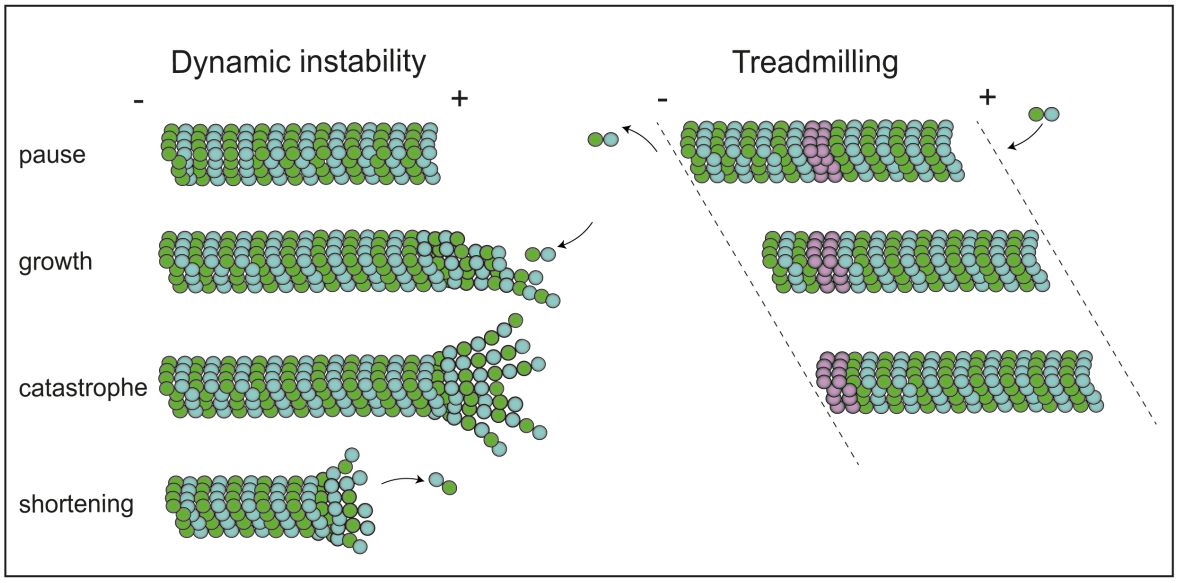

Figure 1.4 Treadmilling and dynamic instability
Two inner properties of the microtubule are the dynamic instability (tubulin subunits association or dissociation at microtubule plus end that can result in the pause, growth, catastrophe and shortening processes), and the treadmilling (subunits are added in one end and removed at the other resulting in the apparent movement of the filament).

GTP hydrolysis converts the GTP bound-tubulin into GDP bound-tubulin. As GTP-bound protofilaments are straight, with multiple lateral contacts, assembly into the final cylindrical conformation rely on GTP hydrolysis that is both intrinsic and essential to filament assembly with the rate of GTP hydrolysis being the primary determinant of whether microtubules grow or shrink. The GTP/GDP bound state affects microtubule dynamics. Tubulin dimers polymerize and depolymerize at microtubule extremities, resulting in cycles of assembly and disassembly. Two mechanisms allow microtubules to display different polymerization behaviors essential for their functions, namely dynamic instability and treadmilling (**Figure 1.4**). The hydrolysis of GTP is at the bases of dynamic instability (Cassimeris, Pryer and Salmon, 1988). The hydrolysis of GTP lags behind the binding of new GTP-tubulin; this lag creates a cap of GTP-tubulin at the microtubule end, which constrains the

curvature of the protofilaments. When GTP bound to β-tubulin is hydrolyzed to GDP, the constraint is removed and the protofilament becomes highly unstable as the stored energy in the lattice (the lateral surface of microtubules) is released. The hydrolysis weakens the binding affinity of tubulin for adjacent molecules, thereby favoring rapid shrinking of the microtubule. A typical microtubule will fluctuate every few minutes between growing and shrinking (Burbank and Mitchison, 2006). Dynamic instability allows the cell to rapidly reshape microtubules in response to cell needs. The reorganization of the mitotic spindle during mitosis strictly depends on the properties that allow arrays of microtubules to adapt quickly to the environment adopting new spatial arrangements. Treadmilling is the continuous loss of GDP bound subunits at the minus end and the association of GTP tubulin subunits at the plus end so that the microtubule stays at constant length but individual subunits move along (Waterman-Storer and Salmon, 1997) (Rodionov and Borisy, 1997).

During cell cycle progression, microtubules length and dynamics are controlled by microtubule-associated proteins (MAPs) and motor proteins.

1.2.2 Different types of MTs

During mitosis, the different position, orientation, and length of the microtubules fibers not only shape the mitotic spindle but also underly the heterogeneity of functions displayed by this complex machinery. The yeast spindle is composed solely of 40 microtubules, of which 2 or 3 are astral microtubules (aMTs), 32 are kinetochore microtubules (kMTs) and 8 are interpolar microtubules (iMTs) (Wittmann, Hyman and Desai, 2001) (**Figure 1.5**).

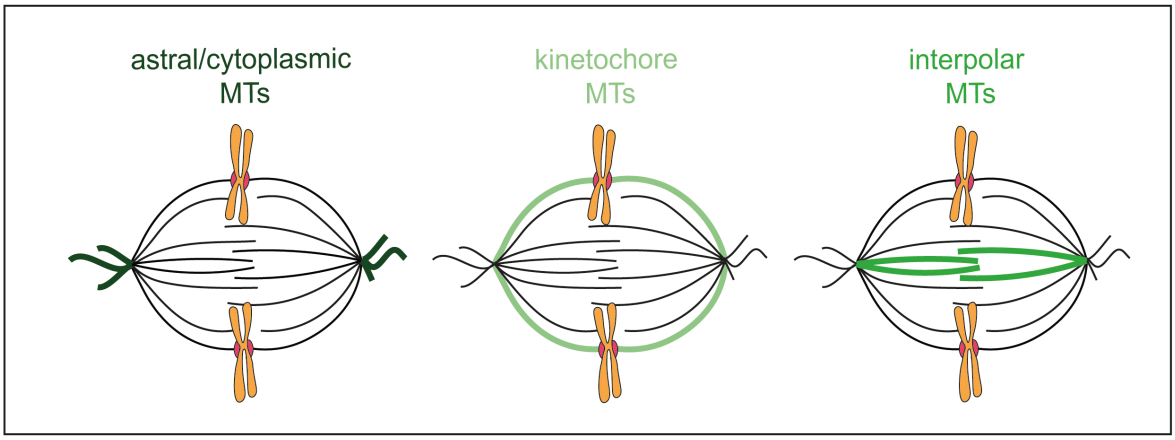

Figure 1.5 Different types of microtubules of the mitotic spindle
The founding blocks of the mitotic spindle are three classes of microtubules: astral microtubules (aMTs), kinetochore microtubules (kMTs), and interpolar microtubules (iMTs).

The astral microtubules are the only cytoplasmic microtubules, they nucleate minus ends at the Spindle Pole Body (SPB) and extend plus ends toward the cell cortex (Wittmann, Hyman and Desai, 2001). Astral microtubule interaction with and sliding along the cell cortex ensure the orientation of the spindle with respect to the division axis and, as the entire nuclear contents are moved along with the spindle, they are responsible also for nuclear positioning at the bud neck (Palmer *et al.*, 1992). Astral microtubule-mediated spindle positioning is controlled by two redundant pathways of which Kar9 and Dynein 1 are the central members. Kar9 is a protein involved both in karyogamy and in spindle positioning (Manatschal *et al.*, 2016). In the latter it acts as a cytoplasmic tether or adaptor linking the cytoplasmic microtubules to a specific site at the bud cortex (Manatschal *et al.*, 2016).

Dynein is a large cytoplasmic polypeptide member of the minus-end directed family of motor proteins that specifically localizes on astral MTs (di Pietro, Echard and Morin, 2016). Each individual pathway is dispensable, provided that the other one remains functional. The Kar9 pathway is activated earlier in time with respect to the Dynein one and serve the purpose of directing astral MTs from one spindle pole body (SPB) into the emerging bud, where they are captured at the cell cortex, and their activity causes the

movement of the spindle toward the mother-bud neck prior to anaphase (Manatschal *et al.*, 2016). After Kar9, Dynein is required to generate the force needed for nuclear positioning (di Pietro, Echard and Morin, 2016). During anaphase, the Dynein 1 pathway is responsible for the astral MTs plus-ends directed sliding along the cell cortex that results in the final orientation of the spindle. Indeed, as the spindle elongates, one SPB is pulled into the bud and the other is retained into the mother cell, placing the spindle along the mother-bud axis (di Pietro, Echard and Morin, 2016).

Within the nucleus, the SPB organizes two kinds of microtubules: the kMTs and the iMTs. One kinetochore microtubule attaches to a single kinetochore, while several interpolar microtubules extending from the two poles interdigitate in the middle of the structure, the midzone, providing stability to the bipolar spindle (M. Winey and Bloom, 2012). These two classes of microtubules work synergistically in the accomplishment of chromosome segregation. The extension of kinetochore microtubule plus ends allows kinetochore MTs to "explore" space and to find and bind sister chromatid kinetochores. Indeed, as the initial attachment is asynchronous and stochastic, it is a transient contact that has to be converted into a stable interaction for proper bipolar attachment, with the two sister chromatids binding to kMT emating from the opposite sides of the cell (Tanaka, 2010). Once the correct "bipolar" configuration is achieved, the chromatids are separated, through the removal of the linkages that holds them together from their synthesis (Guacci, Koshland and Strunnikov, 1997), and segregated by the shortening of kinetochore microtubules first (anaphase A) (Lodish *et al.*, 2000) and next by the pulling forces generated by the interpolar microtubules (anaphase B) (Scholey, Civelekoglu-Scholey and Brust-Mascher, 2016). During anaphase A, the poleward movement of the chromatids is generated by the progressive depolymerization of kinetochore MTs plus-end (Guacci, Koshland and Strunnikov, 1997). Successively, the concomitant extension of interpolar MT plus-ends together with their sliding produce the outward directed force necessary for pushing the spindle poles apart (Scholey, Civelekoglu-Scholey and Brust-Mascher, 2016).

1.3 The mitotic spindle cycle

Microtubule behaviors defines the mitotic spindle cycle, that is strictly intertwined with the chromosome cycle to ensure proper cell division. The mitotic spindle cycle begins with MTs nucleation that occurs from a specialized organelle, the centrosome, or Spindle Pole Body (SPB) in yeast, that represents the Microtubule Organizing Centers (MTOC) (Rüthnick and Schiebel, 2018). The G1 cell inherits a single centrosome that has to be duplicated once in the cell cycle in order to establish the bipolar structure essential for the accurate partitioning of the genetic material. To this end, correct centrosome duplication is a critical first step and therefore it requires a tight control to ensure proper coordination with DNA replication and partitioning.

Once the centrosome correctly duplicates, the spindle establishes the bipolar arrangement in which uniformly oriented microtubules, aligned with their minus end retained at and their plus end that radiate out from the two poles, organize in the two symmetric arrays of the bilobated structure (M. Winey and Bloom, 2012).

As cells progress through to metaphase, the microtubule turnover increases and this is thought to help correct erroneous attachments that occur during bipolar chromosome alignment, the configuration in which sister kinetochores are bound to kMTs emanating from the opposite poles (Lee and Spencer, 2004). In this configuration, the cohesin link that tethers the chromatids together preserves the identity of each pair of chromosomes until biorientation is achieved, and at meanwhile, provides a force opposed to the one exerted by the spindle that tends to pull the chromatids in opposite directions (Makrantoni and Marston, 2018). Once each chromosome couple is bipolarly attached by the kinetochore MTs, the cohesin link is removed, and the microtubules segregate the chromatids at the two poles (Makrantoni and Marston, 2018). During anaphase A, sister chromatids are pulled toward the spindle poles through the shortening of the kinetochore MTs fibers. Instead, during anaphase B, the elongation and the outward sliding of the

antiparallel interpolar MTs, increase the interpolar distance thereby pushing the two poles further apart (Scholey, Civelekoglu-Scholey and Brust-Mascher, 2016). Spindle elongation requires the stabilization of microtubule dynamics and the activity of microtubule-motor proteins and Microtubule Associated Proteins (MAPs) (Higuchi and Uhlmann, 2005a) (Anton Khmelinskii *et al.*, 2007) (Anton Khmelinskii & Elmar Schiebel, 2008). Once the sister chromatids have reached the opposite poles of the cell, the mitotic spindle is dismantled (telophase) and the chromosomes decondense. To complete the division process, the cells are next physically separated through cytokinesis, that leads to the physical separation of cytoplasm, cell content and cell membrane into the two daughter cells, each one containing one exact copy of the genetic information of the mother (Wloka and Bi, 2012). This process is generally achieved through a contractile actomyosin ring, that pinches and cuts the cell into two, but additional species-specific events are essential to complete it (Guertin, Trautmann and McCollum, 2002). Despite obvious divergences among species exist the basic mechanisms of cell cycle regulation are highly conserved in the eukaryotic kingdom and legitimate our choice to use *Saccharomyces cerevisiae* as a model organism.

> *"Model organisms are not better because they are more like humans but because they use the same processes as human cells and do so in a manner that facilitates discoveries about these processes. S. pombe's preoccupation with G2 to M phase control is not particularly "human," but without any question it made possible the discovery of Cdc2's role in regulating mitosis, which is shared by all eukaryotic cells"* (Nasmyth, 2001)

1.3.1 Mitotic spindle assembly

1.3.1.1 Spindle pole bodies structure

The yeast spindle pole body (SPB) is the functional equivalent of the vertebrate centrosome and it represents the microtubules organizing center (MTOC) in which the γ tubulin complex constitutes the essential element for MTs nucleation (Farache *et al.*, 2018).

As the budding yeast undergoes a closed mitosis, the SPBs are embedded in the nuclear membrane within a specialized "polar fenestra" facing both the nucleus and the cytoplasm during all the cell cycle (**Figure 1.6**).

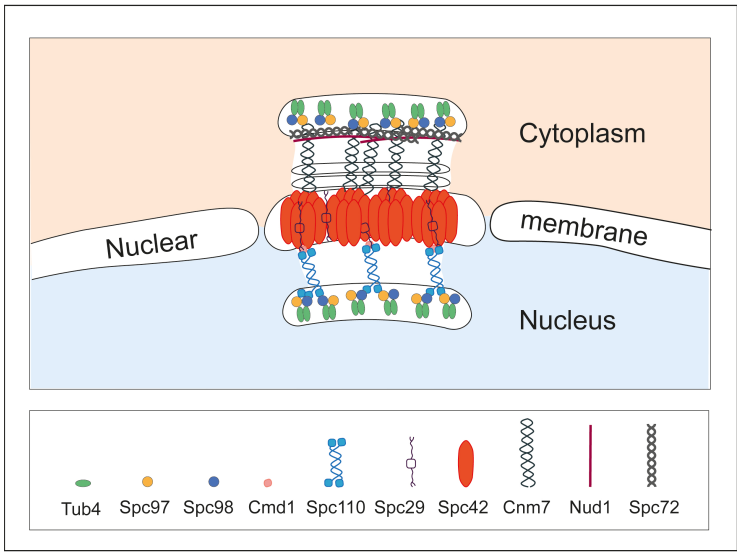

Figure 1.6 The spindle body (SPB) structure
The spindle pole body, the yeast equivalent to the vertebrate centrosome, is a complex structure organized in three layers: with the central one embedded within the nuclear membrane and the other two, namely the inner and outer layers facing the nucleus and the cytoplasm, respectively.

The yeast spindle pole body (SPB) is a plate-like structure embedded in the nuclear envelope and capable of nucleating the three-different kinds of microtubules making up the mitotic spindle (Mark Winey and Bloom, 2012). The SPB is layered in three plaques: an inner and outer plaque facing the nucleus and the cytoplasm respectively, and a central plaque that extends over the nuclear membrane. Comprehensive structural analysis

revealed the SPB as a complex structure composed of almost 20 proteins of which 16 are essential for cell viability (Bullitt *et al.*, 1997) (Kilmartin, 2014). The SPB is organized around a crystalline core of Spc42 proteins that constitute the central plaque The Yeast Spindle Pole Body Is Assembled around a Central Crystal of Spc42p (Muller *et al.*, 2005) (Seybold and Schiebel, 2013). The inner and the outer plaques are built up by specific proteins that anchor γ tubulin receptors (Spc110 nuclear receptor and Spc72 cytoplasmic receptor) that, in turn, ligate γ tubulin subunits to nucleate the MTs (Muller *et al.*, 2005) (Seybold and Schiebel, 2013) (Kilmartin, 2014). The nuclear receptor Spc110 is related to the pericentrin family of proteins, in which the MTs nucleating domain is separated from the anchor domain by an extended coiled-coil region (Jaspersen and Winey, 2004). In the nuclear plaque, Spc42 is connected to Spc110 through the Spc29 protein whose binding with Spc110 relies on the association of Spc110 with Calmodulin (Jaspersen and Winey, 2004). On the cytoplasmic side, the association of the linker Cnm67 to Spc42 determines the binding of Nud1, a protein responsible of recruiting both components of the Mitotic Exit Network (Hotz *et al.*, 2012), for the regulation of mitotic late events, and the Spc72 γ tubulin receptor complex (Jaspersen and Winey, 2004).*S. cerevisiae* has the most elemental MT nucleation machinery, the γ tubulin small complex (γ TuSC), a Y-shaped structure consisting of only two γ tubulin molecules each bound to Spc97 and Spc98 (Kollman *et al.*, 2010) (**Figure 1.7**).

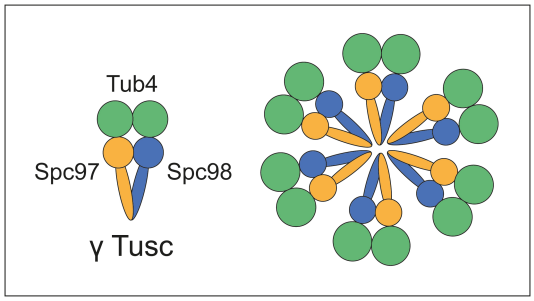

Figure 1.7 The microtubule organizing center (MTOC)
In yeast, the microtubule-organizing center is formed by heterodimers of Spc97 and Spc98 that by recruiting γ tubulin nucleate microtubule filaments in the cell.

Spc97 and Spc98 belong to the gamma tubulin protein complex family (GCP) and are homologs of GCP2 and GCP3 respectively (Kollman *et al.*, 2010). While the yeast γ TuSC is composed of only two proteins of this family, in other eukaryotes multiple γ TuSC associates with multiple GCP proteins (GCP4-6 proteins) to form the γ tubulin ring complex (γ TuRC). Despite the lack of additional subunits, the direct association of multiple γ -TuSC to oligomers of Spc110 proteins determines the formation of a ring-like MT-nucleation template that is consistent with the 13-folds microtubule structure (Kollman *et al.*, 2010).

1.3.1.2 Spindle pole bodies duplication

Mitotic spindle assembly initiates when the single SPB duplicates, establishing the bipolar structure that ensures accurate chromosome segregation. As the new SPB is not generated *de novo,* but from the duplication of the inherited one, the SPB duplication is considered a conservative event. In particular, the new SPB originates from the development of a structure connected to the old one by the half bridge (**Figure 1.8**).

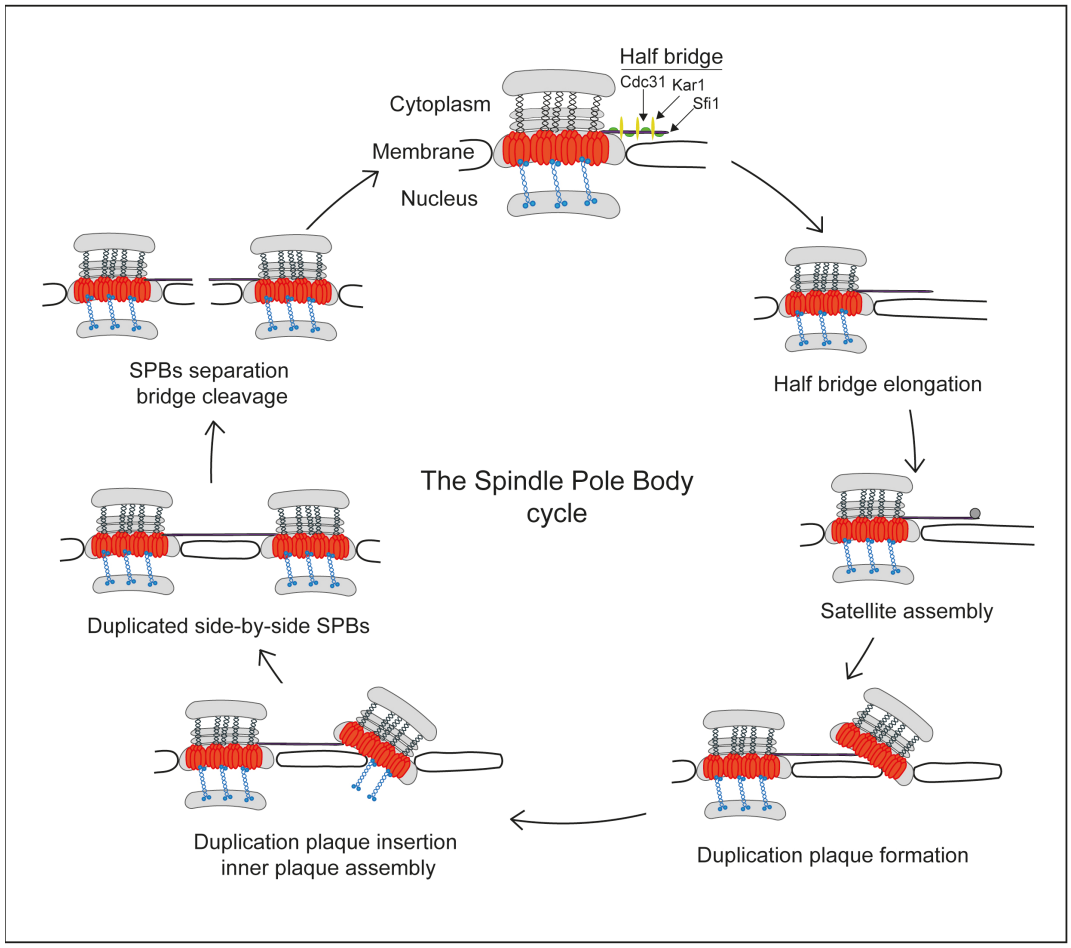

Figure 1.8 The spindle pole body (SPB) duplication.
The phases of the spindle pole body duplication are shown. The spindle pole body cycle starts in G1 and it is completed by the end of S phase. 1) in G1 the SPB carry a half bridge composed by Cdc31, Kar1 and Sfi1 proteins; 2) the half bridge elongates; 3) the satellite assembles at the distal tip of the half bridge; 4) the satellite develops the central and the outer plaques; 5) while inserting into the nuclear envelope, the new SPB forms inner plaques components; 6) the two SPBs lie side by side embedded in the nuclear membrane;7) the severing of the bridge results in SPBs separation.

The half-bridge is a modified region of the nuclear envelope (NE) that extends from the central plaque and faces both the nuclear and the cytoplasmic sides of the membrane (Short, 2015) (Rüthnick and Schiebel, 2016) (Kilmartin, 2014). Components of the half

bridge are Sfi1, Cdc31, Kar1 and Mps3 (Rüthnick and Schiebel, 2016) proteins. Sfi1 is a Centrin-binding protein that spans the entire length of the cytoplasmic side of the half-bridge (Rüthnick and Schiebel, 2016). Sfi1 is organized with the N-terminal in contact with and the C-terminal far from the central plaque of the SPB (Rüthnick and Schiebel, 2016). The region in between is mainly α-helical and exposes 21 Centrin-binding repeats *via* which Sfi1 makes contacts with multiple Centrin proteins and with Kar1. Cdc31 is the yeast Centrin, a ubiquitous centrosome component, consisting in a small Ca^{2+} binding protein, closely related to Calmodulin (Rüthnick and Schiebel, 2016). Kar1 and Mps3 are membrane-anchored proteins that are responsible for the insertion of the newly duplicated SPB within the cytoplasmic and nuclear membrane respectively (Seybold *et al.*, 2015) (Rüthnick and Schiebel, 2018). The half bridge doubles its length during anaphase, so that the nascent daughter cell will receive one SPB bearing a completed bridge (Seybold and Schiebel, 2013) (Seybold *et al.*, 2015). The extension of the half-bridge is accomplished by the antiparallel dimerization of additional Sfi1 molecules that bind, with their C-terminal, to the C-terminal of the ones already positioned (Rüthnick and Schiebel, 2018). In this antiparallel arrangement, the C termini lie at the center of the bridge, and the distal N termini constitute the daughter-SPB assembly platform (Rüthnick and Schiebel, 2018). As the half bridge extension represents the very early step of SPB duplication and hence, of bipolar spindle assembly, it was demonstrated that a tight balance between phosphatase and opposing kinases plays a crucial role in regulating SPB duplication, thereby providing a potential licensing mechanism (Tanaka, 2014). The overall regulation of the cell cycle is based on a fundamental antagonism between kinase and phosphatase activities that determine the phosphorylation state of targeted substrates hence the progression through the cycle transitions. In general, entry into mitosis is driven by rising mitotic kinase activity while exit from mitosis provides for the decline of the kinase activity and for the reversal of mitotic phosphorylation events (Uhlmann, Bouchoux and López-Avilés, 2011). As well as other essential processes, also spindle morphogenesis is subjected to cell cycle

control. Specific cyclin-CDK complexes (**Box 1**) have been shown to positively and negatively regulate several steps in the SPB-duplication cycle at different cell cycle phases (Haase, Winey and Reed, 2001) and roles for CDKs main antagonistic phosphatse Cdc14 highlighted (**Box 2**).

Box 1: Cyclins and cyclin-dependent kinases

Cyclin dependent kinases (CDKs) are a family of Serine-Threonine kinases that guide cell cycle progression up to metaphase.
CDKs are regulated mainly *via* the association with a set of regulatory subunits called cyclins. Cyclins levels fluctuate during the cell cycle. Besides contributing to CDKs activation, the different cyclins serve to confer substrate specificity to the kinases.
This principle holds true for all Eukaryotes, with the exquisite difference that in yeast is a single CDK, namely Cdc28, that guides cell cycle progression whereas In vertebrate, on top of different classes of phase-specific cyclins, several CDKs also exist.

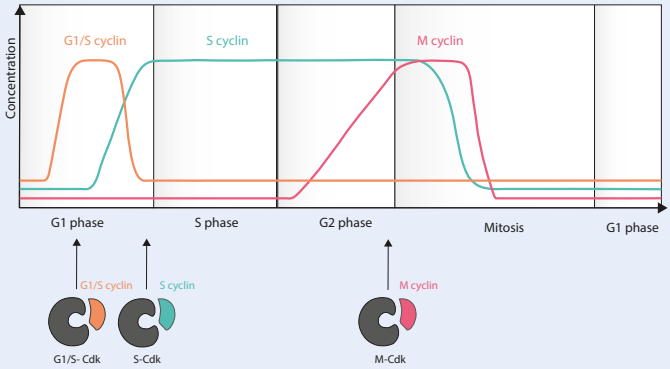

The figure shows how yeast cyclins are expressed during the cell cycle.

Box 2: Cdc14 phosphatase

In budding yeast, the final stages of mitosis are triggered by conserved protein phosphatase Cdc14, which is responsible for both CDKs inactivation and reversal of the phosphorylation events mediated by these kinases. Cdc14 itself is regulated by being sequestered in the nucleolus by binding to its inhibitory subunit Cfi1 (also known as Net1). Cfi1 sequesters and keeps Cdc14 inactive in the nucleolus until metaphase, but releases it during nuclear division. Two regulatory networks, the Cdc Fourteen Early Anaphase Release network (FEAR) and the Mitotic Exit Network (MEN) are required for the release of Cdc14 from Cfi1. The FEAR network promotes Cdc14 release from the nucleolus during early anaphase, whereas the MEN maintains Cdc14 in a released state during late stages of anaphase and telophase.

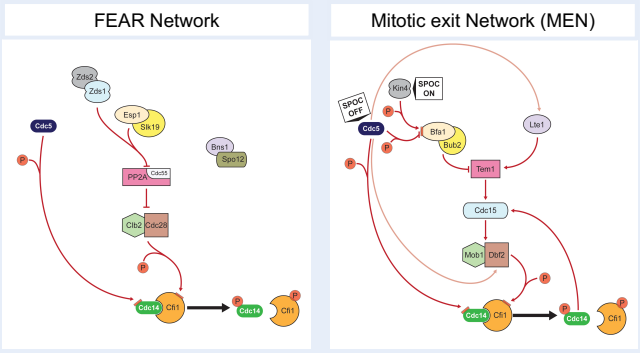

A schematic representation of the FEAR and MEN network is shown

Cdc14 leads several mitotic spindle dynamics. During anaphase, the progressive activation of the phosphatase and the consequent drop of the kinase activity allows for the formation of the bridge (Tanaka, 2014) (Rüthnick and Schiebel, 2016). In particular, it is the removal of CDK-mediated-inhibitory phosphorylation of Sfi1-C terminus that promotes the dimerization of the half bridge into the bridge (Tanaka, 2014) (Rüthnick and Schiebel, 2016). Other regulatory kinases are implicated in SPB duplication including the Mps1 kinase and the Polo-like kinase Cdc5 (Tanaka, 2014). After Cdc14 dephosphorylation, Mps1 promotes the extension of the bridge by phosphorylating Cdc31, and thus, inducing conformational changes in the Centrin-binding protein Sfi1 (Tanaka, 2014). Beside Cdc31, Mps1 regulates also other half-bridge and core SPB components including Spc29 and Kar1. Concerning the Polo like kinase, similarly to CDK1, but to a lesser extent, Cdc5 phosphorylation of Sfi1 is required to block an additional round of duplication during mitosis (Tanaka, 2014). In budding yeast, Cdc5 is the only member of the Polo like family of kinases and represents an integral part of the cell cycle engine.

The new SPB is initially formed by the recruitment of components of a SPB precursor, the satellite (Rüthnick and Schiebel, 2018). Soluble components of the satellite are Cnm7, Nud1, Spc42, and Spc29 whose overall structure assembles at the distal tip of the bridge, thereby lying on the cytoplasmic side of the nuclear envelope (Rüthnick and Schiebel, 2016). Next, the satellite expands into a duplication plaque, another intermediate form of the SPB, whose structure resembles the one of the cytoplasmic side of the mature SPB (Rüthnick and Schiebel, 2016). The development of the satellite into the duplication plaque is sustained by G1-cyclin-CDK-mediated phosphorylation (Rüthnick and Schiebel, 2016). CDK-mediated phosphorylation of Spc42 is thought to promote the self-assembly of the Spc42 hexagonal lattice, a superstructure forming the inner layer (Rüthnick and Schiebel, 2016). Concomitant with this, the duplication plaque embeds in the nuclear envelope where it assembles the last, nuclear layer of the SPB.

1.3.1.3 Spindle pole bodies separation

The two SPBs remain nearly adjacent within the membrane and connected by the bridge until late S phase self-assembly of the Spc42 hexagonal lattice, a superstructure forming the inner layer (Rüthnick and Schiebel, 2016).

Soon after the accomplishment of the replication of the genetic material, the bridge is severed, the old and the new SPBs start separating, allowing for the formation of the two poles of the short bipolar spindle (**Figure 1.8**). SPB separation requires the activities of Cin8 and Kip1, two kinesin-5 (BimC) motor proteins that play a role both in spindle assembly and elongation (Hoyt *et al.*, 1993) (David J. Sharp, Rogers and Scholey, 2000). Although BimC family members are generally processive plus-end directed motor proteins, it has recently been shown that both Cin8 and Kip1 can switch directionality and move in both the directions on spindle MTs (Gerson-Gurwitz *et al.*, 2011) (Düselder *et al.*, 2015) (Bell *et al.*, 2017). The significance of this is not yet fully understood. Cin8 and Kip1 are known to have partially overlapping functions in spindle assembly, as their concomitant absence prevents the duplicated SPBs from separating (Hoyt *et al.*, 1993) (David J. Sharp, Rogers and Scholey, 2000) , promotes collapse of the spindle and induces cell death. The overlap in functions of these proteins underlies the finding that neither of them is *"per se"* essential for cell viability albeit their involvement in essential cell cycle events (Hoyt *et al.*, 1993) (David J. Sharp, Rogers and Scholey, 2000). Although either Cin8 or Kip1 function alone is sufficient to assemble the spindle, at the restrictive growth temperature of 37°C the function of Cin8 becomes essential for this process (Hoyt *et al.*, 1993). The reason for it remains to be elucidated. The failure in SPBs separation of *cin8Δ kipΔ* cells is partially rescued by the deletion of the kinesin-14 minus-end-directed motor Kar3, suggesting that the SPBs separation relies on counteracting forces exerted by the two class of proteins (Hoyt *et al.*, 1993). Besides motors, also the microtubule-associated protein (MAP) Ase1 is implicated in SPBs separation (Crasta *et al.*, 2006a). Ase1 is a MT binding and bundling protein, firstly described and named for its role during anaphase

spindle elongation, where it localizes and stabilizes the midzone by organizing antiparallel MTs into bundles (Schuyler, Liu and Pellman, 2003a). Midzone localization but also bundling activity are common features shared by Cin8 and Kip1 motors, and Ase1 non-motor protein (Bell *et al.*, 2017). It is now well established that the shearing force generated by the MTs bundling activity is key in the scission of the inter-SPB bridge (Crasta *et al.*, 2006a). Kinesin-5 motor expression is cell cycle regulated: they peak in mitosis and their stability relies on the Anaphase Promoting Complex or Cyclosome (APC/C) ubiquitin-mediated pathway (**Box 3**) (Crasta *et al.*, 2006a).

Box 3: The anaphase promoting complex/ cyclosome

The anaphase Promoting Complex or Cyclosome (APC/C) is a multi subunit E3 ubiquitin ligase, responsible of transferring ubiquitin, a small signalling molecule, onto substrates; thereby targeting them for proteasome mediated degradation.

APC/C activation requires the interaction of the core APC/C complex with substrate specific activator proteins like Cdc20 and Cdh1, the mitotic co-activators of the APC/C. Cdc20 activates the APC/C at the metaphase to anaphase transition towards its early targets including S-phase and mitotic cyclins and Securin (Pds1 in yeast).

While, at exit from mitosis, the APC/C now bound to Cdh1, targets for degradation other mitotic proteins as mitotic cyclins, Cdc5. Ipl1 and Cdc20,

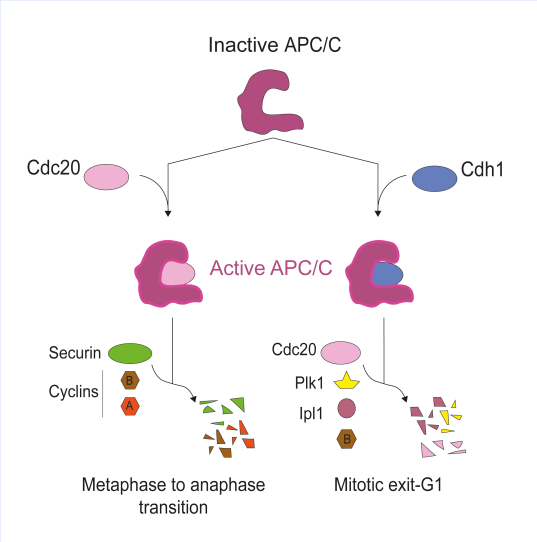

In budding yeast the APC/C complex interacts with specific coactivators required for substrate specificity.

APC/C activation requires the interaction of the core APC/C complex subunits with substrate specific activator proteins like Cdc20 and Cdh1. Cin8, Kip1 and Ase1 are all targeted for degradation by the APC^{Cdh1} during anaphase, and this degradation appears to be required for the normal timing of spindle disassembly (Crasta *et al.*, 2006a) (Qiao *et al.*,

2010). APC/C^{Cdh1} activity persists throughout G1 until the beginning of S phase, when increasing CDK1 levels leads to the inactivation of the APC^{Cdh1}allowing for the accumulation of the two kinesin-5 motor proteins Cin8 and Kip1 (Crasta *et al.*, 2006a) (Qiao *et al.*, 2010). Besides inactivating the APC^{Cdh1} complex, CDK1 positively regulates the splitting of the bridge both in a direct and indirect manner (Crasta *et al.*, 2006a). First, the CDK1- mediated phosphorylation of the C-terminus of Sfi1 determines the disassembly of Sfi1 antiparallel oligomers (Tanaka, 2014) (Rüthnick and Schiebel, 2016). Moreover, it seems that Cdk phosphorylation of Cdh1 primes the binding of the polo-like kinase Cdc5. CDK1-Cdc5 combined action results in the fission of the Sfi1-Sfi1 interface in the bridge allowing both for the formation of the bipolar spindle but also to regenerate the half-bridge structure on which the satellite will form in the next cell cycle (Rüthnick and Schiebel, 2016).

1.4 Metaphase and kinetochore splitting

Following the completion of SPB duplication, the mitotic spindle is short, with a length of 0,6 μm and the two SPBs facing each other.

Rapidly transiting toward metaphase, the spindle continues to elongate reaching a length of approximately 1 or 2 μm. Even though, in yeast, these transitions are difficult to detect, metaphase is defined as the moment in which chromosomes are condensed and captured by kinetochores MTs to bipolarly attach into the mitotic spindle. Proper chromosome capturing relies on a search and capture mechanism by which kinetochore MTs emanating from opposite SPBs search and interact with the two sister kinechores of each sister chromatid couple. This kind of attachment, named bipolar or amphitelic (sister kinetochores bound to opposite poles of the spindle), is the only one capable to guarantee proper chromosome segregation. Mechanisms are in place to correct faulty attachments and promote bi-oriented kinetochores binding (Heald and Khodjakov, 2015).

1.4.1 Kinetochore structure

The interaction between chromosomes and microtubules is mediated by the kinetochore (KT), a multi protein complex that assembles on the centromere, a specialized repetitive sequence of DNA, that in mitotic, condensed, chromosomes appears as a constricted region where sister chromatids are at their closest (**Figure 1.9**).

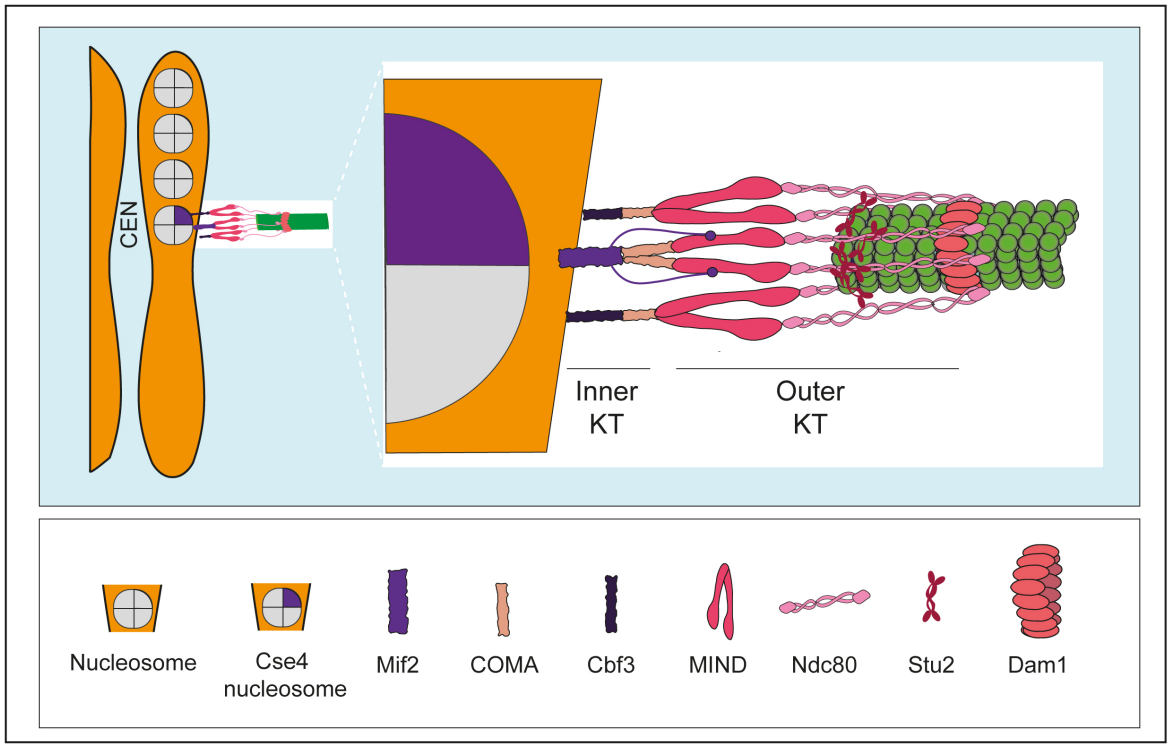

Figure 1.9 The kinetochore (KT)
The kinetochore is a complex structure hierarchically assembled on centromeric DNA. The main complexes of the inner and outer yeast kinetochore are shown.

In yeast, centromeres consist of a 125-bp stretch comprised of three elements (CDE I, II, and III). This type of centromeric arrangement, also known as point-CEN, is very different from the centromeres found in vertebrates or even fission yeast, where centromeres can extend over many kilo- and megabases (regional CENs) or even along the entire length of the chromosomes as in *Caenorhabditis elegans* (Hegemann and Fleig, 1993) (Oegema *et*

al., 2001). Despite a great similarity in functions and design, stricking differences are appreciated among species.

The yeast kinetochore is composed by approximately 65 proteins, hierarchically assembled, and mainly organized into multiprotein subcomplexes (ranging from two to ten subunits per complex). If from a morphological point of view, the vertebrate kinetochore seems far more complex than its yeast counterpart, it appears that at the molecular level, all organisms studied so far, contain kinetochores similar in compositions as they share a surprisingly large number of proteins. An explanation for the apparent discrepancy between morphological and molecular data is that the kinetochores of metazoans are assembled from repeated subunits.

The second unique feature of the budding yeast kinetochore is that the stoichiometry of the interaction between kMT and kinetochore is 1:1, meaning that only a single microtubule attaches to each kinetochore. In higher eukaryotes this binding, can reach stoichiometry of 20:1 up to 40:1 with one sister KT requiring the binding of a set of 20 to 40 microtubules. Consequently, it is not surprising that while the budding yeast contains a single kinetochore-assembly unit (point-CEN), in higher eukaryotes it is common to find extended regions of centromeric DNA that provide for the assembly of multiple kinetochores capable of binding multiple MTs.

What's universal across organisms is that kinetochore complexes assemble on centromeric sequences (CENs) containing nucleosomes including the specialized histone H3 variant CENP-A (Cse4 in budding yeast) (Mellone *et al.*, 2003) (Black and Bassett, 2008) and are organized in two parts: an inner part, that directly binds chromosome CENs and an outer part that interacts with spindle MTs

The inner kinetochore is built upon the Cse4 nucleosome by the initial binding of Mif2 (CENP-C in human). This binding serves as a seed for the assembly of other proteins and proteins sub-complexes including CBF3, Mif2, Mtw1, COMA, and Cnn1 (Goh and Kilmartin, 1993) (Sorger, Severin and Hyman, 1994) (He *et al.*, 2001). The outer

kinetochore, is considered a linker structure with the purpose of connecting the inner layer to microtubules. The need for a linker structure comes from the fact that no proteins in direct contact with centromeric DNA displays microtubule-binding activity. Additional functions of these complexes include: i) conveying the forces generated by microtubule dynamic instability to the inner kinetochore proteins thereby allowing centromere oscillations during metaphase and poleward chromosome movement during anaphase, ii) surveiling the kinetochore attachement status through the recruitment of checkpoint proteins, and iii) monitoring the quality of kinetochore-microtubule attachments *via* the "tension-sensing" machinery.

Key within the outer kinetochore is the conserved Ndc80 complex (Hec1 complex), that associates with other protein complexes including Spc105 and Dam1 (De Wulf, Odekerken-Schröder and Van Kenhove, 2003) (Lampert and Westermann, 2011). Ndc80 is a heterotetrameric complex made of four protein subunits: Spc24, Nuf2, Spc25, and Ndc80. It assembles as a long rod with a globular head at both extremities. The unstructured N-terminal domain of the globular head, exposed toward the microtubule interface, mediate the binding to microtubules (Ciferri, Musacchio and Petrovic, 2007) via binding to the Dam1 ring, a heterodecamer structure consisting of multiple Dam1 complexes organized as a ring around the microtubules plus end. Concomitantly the other head binds proteins of the inner kinetochore. Given its peculiar function Ndc80 is defined as a crucial bridge (van Hooff *et al.*, 2017).

Given that microtubule plus ends continuously grow and shrink it is important to understand how microtubules can de/polymerize while staying attached to KT. For the polymerization of the microtubule plus end it is proposed that proteins associates forming a cap that prevents is from slipping out of the ring (Asbury *et al.*, 2006). For depolymerizing microtubules, it is proposed that the distal bending of the depolymerizing filaments might let the ring run toward the SPB, moving the chromosome with it (Asbury *et al.*, 2006). The stability of the Kinetochores-microtubules structure relies on the presence of several motor

proteins and MT-associated proteins (MAPs) that seem to be recruited via the "linker" complexes at outer Kintetochore (Pagliuca *et al.*, 2009).

1.4.2 Kinetochore-microtubule attachment

Another peculiarity of the budding yeast is that by undergoing a closed mitosis, kinetochores are in the proximity of the SPBs during most of the cell cycle (Winey *et al.*, 1995). It was observed that they are continuously associated with the SPB *via* microtubules except for the time required for the replication of the centromeric DNA sequence (Kitamura *et al.*, 2007). DNA replication calls for the disassembly of the kinetochore that is promptly reconstituted soon afterwards and immediately reconnected to the microtubules. Kinetochore capture is indeed observed already in S phase when a contact is established between kinetochores and microtubule lattice (**Figure 1.10 A**). The larger surface of the microtubule lattice facilitates the kinetochore-microtubule interaction providing higher possibilities for making a contact, in contrast to the more restrained microtubule tip.

The capture of kinetochores is explained by a "search-and-capture" mechanism. According to this model microtubules, by extending their dynamic plus ends, explore the space up to when they eventually encounter and bind kinetochores. Albeit intriguing, this serendipitous mechanism *per se* doesn't seem to provide a proper explanation for the efficiency of the physiological microtubule-kinetochore binding observed and calls for additional mechanisms contributing to the process.

The observation that, in organisms performing an open mitosis, a gradient of Ran-GTP forms around chromosomes and guides the directionality of kinetochore microtubule extension allows for the hypothesis that this gradient may contribute to the process (Wollman *et al.*, 2005). The Ran-GTP gradient model doesn't seem to provide a suitable

explanation also for the budding yeast, that is relatively too small to produce an effective gradient. An alternative possibility comes from the observation that the kinetochores are capable of nucleating microtubules that can associate with SPB-nucleated microtubule, thereby facilitating the association of the kinetochore with the lateral surface of SPB-nucleated microtubule (**Figure 10 B**) (Tanaka *et al.*, 2005) (Tanaka and Desai, 2008) (Tanaka, 2010).

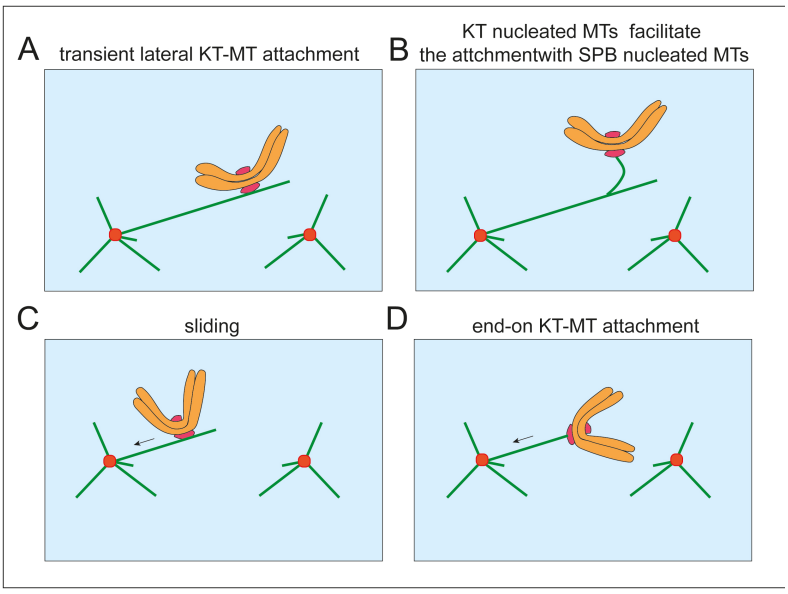

Figure 1.10 Biorientation of the kinetochore-microtubule (KT-MT) attachment
Biorientation of KT-MT attachment is achieved through sequential steps: establishment of KT-MT lateral attachment (a) requires KT nucleated MTs to facilitate kinetochore binding to the lateral surface of SPB nucleated kMTs (b) next sliding of the chromosome kinetochore toward the relative SPB stabilize the interaction (c) leading to conversion of the lateral KT-MT attachment to an end-on attachment when the KT is bound to the distal tip of the kMT (d).

Once the kinetochore is bound to the lateral surface of the microtubule, stabilization of the binding requires kinetochore movement along the MT toward the pole. This process, known as “sliding”, in budding yeast is partially mediated by Kar3 a minus end directed motor member of the Kinesin-14 family (Tanaka *et al.*, 2005) (Tanaka and Desai, 2008) (Tanaka, 2010) (**Figure 1.10 C**). Since Kar3 is a non-processive motor, the sliding of the kinetochore along the microtubule often causes the detachment of the kinetochore and results slower compared to the one mediated by the Dynein1 motor in animal cells. The

sliding of the kinetochore along the microtubules continues till the shrinking plus end reaches the kinetochore site on the lattice. At this point the orientation of the kinetochore changes and it binds at the microtubule plus tip (**Figure 1.10 D**). The conversion from lateral to the "end-on KT-MT" attachment is controlled by the microtubule associated protein Stu2 (ch-TOG in human). If the conversion fails, Stu2 induces the rapid polymerization of the microtubule tip preventing the dissociation of the kinetochore. The different kinetochore attachments on microtubules require different partner regulators. The stabilization of the end-on attachment involves the loading of the Dam1 complex on kinetochores that is, in turn, dependent of Ndc80 complex. The Dam1 complex is capable of converting the energy generated from the curling of microtubule plus-end depolymerization into a force that pulls the kinetochore toward the pole. This mechanism is similar to the one applied during anaphase A, where kinetochore end-on movement toward the pole is guided by microtubule depolymerization as well.

1.4.3 Biorientation of sister kinetochores attachment

Once the microtubule has driven the kinetochore toward the pole, another microtubule, emanated from the opposite pole, has to bind to the sister kinetochore in order to establish the bipolar or amphitelic attachment of the chromatids. Mainly two mechanisms facilitate the bipolar settlement: the kinetochore geometry and the restraint exerted by the presence of the cohesin complex between the chromatids (**Box 4**).

Box 4: Cohesin complex

The cohesin is a ring shaped complex responsible of coupling each pair of chromosome till their separation in anaphase. The complex consists of two members of the SMC family, Smc1 and Smc3, and two non-SMC proteins, the a-kleisin subunit Scc1/Mcd1 and Scc3.

Smc1 and Smc3 proteins are formed by two globular domains at N- and C- terminus connected by a long coiled-coil region at the center of which there is a third globular domain, the hinge domain. The antiparallel association of the coiled coil regions of Smc1 and Smc3 heterodimers make N- and C-terminus of each monomers in contact, thus establishing a functional ATPase domain. The Scc1 kleisin subunit binds to the SMC heads, and this, together with the association of Scc3, stabilizes the interactions within the complex and closes the ring.

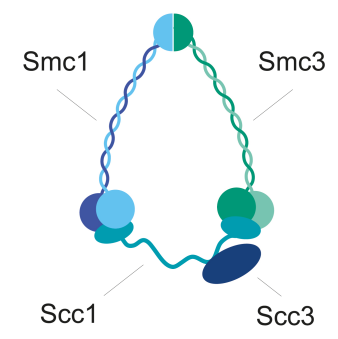

Overview of the cohesin complex consisting of four core subunits: Smc1, Smc3, Scc1 and Scc3

The back-to-back geometry of the sister kinetochores, with the two kinetochores facing the opposite poles of the cell, favors the attachment of the kinetochores to the microtubules originating from the opposite poles. Once KTs are bipolarly attached to the spindle, microtubule pull the sister chromatids towards the poles. The pulling force exerted by microtubules is opposed by the cohesin that tethers the chromatids together. This tug-of-war generates tension, that is sensed by the cell and translated into the validation of proper bipolar attachment by the Spindle Assembly Checkpoint (SAC) (Corbett, 2017). If errors occur, correction mechanisms are activated to establish a proper bipolar, amphitelic attachement, the only configuration that satisfies the conditions for an equal distribution of the chromosomes between the two daughter cells. Erroneus non-bipolar attachements include: syntelic (sister KTs attached to the same SPB), monotelic (one sister KTs attached to one pole, the other KT is not bound) and merotelic (one of the two sister KTs attached to both the SPBs) attachments (Lampson *et al.*, 2004) (Pinsky and Biggins, 2005)(**Figure 1.11**).

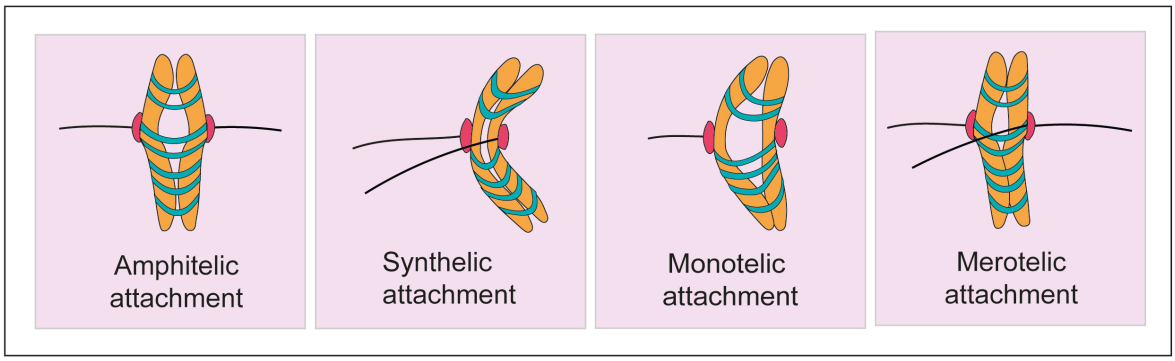

Figure 1.11 Schematic representation of possible (KT-MT) attachments

Tensionless attachments trigger the SAC that prevents cohesin cleavage (**Box 5**), hence chromosome separation and anaphase progression till all the chromatids are correctly attached.

Box 5: The metaphase to anaphase transition

Anaphase onset coincides with sister chromatids separation and require the removal of cohesins from chromosomes, achieved through the proteolytic cleavage of the cohesin subunit Scc1. Scc1 is cleaved by the separase Esp1, which is maintained in an inactive state till metaphase by the Securin Pds1.
Only once all the chromosomes are bipolarly attached to the spindle, and the checkpoint is switched-off, Cdc20 activates the APC/C that, in turn i) releases Esp1 by degrading its inhibitor Pds1 and jj) inactivates the mitotic CDK1 by cyclin B degradation. APC/C signalling cascade regulates both sister chromatids separation, through cohesin cleavage, and by decreasing the kinase activity ensures chromosome segregation and the begin of mitotic exit.

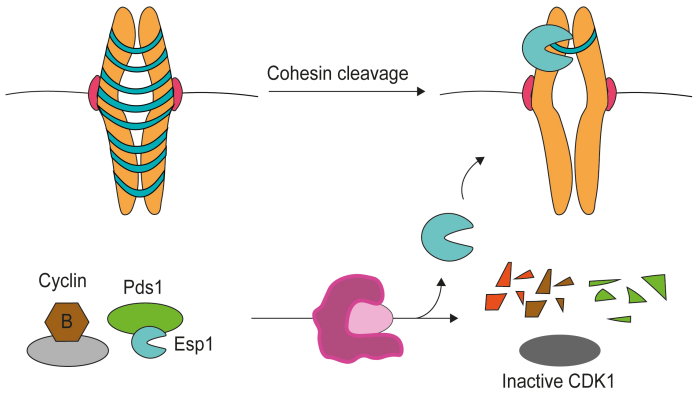

A schematic representation of the FEAR and MEN network is shown

To inhibit anaphase onset the SAC acts by inhibiting the APC/C^{Cdc20} (**Figure 1.12**)

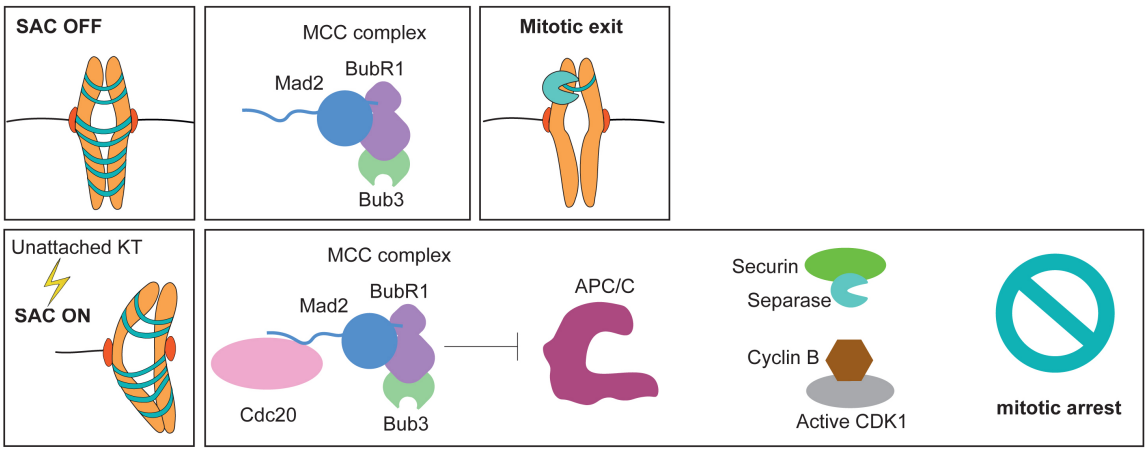

Figure 1.12 The spindle assembly checkpoint (SAC)
Unattached kinetochores are sensed by the spindle assembly checkpoint a surveillance pathway which halt cell cycle progression by sequestering the APC/C cofactor Cdc20.

The SAC generates the mitotic checkpoint complex (MCC), which is composed of Mad2, BubR1/Mad3, and Bub3. The MCC inhibits the APC/C through the direct association of Mad2 with the APC/C cofactor Cdc20. In addition, other members of the SAC as Bub1, BubR1, Mad1, and Mps1 help the MCC-mediated inhibition of Cdc20 (Musacchio and Salmon, 2007) (Vleugel *et al.*, 2012). Mad2 is responsible for the sequestration of Cdc20, and their binding depends on the previous interaction between Mad2 and Mad1. Indeed, the interaction Mad2-Mad1 changes the Mad2 status from an open-conformation (O-Mad2) to a closed-conformation (C-Mad2), increasing its affinity for Cdc20 and ensuring efficient MCC formation (De Antoni *et al.*, 2005) (Mapelli *et al.*, 2007). Fundamental to recruit Mad2 at unattached KTs is the kinase Mps1 (Yamagishi *et al.*, 2012) (London and Biggins, 2014); when the KT binds to microtubules, Mps1 activity is lost and it stops producing MCC. In addition, an "error correction" mechanism exists that upon low tension signal (e.g. synthelic attachment) indirectly activates the SAC through the generation of unattached kinetochores which are the only source for SAC signal (Krenn and Musacchio, 2015). This mechanism has been suggested to depend on the activity of

Ipl1 (Biggins and Murray, 2001) the only member of the conserved serine/threonine Aurora B kinase family (**Figure 1.13**).

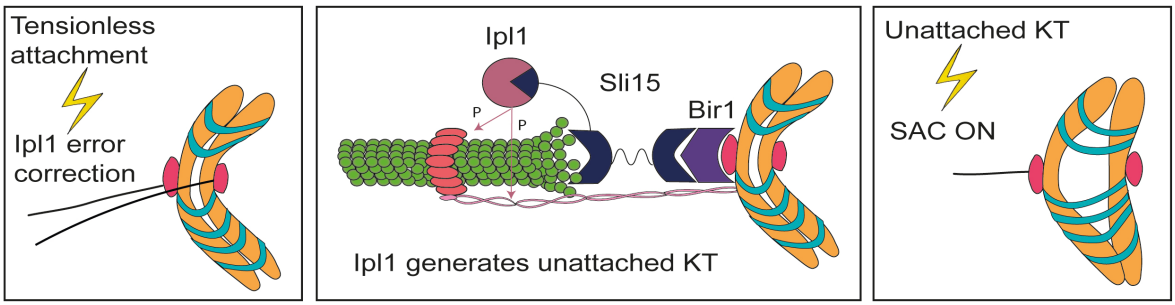

Figure 1.13 Error correction
Tensionless attachments are sensed by the Aurora yeast member Ipl1. Ipl1 destabilize KT-MT attachment generating unattached kinetochores that i) can establish a new correct attachment or ii) activate a SAC dependent response.

Ipl1 is a component of the Chromosome Passenger Complex (CPC) together with Sli15 (INCENP), Bir1 (Survivin) and Nbl1 (Borealin). The CPC relocates during the cell cycle, being in metaphase at the centromeres, where it promotes biorientation, and in anaphase at the spindle to prevent further re-orientation. Ipl1 phosphorylation of kinetochore components weakens KT-MT attachment and promote their turnover. In particular, Ipl1 mediated phosphorylation of Dam1 and Ndc80 reduces their affinity with microtubules promoting their disassembly thereby facilitating re-orientation of KT-MT attachments. Whereas, in the case of bi-oriented kinetochores, the tension generated spaces the kinetochores away from inner sister centromeres, hence preventing Ipl1 from phosphorylating its KTs substrates, resulting in stable KT-MT attachments. A serious threat is presented when merotelic attachments occurs. These attachements generate tension across sister kinetochores and do not produce unattached kinetochores, hence they are undistinguishable from the amphitelic ones and similarly they do not engage the SAC. Several findings indicate that the centromeric pool of the Aurora B kinase plays a central role in correcting these errors. Aurora B results enriched at merotelic attachment sites and

its inhibition causes an increase in the number of merotelic attachments (Liu *et al.*, 2009) (Liu *et al.*, 2010).

1.5 Anaphase movements

When all chromosome kinetochores are correctly bipolarly attached, the SAC is satisfied and cells can progress through anaphase. The checkpoint inactivation allows Cdc20 to activate the APC/C thereby triggering a signalling cascade that culminates with the activation of the separase Esp1. Esp1 triggers parallel signaling cascades that result both cohesin cleavage and spindle elongation providing a functional link for the timely coordination of chromosome separation and segregation. Cohesin cleavage has long been considered the point of no return for anaphase completion but recent data indicate that after cohesin cleavage, additional mechanisms exist that prevent spindle elongation hence anaphase progression if conditions go awry (Roccuzzo *et al.*, 2015)

Anaphase spindle elongation can be divided into anaphase A and anaphase B. During anaphase A sister chromatids move toward the SPB they are in contact with. This poleward movement is achieved through the shortening of th kinetochore microtubules. During anaphase B sister chromatids are further segregated apart by the progressive elongation of the interpolar microtubules that results in an increase in the pole to pole distance (Pearson *et al.*, 2001). Kinetochore and interpolar microtubules work synergistically to achieve chromosome segregation, however the dynamics of the two classes of microtubules are driven by distinct molecular mechanisms (Scholey, Civelekoglu-Scholey and Brust-Mascher, 2016) (Asbury, 2017).

1.5.1 Spindle mechanics during anaphase A

The features of microtubules dynamics behind the poleward movement of the sister chromatids during anaphase A vary in different model organisms, in which the shortening of kinetochores microtubules can be observed at either or both extremities.

In budding yeast anaphase A, the force necessary to drive chromosome segregation is generated by the progressive shortening of kinetochore microtubules through depolymerization at their plus end. Understanding how kinetochore microtubules can depolymerize while securely maintaining chromosome kinetochores attached to the same extremities is puzzling. As motor proteins are generally involved in regulating microtubule dynamics while walking on microtubule, it is tempting to assume they may contribute to this dragging poleward chromosome movement as well. Although such a contribution during anaphase A is observed in other organisms, the observation that in budding yeast the disassembly of kinetochore plus-end occurs even in the absence of minus-end directed motors, suggests that chromosome movement is not only achieved through the activity of minus-end motors (Asbury, 2017).

Two models provide an explanation for how kMT disassembly can be coupled to chromosome binding and dragging: the biased diffusion and the conformational wave (**Figure 1.14**).

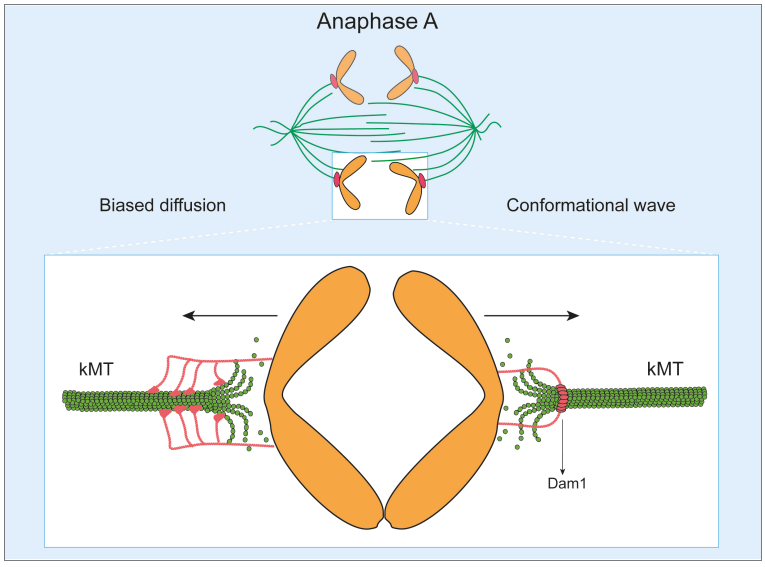

Figure 1.14 Anaphase A
Graphic representation of two putative models (Biased diffusion and Conformational wave) explaining chromosome movement during anaphase A.

In the biased diffusion model an array of fibrils of microtubule binding elements at the kinetochore attaches, pulls and detaches the shrinking microtubule lattice at or near the plus end tip. In the conformational wave model, kMT plus end disassembly and the Dam1 complex in yeast are the main factors involved. During the shortening, the depolymerizing plus-end bends, and the curvature pulls toward the kinetochore, determining the sliding of the Dam1 complex and hence of chromosome kinetochore. These two models are not mutually exclusives and a Hybrid model in which the force is produced by the combination of the two mechanisms can also be envisioned (Asbury, 2017). The latter would provide a good explanation for the coupling-tip mechanism. None of the existing models is exhaustive enough suggesting that further studies are required to fully understand this process.

1.5.2 Anaphase B

In *S. cerevisiae,* the completion of chromosome segregation is achieved mainly *via* anaphase B, when the progressive increase in the length of the interpolar microtubules results in spindle elongation hence poles separation.

In yeast, the elongation of the spindle is biphasic with a first phase where the spindle elongates fast (0.54 μm /min) going from a length of 1,5-2 μm (metaphase spindle) to a length of 4-6 μm (early anaphase) followed by a second phase where, MTs elongation rate decreases (0.21 μm /min) leading the spindle to reach the final length of approximately 8-10 μm (Straight, Sedat and Murray, 1998) (Movshovich *et al.*, 2008).

Multiple mechanisms contribute to the elongation of the spindle including the polymerization and the outward sliding of antiparallel interpolar microtubule and the cortical pulling mediated by the astral microtubules.

For yeast anaphase B spindle elongation, the best mechanistic explanation comes from the sliding filaments/midzone pushing model (**Figure 1.15**).

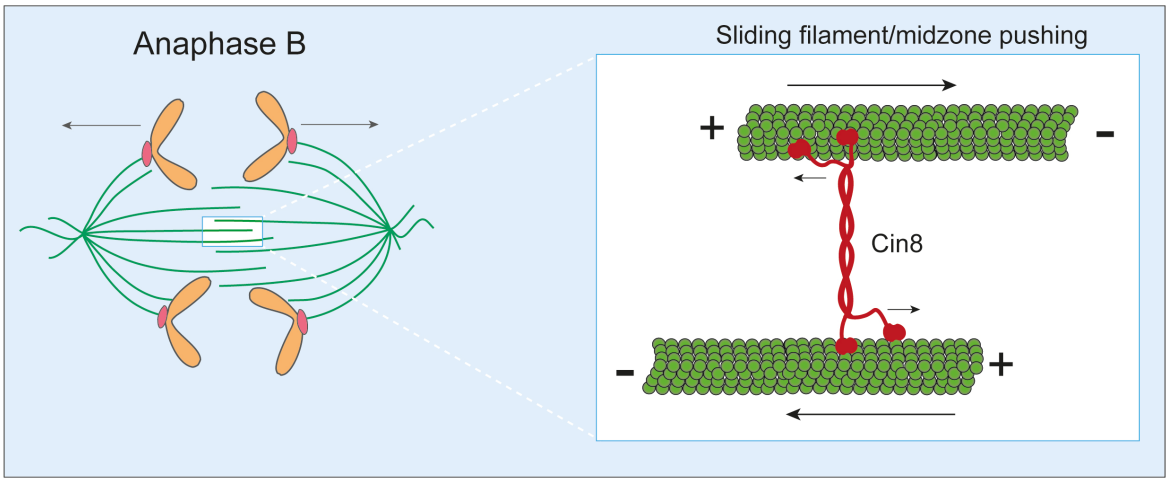

Figure 1.15 Anaphase B
In yeast, anaphase B spindle elongation is mainly achieved through a sliding filament/midzone pushing mechanism in which interpolar overlapping microtubules at the spindle midzone are crosslinked and slid by homotetrameric kinesin-5 motors.

According to this model, microtubules growing from the two poles meet in an anti-parallel arrangement right at the midzone. Here their overlapping plus ends are cross-linked by plus-end directed motors, that, by sliding apart the fibers, generate the pushing forces responsible for reducing the length of the overlaps and increasing the distance between the poles.

Therefore, the midzone region, beside being essential for the maintenance of spindle bipolarity, can be envisioned as the hub for the recruitment of factors necessary for the forces required to stabilize and elongate the spindle. Indeed, at anaphase, several proteins essential for spindle elongation localize selectively to the midzone as a consequence of changes in their phosphorylation status. In yeast, the phosphatase responsible of dephosphorylating multiple proteins implicated in microtubules stabilization is Cdc14.

1.5.2.1 Microtubule-associated proteins (MAPs)

Phospshorylation is the main mechanism of MAPs regulation. Upon entry into mitosis mitotic-CDKs command the increase in MT dynamics to permit the formation of the mitotic spindle and the attachment of the spindle MTs to sister chromatids KTs. Later on, spindle elongation and chromosome segregation require the stabilization of the anaphase spindles and indeed the metaphase-to-anaphase transition overlaps with a remarkable decrease in MT turnover. The activation of the separase Esp1 coordinates sister chromatid separation with the activation of the phosphatase Cdc14, whose dephosphorylation of multiple MAPs is required to stabilize the elongating anaphase spindles (Higuchi and Uhlmann, 2005a).

In budding yeast, the microtubule associated protein Ase1 (the yeast homolog of vertebrate PRC1/MAP65) is central for the assembly of the spindle midzone in anaphase. The spindle midzone is defined as a region in the middle of the *spindle* where the microtubules emanated from opposite poles overlap. Ase1 homodimers bundle anti-parallel MTs at the spindle midzone (Schuyler, Liu and Pellman, 2003b) thereby establishing a landmark for the recruitment of all midzone organizers. Ase1 is expressed in mitosis, likely after bipolar spindle formation, and its APC/C^{Cdh1}-mediated degradation contributes to the disassembly of the spindle upon exit from mitosis (Juang *et al.*, 1997). Prior to anaphase onset, Ase1 is kept inhibited by S phase-CDK-mediated phosphorylation events. At anaphase onset, Cdc14 removes these inhibitory phosphorylations allowing for Ase1 binding to the central spindle and, ultimately, midzone establishment.

The lack of this dephosphorylation results in the delocalization of multiple midzone components and delays the switch from fast to slow elongation rate of the spindle (Anton Khmelinskii *et al.*, 2007).

Once bound, Ase1 recruits the Esp1-Slk19 complex, whose role is to restrict the spindle midzone to the middle of the mitotic spindle (Jensen *et al.*, 2001) (Sullivan and Uhlmann, 2003). Esp1-Slk19 recruitment to the spindle also requires the chromosomal passenger

complex (CPC) (Ruchaud, Carmena and Earnshaw, 2007). This complex associates with KTs up to when Cdc14 dephosphorylation of its subunit Sli15 re-localizes the entire complex to the spindle MTs, a movement necessary for its role in spindle midzone assembly (Pereira and Schiebel, 2003). Premature CPC binding to MTs is prevented through combinatory phosphorylation of Sli15 by CDKs and Ipl1 itself (Nakajima *et al.*, 2011).

Mounting evidences suggest that one function of Cdc14 in regulating the spindle behaviour is to influence the activity of different MAPs to anaphase. The role of the phosphatase is not restricted to Ase1 and Sli15 but additional proteins associated to the spindle are Cdc14 substrates. The spindle-stabilizing protein Fin1 requires Cdc14-mediated dephosphorylation to interact with SPBs and MTs of elongating anaphase spindles and upon mitotic exit is targeted to degradation by the activated APC/C^{Cdh1} ubiquitin ligase (Woodbury and Morgan, 2007).

The kinetochore DASH component Ask1 is another mitotic protein whose activity is regulated through CDK phosphorylation and Cdc14-mediated dephosphorylation (Li and Elledge, 2003). Also the MAP Stu2 (Yin *et al.*, 2002) needs to be dephosphorylated by Cdc14 to localize to the spindle. These Cdc14-dependent dephosphorylation events directly contribute to reduce MT dynamics at anaphase onset (Higuchi and Uhlmann, 2005a).

1.5.2.2 Kinesin-related motor proteins

Microtubule motor proteins are a class of proteins that use the energy derived from ATP hydrolysis to generate the mechanical energy required to move and segregate spindle-attached chromosomes. In *S. cerevisiae* five kinesin-related motor proteins (Cin8, Kip1, Kar3, Kip3 and Kip2) exist. Although overall essential for cell division the overlap in functions observed for these proteins indicate that none of them is *per se* indispensable for cell viability (Hildebrandt and Hoyt, 2000).

Cin8 and Kip1 are members of the kinesin-5 (BimC) subfamily of motor proteins. Remarkably, while BimC family members are generally processive plus-end directed motors it has been shown that Cin8 can switch its directionality and move in both the directions on spindle MTs (Gerson-Gurwitz *et al.*, 2011) (Roostalu *et al.*, 2011). The significance of this remains unclear.

Cin8 and Kip1 share a high sequence similarity in the motor (force-producing) domain and act by sliding apart anti-parallel MTs to generate an outwardly-directed force important to establish proper spindle dynamics. Before anaphase onset Cin8 and Kip1 are required for SPBs separation and bipolar spindle formation (M A Hoyt *et al.*, 1992a) (Roof, Meluh and Rose, 1992). At anaphase they participate in the stabilization of the spindle midzone (Gerson-Gurwitz *et al.*, 2009) (Fridman, Gerson-Gurwitz et al. 2009) and regulate the switch from the fast to the slow phase of anaphase B spindle elongation (Straight, Sedat and Murray, 1998) (Movshovich *et al.*, 2008) (Fridman, Gerson-Gurwitz et al. 2009).

In addition to the motor domain Cin8 possesses a self-association domain as well as a tetramerization domain and it is active only as homotetramer. This particular structure seems to be fundamental for the cross-linking and sliding apart of anti-parallel MTs as suggested by the finding that homodimers of Cin8 can bind to MTs but are not functional (Hildebrandt and Hoyt, 2001).

The expression of Kinesin-5 motors is cell cycle regulated and resembles the pattern of mitotic cyclins. They peak in mitosis and their stability relies on the APC/C activity with Cin8 being targeted for degradation late in anaphase by the APC/C^{Cdh1} (Hildebrandt and Hoyt, 2001) and Kip1 earlier in anaphase by the APC/C^{Cdc20} (Gordon and Roof, 2001). In respect to their functions two patterns of regulation are proposed. Early functions (i.e. SPBs separation and bipolar spindle formation) are mediated by CDKs in two ways. On the one hand CDKs phosphorylation of Cdh1 keeps the APC/C^{Cdh1} inactive indirectly stabilizing the motors (Crasta *et al.*, 2006b) (Crasta *et al.*, 2008), on the other hand mitotic CDKs directly phosphorylate Cin8 and Kip1 thereby promoting their activity in SPBs

separation and bipolar spindle formation (Chee and Haase, 2010b). On the contrary late functions are under the control of the phosphatase Cdc14 in at least two ways. On the one hand Cdc14 facilitates the interaction of Cin8 with the short anaphase spindle directly by reversing CDK mediated phosphorylation events (Rachel Avunie-Masala *et al.*, 2011), on the other hand Cdc14 dephosphorylation of Ase1 indirectly induces Cin8 recruitment to spindle midzone where it drives spindle elongation (Khmelinskii *et al.*, 2009).

Kar3 belongs to the family of microtubule minus-end-directed kinesin-14 motor proteins (deCastro *et al.*, 2000). Kar3 produces inwardly-directed forces antagonizing the outwardly-directed forces generated by the kinesin-5 motors (Saunders *et al.*, 1997). Its activity depends on the heterodimerization with the non-motor proteins Cik1 or Vik1, two accessory subunits associated to different functions (Manning *et al.*, 1999). The Kar3/Vik1 complex localizes to SPBs while the Kar3/Cik1 one mainly accumulates on astral MTs (Manning *et al.*, 1999). In agreement with their localization Kar3/Vik1 cross-links and stabilizes parallel MTs at the SPBs while Kar3/Cik1 slides, stabilizes, and depolymerizes cytoplasmic MTs and seems to be the complex involved in spindle and nucleus orientation and positioning (Maddox *et al.*, 2003) (Sproul *et al.*, 2005) (Gardner *et al.*, 2008) (Chen, Rayment and Gilbert, 2011).

Kip3 is a member of the kinesin-8 family of motor proteins and possess a plus-end specific MTs depolymerase activity that correlates with its catastrophe-promoting effect in cells (Gupta *et al.*, 2006) (Varga *et al.*, 2006). The role of Kip3 is determined by the cooperative interactions with other Kip3 motors (Varga *et al.*, 2009). This motor localizes predominantly onto cytoplasmic MTs and SPBs to regulate astral MTs length and nuclear migration (DeZwaan *et al.*, 1997). Kinesins-8 are required to restrain MTs length especially by promoting catastrophe of longer MTs over shorter ones (Tischer, Brunner and Dogterom, 2009), and negatively regulating the MTs elongation rate (Du, English and

Ohi, 2010). Kip3 also contributes to metaphase KTs clustering in the nucleus (Wargacki *et al.*, 2010).

Kip2 as well as Kip3 are prevalently cytoplasmic motor proteins, but Kip2 localizes exclusively on astral MTs and not at SPBs. Provided with MTs polymerizing activity Kip2 antagonizes Kip3 in the process of nuclear positioning. Loss of Kip2 results in short astral MTs. In contrast, in *kip3* mutants the cytoplasmic MTs are significantly longer than normal (Cottingham and Hoyt, 1997) (Miller *et al.*, 1998). Kip2 serves also to target cargo-proteins such as Bik1 and dynein to the plus-ends of astral MTs, required to orient the nucleus towards the bud-neck (Carvalho *et al.*, 2004).

1.5.2.3 The polo-like kinase family

Polo-like kinases (Plk) are a family of serine/threonine protein kinases that play important roles throughout the cell cycle. Their name comes from the abnormal spindle poles phenotype observed in *Drosophila* mutants (Sunkel and Glover, 1988). There are four Plk family members; among them Plk1 is the best characterized. Budding yeast, contains a single Polo-like family member (Cdc5) that is a memer of the Plk1 family.

Plk1 has been implicated in several critical functions in basically all sub-phases of mitosis. It is associated with CDK activation, centrosome maturation, mitotic spindle assembly, kinetochore function, chromosome cohesion, mitotic exit and cytokinesis (Barr, Silljé and Nigg, 2004). In respect to spindle elongation, the critical role of Plk1 in the process has been highlighted by the finding that treating cells with a Plk1 inhibitor blocked anaphase B spindle elongation but did not impact on spindle midzone assembly or anaphase A (Brennan *et al.*, 2007b). Although Plk1 is a candidate for controlling anaphase spindle elongation its role in the process has not been defined. Plk1 phosphorylation could either activate motor proteins or alter the dynamics of microtubules. In agreement with this hypothesis are the findings that a comprehensive study of the Plk1-dependent

phosphoproteome of the human mitotic spindle identified Plk1 phosphorylation sites on centrosomal, MT-associated proteins (MAPs), and motor proteins including the MAP PRC1 (Ase1 in yeast) and the kinesin 5 Eg5 (Cin8 in yeast) (Santamaria *et al*., 2011) and Plk1 localizes to the spindle midzone immediately after anaphase, where it directly phosphorylates the midzone kinesin MKLP2 (Neef *et al.*, 2003) thereby guiding its localization (Carmena *et al.*, 1998).

1.6 Spindle disassembly

Once sister chromatids segregation is completed the cell exit from the cycle of division dismantling of the mitotic spindle. Spindle disassembly occurs in telophase and the accountable microtubule dynamics involved are tightly coordinated with cell cycle progression. As the spindle elongates, the number of the interpolar microtubules decrease to two for each SPB. Spindle disassembly consists in the depolymerization of the few interpolar microtubule and ultimately in the splitting of the two halves of the typical metaphase shaped spindle (Maddox, Bloom and Salmon, 2000). To split in two, the mitotic spindle has to dismantle the midzone region. This process coincides and is coordinated by the APC/C Cdh1 targeted degradation of several midzone stabilizing proteins: Ase1 (Juang *et al.*, 1997), Fin1 (Woodbury and Morgan, 2007) and Cin8 (Hildebrandt and Hoyt, 2001).

Other effectors of midzone disassembly are Ipl1 and Kip3. Ipl1 kinase mediated phosphorylation of the plus end binding protein Bim1 causes its detachment from the microtubules and consequently the progressive shortening of microtubule plus end (Zimniak *et al.*, 2009). Finally, also the depolymerizating activity of Kip3 is necessary for the depolymerization of interpolar MTs (Straight, Sedat and Murray, 1998).

2 Materials and methods

2.1 Plasmids, primers and strains

2.1.1 Plasmids and primers

All plasmids and primers that were used in this study are listed in **Table 2.1** and **Table 2.2**, respectively.

2.1.2 Bacterial strains

The genotypes of the *Escherichia coli* (*E. coli*) bacterial strains that were used as hosts for plasmid amplification and for recombinant protein expression are listed in **Table 2.3**. Chemically competent cells were used for the transformations.

2.1.3 Yeast strains

All *Saccharomyces cerevisiae* (*S. cervisiae*) yeast strains that were used in this study are isogenic to the W303 (*ade2-1, can1-100, trp1-1 leu2-3,112, his3-11,15, ura3*) background, except for the mating type tester strains Ry72 and Ry73. The majority of the strains were generated by dissecting sporulated heterozygous diploid strains obtained by crossing haploid strains of opposite mating type (see section 2.5.1 for procedure). The relevant genotypes of all yeast strains used in this study are listed in **Table 2.4**.

2.2 Growth media and growth conditions

2.2.1 Growth media for *E. coli*

Bacterial cells were grown in Luria Broth (LB) medium with the following composition:

LB: 1% bactotryptone (DIFCO)
0.5% yeast extract (DIFCO)
1% NaCl
pH 7.25

The LB medium was supplemented with 50 μg/ml ampicillin (LB + amp). For solid media, 2% agar (DIFCO) was added to the medium. All strains were grown at 37°C.

2.2.2 Growth media for *S. cerevisiae*

Yeast cells were grown in rich medium Yeast Extract Peptone (YEP) or Sythetic Complete (SC) with the following composition:

YEP: 1% yeast extract
2% bactopeptone
0.015% L-tryptophan
pH 5.4

The YEP medium was supplemented with 300 μM adenine and either 2% glucose (Yeast Extract Peptone Dextrose, YEPD), or 2% raffinose (Yeast Extract Peptone Raffinose, YEPR), or 2% raffinose and 2% galactose (Yeast Extract Peptone Raffinose Galactose, YEPRG) as carbon sources. For solid media, 2% agar (DIFCO) was added to the medium.

SC: 0.15% yeast nitrogen base (YNB, DIFCO) without amino acids and ammonium sulfate.
0.5% ammonium sulfate
200 nM inositol

The SC medium was supplemented with either 2% glucose (Synthetyc Complete Dextrose, SCD), or 2% raffinose (Synthetyc Complete Raffinose, SCR), or 2% raffinose and 2% galactose (Synthetyc Complete Raffinose Galactose, SCRG) as carbon sources and amino acids as required. For solid media, 2% agar (DIFCO) was added to the medium.

All strains were grown at 23°C unless otherwise stated. Growth conditions for individual experiments are described in the corresponding figure legend.

2.3 DNA-based procedures

2.3.1 *E. coli* transformation

50 µl of fresh chemically competent Top10 cells were thawed on ice for approximately 10 minutes prior to the addition of plasmid DNA or the ligation mixture. Cells were incubated with DNA on ice for 30 minutes and then subjected to a heat shock for 30-45 minutes at 37°C. After the heat shock, cells were returned to ice for 2 minutes. Finally, 950 µl LB medium was added to the reaction tube. The cell suspension was incubated on a shaker at 37°C for 45 minutes before plating onto LB and ampicillin plates. The plates were incubated overnight at 37°C.

2.3.2 Plasmid DNA isolation from *E. coli* (mini prep)

Clones were picked from individual colonies and used to inoculate 2 ml LB and ampicillin and grown overnight at 37°C. Bacterial cells were transferred to micro-centrifuge tubes and pelleted for 5 minutes at 8000 rpm. Minipreps were performed with QIAprep Spin Miniprep Kit (Quiagen) following the manufacturer's instructions. Plasmids were eluted in 30 µl sterile double-distilled water (ddH_2O).

2.3.3 Plasmid DNA isolation from *E. coli* (maxi prep)

Plasmid-containing cells were inoculated in 100 ml LB and ampicillin and grown overnight at 37°C. The cells were then recovered by centrifugation for 10 minutes at 5000 rpm. Maxipreps were performed with QIAprep Spin Maxiprep Kit (Quiagen) following the manufacturer's instructions. Plasmids were eluted in 500 µl ddH_2O.

2.3.4 High efficiency LiAc-based yeast transformation

Yeast cells were grown overnight in 50 ml YEPD or the appropriate medium, allowing them to reach the stationary phase. On the following morning, the cell culture was diluted to OD_{600} = 0.2 and allowed to grow several cycles until it had reached an OD_{600} of 0.4-0.7. Cells were then harvested at 3000 rpm for 3 minutes and washed with 50 ml ddH_2O. The pellet was then transferred to an eppendorf tube with 1 ml ddH_2O and washed with 1 ml 1X Tris-EDTA Lithium-Acetate (TE/LiAc) solution. The cells were then resuspended in 250 µl 1X TE/LiAc solution. Aliquots of 50 µl of competent cells were used for each transformation reaction with 300 µl 1X Polyethylene Glycol Tris-EDTA Lithium-Acetate (PEG/TE/LiAc) solution, 5 µl 10 mg/ml single-stranded salmon sperm denatured DNA and "x" µl (max up to 10 µl) DNA. After gentle mixing, the transformation reaction was incubated on a rotating wheel for 30 minutes at room temperature (RT). The cells were heat-shocked at 42°C for 15 minutes and then centrifuged for 3 minutes at 3000 rpm. The pellet was resuspended in 200 µl 1X TE and the cell suspension was plated on appropriate auxotrophy selective medium. In case of selection for resistance to the antibiotic G418, the pellet was resuspended in 200 µl 1X TE and the cell suspension was plated on YEPD to allow the cells to recover after the heat-shock before exposure to antibiotics. After two days, the resulting colonies were replicated on a YEPD plate containing 220 µm/ml G418.

10X TE:	0.1 mM Tris, bring to pH 8.0 with HCl 10 mM EDTA pH 8
10X LiAc:	1 M LiAc, bring to pH 7.0 with acetic acid
1X TE/LiAc:	1X TE 1X LiAc
1X PEG/TE/LiAc:	1X TE 1X LiAc 40% PEG 4000

2.3.5 Smash and Grab yeast genomic DNA isolation

Cells were picked from individual yeast colonies and inoculated in 200 µl lysis buffer. 200 µl phenol/clorophorm/isoamyl alcohol 25:24:1 (SIGMA) and 1 volume of glass beads were added to the cell suspensions and the tubes were shaken for 10 minutes on Vxr Ika-Vibrax shaker. The tubes were then centrifuged twice for 4 minutes at 13000 rpm and the upper aqueous layer was transferred to new tubes. 1 ml ice-cold 100% ethanol was added to precipitate the DNA. After gently mixing the solution, the tubes were centrifuged for 4 minutes at 13000 rpm. The supernatants (SN) were then removed, the pellets were air-dried and the DNA was resuspended in 50 µl 1X TE.

Lysis buffer: 2% Triton X-100
1% SDS
100 mM NaCl
10 mM Tris, bring to pH 8.0 with HCl
1 mM EDTA pH 8.0

2.3.6 Yeast genomic DNA extraction

Yeast cells of the desired strain were grown in 10 ml YEP containing the appropriate sugar to stationary phase. The cells were collected through centrifugation and then washed with 1 ml of solution I. The pellet was then transferred into 0.4 ml of solution I, together with 14 mM β-mercaptoethanol. After mixing, 0.1 ml of a 2 mg/ml Zymoliase 100T solution were added and the tube was incubated at 37°C until spheroplasts were formed (20-30 minutes), which was verified by optical microscopy. After 30 minutes centrifugation, the pellet was carefully resuspended in 0.4 ml 1X TE. After the addition of 90 µl of solution II, the tube was mixed and incubated for 30 minutes at 65°C. 80 µl of potassium acetate (KAc) 5 M, were then added and the tube was incubated on ice for at least 1 hour. The tube was then centrifuged for 15 minutes and the supernatant was transferred in a new

tube, and the DNA was precipitated and washed with 100% ethanol. The dried pellet was carefully resuspended in 0.5 ml 1X TE. 25 µl of 1 mg/ml RNAse was added and the solution was incubated for 20 minutes at 37°C. The DNA was then precipitated by the addition of 0.5 ml isopropanol, followed by centrifugation. The pellet was washed with cold 70% ethanol, air-dried and finally resuspended in 50 µl TE 1X.

Solution I:	0.9 M sorbitol
	0.1 M EDTA, pH 7.5
Solution II:	1.5 ml EDTA, pH 8.5
	0.6 ml Tris base
	0.6 ml 10% SDS

2.3.7 Enzymatic restriction of DNA

For diagnostic DNA restriction, 0,5-2 µg plasmid DNA were digested for 2 hours at 37°C with 1-10 units of the appropriate restriction enzyme (New England Biolabs, NEB). The volume was adjusted depending on the DNA volume and concentration to 20-50 µl with the appropriate buffer and ddH_2O.

For preparative DNA restriction, 5-10 µg plasmid DNA were incubated for 2 hours at 37°C with 1-10 units of restriction enzyme. The enzymes sensitive to heat inactivation were inactivated at 65°C for 20 minutes. The enzymes not sensitive to heat inactivation were inactivated at 65°C for 5 minutes with 6 mM EDTA pH 8. The DNA was then precipitated by addition of 1/10 volume 3 M Sodium Acetate (NaAc) and 3 volumes of 100% isopropanol, followed by centrifugation at 13000 rpm for 15 minutes. The pellet was washed with 200 µl 70% ethanol and finally resuspended in 10 µl ddH_2O, in the case of integrative plasmids, for transformation into yeast.

2.3.8 DNA amplification through polymerase chain reaction

The DNA was amplified using polymerase chain reaction (PCR). PCR was performed using genomic yeast DNA or plasmid DNA as template. Amplification of a DNA fragment requires two oligonucleotides flanking the interesting region, working as primers for the DNA polymerase. Phusion DNA polymerase and ExTaq (TaKaRa) DNA polymerase were used.

Reaction mix:	template DNA	1 µl
	reaction buffer	1X
	dNTPs	0.2 mM
	forward primer	1 µM
	reverse primer	1 µM
	DNA polymerase	1-2 units
	ddH_2O	to 20 µl

DNA amplification was performed with a Biometra T3000 Thermocycler with the following general procedure:

1. heat shock step	5’	at 95°C
2. denaturation step	1’	at 95°C
3. annealing step	1’	at 50-58°C
4. extension step	1’/kb	at 72°C
5. repeat 20-25 times steps from 2 to 4		
6. extension step	10’	at 72°C
7. end	hold	at 4°C

2.3.8.1 PCR-mediated gene modification

The *pGAL-10* promoter and *3-HA* tag were introduced at the N- and C- terminus of *DYN1*, respectively, as described by Longtine M. S. and colleagues (Longtine, McKenzie et al. 1998). To place *DYN1* under the p-GAL promoter and insert the *3-HA* tag at the C-terminus of the gene, *cdc14-1 cdc5-as1* (Ry1602) cells were transformed with the PCR

fragment obtained using Rp89 plasmid as template, and F4-pGAL and R3 pGAL 3-HAas primers. The *p-GAL-10* and *3-HA* insertion was assessed by PCR on the entire genome of the transformed strains (see section 2.3.5 for details), using Cc dyn F and Cc dyn R as primers.

2.3.8.2 Site-directed mutagenesis of CIN8

CIN8 was mutagenized according to the QuickChange Site-Directed mutagenesis kit (Stratagene) instructions. Plasmid Rp173 containing *CIN8* open reading frame (Mp7) under the control of its endogenous promoter (841bp fragment) was used as template in the amplification reactions. The set of primers used to introduce the mutations are listed in **Table 2.2**. The mutagenesis mixture contained 5 µl buffer, 3 µl quick solution, 10 ng DNA template, 125 ng of each primer, 1 µl dNTP mix, 1 µl *Pfu Turbo* DNA polymerase, and water up to 50 µl. The template DNA was eliminated with digestion with DpnI, a restriction enzyme that cleaves only methylated DNA. 2 µl of the mixture were used to transform XL10-Gold bacterial cells in order to recover and amplify the mutated plasmids. The plasmids were then sequenced to ascertain that the only mutation they carried was the one we intended to insert.

The primers used in the sequencing reaction are listed in **Table 2.2**.

The amplification of mutated *CIN8* was performed using the following PCR parameters:

1. heat shock step	30 sec	at 95°C
2. denaturation step	30 sec	at 95°C
3. annealing step	1’	at 55°C
4. extension step	11’	at 68°C
5. repeat 18 times steps from 2 to 4		
6. extension step	7’	at 68°
7. end	hold	at 4°C

2.3.9 Agarose gel electrophoresis

Following the addition of 1/5 volume of bromophenol blue (BPB) solution, DNA samples were loaded on 0.8% - 1% agarose gels along with DNA markers. The gels were made in 1X Tris-Acetate-EDTA (TAE) buffer containing 1x sybrsafe (Invitrogen) and run at 80-120 volts (V) until the desired separation was achieved. The DNA bands were visualized under a UV lamp (radiation wavelength 260 nm).

BPB solution: 0.2% BFB in 50% glycerol

10X TAE buffer: 0.4 M Tris acetate
0.01 M EDTA

2.3.10 Purification of DNA from agarose gel

Cut DNA was first loaded into an agarose gel to separate the DNA fragments by electrophoresis. The DNA fragment of interest was then excised from the agarose gel with a sharp scalpel. DNA extraction was performed with QIAquick Gel Extraction Kit (Quiagen) following the manufacturer's instructions. The DNA fragments were eluted in 30-50 µl ddH_2O.

2.3.11 DNA ligation

50 ng vector DNA was ligated with a 3- and 6-fold molar excess of insert DNA in the following conditions: 10X T4 DNA ligase buffer, 1 µl T4 DNA ligase (New England Biolabs, NEB) and ddH_2O up to 10 µl. The reactions were incubated overnight at 16°C, followed by transformation of the entire ligation reaction into *E. coli*.

2.3.12 Southern blotting

Southern blot analysis was employed to assess the number of *CIN8-3HA* constructs integrated in the genome after transformation. DNA was extracted from cells as described in section 2.3.6, digested with SalI and resolved on 0.8% agarose gels. The agarose gels were stained by incubation in 1X TAE added with 1X SybrSafe for 30 minutes to assess the electrophoretic run. The gels were then sequentially incubated for 30 minutes in a depurination solution, twice for 20 minutes in a denaturing solution, and twice for 20 minutes in a neutralizing solution. After each incubation, the gels were rinsed with ddH_2O. The DNA fragments were then transferred overnight to positively charged nylon membranes (Amersham Hybond-N+, GE Healthcare), using capillary blotting in 20X SSC buffer. The DNA was fixed to the membranes by UV crosslinking with the Stratalinker UV crosslinker. To detect the *CIN8-3HA* construct, a probe specific for *CIN8* was used. The probe was first prepared by PCR and then 32P-labeled with Prime-a-Gene labeling system (Promega) following the manufacturer's instructions, and finally purified with the illustra ProbeQuant G-50 Micro Columns (GE Healthcare). The membranes were first incubated in 50 ml pre-warmed PerfectHyb Plus Hybridization Buffer (Sigma) for 60 minutes at 65°C (pre-hybridization), and then overnight at 65°C in 25 ml new, pre-warmed PerfectHyb Plus Hybridization Buffer containing the 32P-labeled probe (hybridization). The membranes were then washed twice in 50 ml pre-warmed washing solution I for 30 minutes at 65°C and twice in 50 ml pre-warmed washing solution II for 30 minutes at 65°C. The membranes were thereafter dried, placed in a cassette and exposed to Amersham Hyperfilm ECL.

20X SSC:	3M NaCl
	0.3M Na citrate
	pH7.5
Depurination Solution:	0.25N HCl

Denaturing Solution:	0.5M NaOH
	1.5M NaCl
Neutralizing Solution:	1.5M NaCl
	1M Tris-HCl, pH 7.4
Washing Solution I:	2X SSC
	1% SDS
Washing Solution II:	0.2X SSC
	1% SDS

2.4 Protein-based procedures

2.4.1 Yeast protein extraction

10 ml of a cell culture at OD_{600} = 0.2-1 were collected and centrifuged for 2 minutes at maximum speed. The resulting pellet was washed with 1 ml cold 10 mM Tris-HCl pH 7.5, transferred to 2 ml Sarstedt tubes and frozen in liquid nitrogen in order to better preserve protein integrity. The pellet was then resuspended in 100 µl lysis buffer supplemented with complete protease inhibitor cocktail (Roche) and phosphatases inhibitors (60 mM β-glycerol phosphate, 0.1 mM Na orthovanadate, 5 mM NaF, and 15 mM p-Nitrophenylphosphate). An equal volume of acid-washed glass beads (Sigma) was added (leaving a layer of SN over the beads) and the tubes were subjected to 3-5 rounds of Fast Prep (speed 6.5 for 45 minutes) at 4°C in order to break the cells. Cell breakage was verified using an optical microscope. Lysed cells were transferred to a fresh tube. In order to quantify the protein content, 10 µl of the lysate were diluted 1:3 with cold 50 mM Tris-HCl pH 7,5 / 0,3 M NaCl and 3 µl were used in the Biorad protein quantification assay. The absorbance was read at λ = 595 nm. 50 µl 3X SDS blue loading buffer were then added to each sample. The samples were boiled at 95°C for 5 minutes, centrifuged at 13000 rpm for 3 minutes and the SN, containing the final protein extract, was collected in a new microcentrifuge tube. Extracts were stored at -20°C.

Lysis buffer:	50 mM Tris-HCl, pH 7.5
	1 mM EDTA, pH 8
	50 mM DTT
3X SDS blue loading buffer:	9% SDS, 30% glycerol
	0.05% bromophenol blue
	6% β-mercaptoethanol
	0.1875 M Tris-HCl, pH 6.8

2.4.2 Yeast protein extraction from TCA treated yeast cells

10 ml of a cell culture at OD_{600} = 0.2-1 were collected and centrifuged for 2 minutes at maximum speed. The resulting pellet was resuspended in an equal volume of ice-cold 5% trichloroacetic acid (TCA) and incubated for 10 minutes on ice. After centrifugation for 2 minutes at maximum speed at 4°C, the pellet was transferred with 1 ml 5% TCA to a 2 ml Sarstedt tube. The tube was centrifuged at 4°C and the SN was discarded. The pellet was frozen in liquid nitrogen in order to better preserve the protein integrity. The pellet was then washed with 1 ml absolute acetone and air-dried. The pellet was then resuspended in 100 µl lysis buffer (see section 2.4.1) supplemented with complete protease inhibitor cocktail (Roche) and phosphatases inhibitors (60 mM β-glycerol phosphate, 0.1 mM Na orthovanadate, 5 mM NaF, and 15 mM p-Nitrophenylphosphate). An equal volume of acid-washed glass beads (Sigma) was added (leaving a layer of SN over the beads) and the tubes were subjected to 3-5 rounds of Fast Prep (speed 6.5 for 45 minutes) at 4°C in order to break the cells. Cell breakage was verified using an optical microscope. 50 µl 3X SDS blue loading buffer (see section 2.4.1) were then added to each sample. The samples were thereafter boiled at 95°C for 5 minutes, centrifuged at 13000 rpm for 3 minutes and the SN, containing the final protein extract, was collected in a new microcentrifuge tube. Extracts were stored at -20°C.

2.4.3 Recombinant protein expression in yeast

2.4.3.1 Generation of centromeric plasmids carrying CIN8, cin8-4A or cin8-11A sequences

The coding sequence of the *CIN8* gene wild type and mutated in 4 and 11 putative Cdc5-consensus sites (*cin8-4A* and *cin8-11A*) were ordered from GenScript. The company sent these synthetic genes cloned with BamHI-SalI into pUC57 plasmids (called Mp1, Mp2 and Mp3, respectively). The *CIN8* wild type, *cin8-4A* and *cin8-11A* coding sequences were

excised from Mp1, Mp2 or Mp3 plasmid for cloning into the centromeric Rp173 plasmid (YCplac22) under the control of the endogenous *CIN8* promoter (841bp long). To this aim, the Mp1, Mp2 and Mp3 plasmids were cut with a double enzymatic digestion using both BamHI and SalI restriction enzymes. The fragments corresponding to *CIN8*, *cin8-4A* or *cin8-11A* coding sequences were cloned into the Rp173 plasmid to obtain Mp4, Mp5 and Mp6 plasmid, respectively. 841 bp of the endogenous *CIN8* promoter were amplified by PCR (as indicated in section 2.3.6) using as template the genome of a wild type W303 strain (Ry1), and PcinN_F and PcinN_R with the addition of KpnI and BamHI restriction sites. The promoter was cloned with KpnI-BamHI into Mp4, Mp5 or Mp6 plasmid to obtain Mp7, Mp8 and Mp9 plasmid, respectively. The Mp7, Mp8 or Mp9 plasmids were then transformed into the strain of interest.

Here below are reported the mutated sequences from the "start" codon ATG to the "stop" codon TAG of *cin8-4A cin8-11A*.

cin8-4A coding sequence:

ATGCCAGCGGAAAACCAAAATACGGGTCAAGATAGAAGCTCCAAC
AGCATCAGTAAAAATGGCAACTCTCAGGTTGGATGTCACACTGTTC
CTAATGAGGAACTGAACATC**GCT**GTAGCTGTGCGATGCAGAGGAA
GGAATGAAAGGGAAATT**GCT**ATGAAAAGCTCCGTTGTGGTAAATGT
TCCAGATATTACAGGTTCTAAAGAAATTGCCATTAACACGACGGGA
GATACCGGTATAACTGCTCAAATGAATGCCAAGAGATACACAGTGG
ACAAAGTCTTCGGTCCCGGCGCTTCCCAGGATCTAATTTTTGATGAA
GTGGCGGGCCCATTATTCCAGGATTTCATTAAAGGTTACAATTGCGC
CGTACTGGTATATGGTATGACGTCAACAGGTAAAACATATACAATG
ACGGGCGACGAAAAGTTATATAATGGTGAATTGAGCGATGCAGCAG
GAATTATACCGAGGGTTCTTTTGAAGTTGTTTGACACATTGGAACTA
CAACAGAACGATTACGTAGTAAAATGTTCGTTCATTGAACTCTACA
ACGAAGAATTGAAGGACCTCTTGGACAGCAATAGCAACGGCTCTAG
TAATACTGGCTTTGACGGCCAATTTATGAAAAAATTGAGGATTTTTG
ATTCAAGCACAGCAAATAATACCACTAGCAACAGTGCTAGTAGTTC
CAGGAGTAATTCTAGGAACAGTTCTCCGAGGTCATTAAATGATCTA
ACACCTAAAGCTGCTCTATTAAGAAAAAGGTTAAGGACAAAATCAC
TGCCGAATACCATCAAGCAACAGTATCAACAACAACAGGCAGTGAA
TTCCAGGAACAACTCTTCCTCTAACTCTGGCTCTACCACTAATAATG
CTTCTAGTAACACCAACACAAATAACGGTCAAAGAAGTTCGATGGC
TCCAAATGACCAAACTAATGGTATATACATCCAGAATTTGCAAGAA
TTTCACATAACAAATGCTATGGAGGGGCTAAACCTATTACAAAAAG
GCTTAAAGCATAGGCAAGTAGCGTCCACTAAAATGAACGATTTTTC

CAGTAGATCTCATACCATTTTTACAATCACTTTGTATAAGAAGCATC
AGGATGAACTATTTAGAATTTCCAAAATGAATCTTGTGGATTTAGCT
GGTTCAGAAAACATCAACAGATCCGGAGCATTAAATCAACGTGCCA
AAGAAGCTGGTTCAATCAACCAAGCTCTATTGACGCTGGGCAGGGT
CATAAACGCACTCGTAGATAAAAGCGGCCATATACCTTTCCGTGAA
TCGAAATTGACCCGCCTGCTTCAAGATGCCCTGGGTGGTAATACGA
AAACCGCACTAATTGCTACTATATCGCCTGCAAAGGTAACTTCTGA
AGAAACCTGCAGTACATTAGAGTATGCTTCGAAGGCTAAAAACATT
AAGAACAAGCCGCAACTGGGTTCATTTATAATGAAGGATATTTTGG
TTAAAAATATAGCTATGGAATTAGCAAAGATTAAATCCGATTTACT
CTCTACAAAGTCCAAAGAAGGAATATATATGAGCCAAGATCACTAC
AAAAATTTGAACAGTGATTTAGAAAGTTATAAAAATGAAGTTCAAG
AATGTAAAAGAGAAATTGAAAGTTTGACATCGAAAAATGCATTGCT
AGTAAAAGATAAATTGAAGTCAAAAGAAACTATTCAATCTCAAAAT
TGCCAAATAGAATCATTGAAAACTACCATAGATCATTTAAGGGCAC
AACTAGATAAACAGCATAAAACTGAAATTGAAATATCCGATTTTAA
TAACAAACTACAGAAGTTGACTGAGGTAATGCAAATGGCCCTACAT
GATTACAAAAAAAGAGAACTTGACCTTAATCAAAAGTTTGAAATGC
ATATTACTAAAGAAATTAAAAAATTGAAATCTACACTGTTTTTACAA
TTAAACACTATGCAACAGGAAGCTATTCTTCAAGAGACTAATATCC
AACCAAATCTTGATATGATCAAAAATGAAGTACTGACTCTTATGAG
AACCATGCAAGAAAAAGCTGAACTAATGTACAAAGACTGTGTGAA
GAAAATTTTAAACGAATCTCCTAAATTCTTCAATGTTGTTATTGAGA
AAATCGACATAATAAGAGTAGATTTCCAAAAATTTTATAAAAATAT
AGCCGAGAATCTTTCTGATATTAGCGAAGAAAATAACAACATGAAA
CAGTACTTAAAAAACCATTTTTTCAAGAATAACCATCAAGAATTACT
GAATCGTCATGTGGATTCT**GCT**TATGAAAATATTGAGAAGAGAACA
AACGAGTTTGTTGAGAACTTTAAAAAGGTCCTAAATGACCACCTTG
ACGAAAATAAAAAACTAATAATGCAGAATCTGACAACTGCAACCA
GCGCGGTTATTGATCAAGAAATGGATCTGTTTGAACCCAAGCGCGT
TAAATGGGAAAAT**GCA**TTTGATCTGATAAATGATTGTGACTCCATG
AATAACGAATTCTATAATAGCATGGCAGCGACGCTATCGCAAATCA
AGAGTACTGTTGATACATCATCAAATTCGATGAATGAGGCTATTTCA
GTCATGAAAGGACAAGTGGAAGAATCGGAGAACGCTATATCCCTTT
TGAAGAACAATACCAAATTTAATGATCAATTTGAGCAGCTTATTAA
CAAGCATAACATGTTGAAAGATAACATTAAAAATTCGATAACATCA
ACACACTCTCATATAACTAATGTGGATGATATCTATAATACGATTGA
AAACATAATGAAAAACTATGGTAACAAGGAAAACGCTACCAAAGA
CGAAATGATCGAGAACATATTGAAGGAAATACCAAATCTAAGTAAG
AAAATGCCGTTAAGGTTATCAAACATAAATAGCAATTCAGTGCAAA
GTGTAATATCGCCCAAAAAGCATGCAATTGAAGATGAAAACAAATC
CAGTGAAAATGTGGACAATGAGGGCTCGAGAAAAATGTTAAAGATT
GAATAG

- cin8-11A coding sequence:

ATGCCAGCGGAAAACCAAAATACGGGTCAAGATAGAAGCTCCAAC
AGCATCAGTAAAAATGGCAACTCTCAGGTTGGATGTCACACTGTTC
CTAATGAGGAACTGAACATC**GCT**GTAGCTGTGCGATGCAGAGGAA
GGAATGAAAGGGAAATT**GCT**ATGAAAAGCTCCGTTGTGGTAAATGT

TCCAGATATTACAGGTTCTAAAGAAATTGCCATTAACACGACGGGA
GATACCGGTATAACTGCTCAAATGAATGCCAAGAGATACACAGTGG
ACAAAGTCTTCGGTCCCGGCGCTTCCCAGGATCTAATTTTTGATGAA
GTGGCGGGCCCATTATTCCAGGATTTCATTAAAGGTTACAATTGCG
CCGTACTGGTATATGGTATGACGTCAACAGGTAAAACATATACAAT
GACGGGCGACGAAAAGTTATATAATGGTGAATTGAGCGATGCAGCA
GGAATTATACCGAGGGTTCTTTTGAAGTTGTTTGACACATTGGAACT
ACAACAGAACGATTACGTAGTAAAATGTTCGTTCATTGAACTCTAC
AACGAAGAATTGAAGGACCTCTTGGACAGCAATAGCAACGGCTCTA
GTAATACTGGCTTTGACGGCCAATTTATGAAAAAATTGAGGATTTTT
GATTCAAGCACAGCAAATAATACCACTAGCAACAGTGCTAGTAGTT
CCAGGAGTAATTCTAGGAACAGTTCTCCGAGGTCATTAAATGATCT
AACACCTAAAGCTGCTCTATTAAGAAAAAGGTTAAGGACAAAATCA
CTGCCGAATACCATCAAGCAACAGTATCAACAACAACAGGCAGTGA
ATTCCAGGAACAACTCTTCCTCTAACTCTGGCTCTACCACTAATAAT
GCTTCTAGTAACACCAACACAAATAACGGTCAAAGAAGTTCGATGG
CTCCAAATGACCAAACTAATGGTATATACATCCAGAATTTGCAAGA
ATTTCACATAACAAATGCTATGGAGGGGCTAAACCTATTACAAAAA
GGCTTAAAGCATAGGCAAGTAGCGTCCACTAAAATGAACGATTTTT
CCAGTAGATCTCATACCATTTTTACAATCACTTTGTATAAGAAGCAT
CAGGATGAACTATTTAGAATTTCCAAAATGAATCTTGTGGATTTAGC
TGGTTCAGAAAACATCAACAGATCCGGAGCATTAAATCAACGTGCC
AAAGAAGCTGGTTCAATCAACCAAGCTCTATTGACGCTGGGCAGGG
TCATAAACGCACTCGTAGATAAAAGCGGCCATATACCTTTCCGTGA
ATCGAAATTGACCCGCCTGCTTCAAGATGCCCTGGGTGGTAATACG
AAAACCGCACTAATTGCTACTATATCGCCTGCAAAGGTAACTTCTG
AAGAAACCTGCAGTACATTAGAGTATGCTTCGAAGGCTAAAAACAT
TAAGAACAAGCCGCAACTGGGTTCATTTATAATGAAGGATATTTTG
GTTAAAAATATAGCTATGGAATTAGCAAAGATTAAATCCGATTTAC
TCTCTACAAAGTCCAAAGAAGGAATATATATGAGCCAAGATCACTA
CAAAAATTTGAACAGTGATTTAGAAAGTTATAAAAATGAAGTTCAA
GAATGTAAAAGAGAAATTGAAAGTTTGACATCGAAAAATGCATTGC
TAGTAAAAGATAAATTGAAGTCAAAAGAAACTATTCAATCTCAAAA
TTGCCAAATAGAATCATTGAAAACTACCATAGATCATTTAAGGGCA
CAACTAGATAAACAGCATAAAACTGAAATTGAAATATCCGATTTTA
ATAACAAACTACAGAAGTTGACTGAGGTAATGCAAATGGCCCTACA
TGATTACAAAAAAAGAGAACTTGACCTTAATCAAAAGTTTGAAATG
CATATTACTAAAGAAATTAAAAAATTGAAATCTACACTGTTTTTACA
ATTAAACACTATGCAACAGGAAGCTATTCTTCAAGAGACTAATATC
CAACCAAATCTTGATATGATCAAAAATGAAGTACTGACTCTTATGA
GAACCATGCAAGAAAAAGCTGAACTAATGTACAAAGACTGTGTGA
AGAAAATTTTAAACGAATCTCCTAAATTCTTCAATGTTGTTATTGAG
AAAATCGACATAATAAGAGTAGATTTCCAAAAATTTTATAAAAATA
TAGCCGAGAATCTTTCTGATATTAGCGAAGAAAATAACAACATGAA
ACAGTACTTAAAAAACCATTTTTTCAAGAATAACCATCAAGAATTA
CTGAATCGTCATGTGGATTCTGCTTATGAAAATATTGAGAAGAGAA
CAAACGAGTTTGTTGAGAACTTTAAAAAGGTCCTAAATGACCACCT
TGACGAAAATAAAAAACTAATAATGCAGAATCTGACAACTGCAACC
AGCGCGGTTATTGATCAAGAAATGGATCTGTTTGAACCCAAGCGCG
TTAAATGGGAAAATGCATTTGATCTGATAAATGATTGTGACTCCAT
GAATAACGAATTCTATAATAGCATGGCAGCGACGCTATCGCAAATC
AAGAGTACTGTTGATACATCATCAAATTCGATGAATGAGGCTATTT
CAGTCATGAAAGGACAAGTGGAAGAATCGGAGAACGCTATATCCCT

TTTGAAGAACAATACCAAATTTAATGATCAATTTGAGCAGCTTATTA
ACAAGCATAACATGTTGAAAGATAACATTAAAAATTCGATAACATC
AACACACTCTCATATAACTAATGTGGATGATATCTATAATACGATTG
AAAACATAATGAAAAACTATGGTAACAAGGAAAACGCTACCAAAG
ACGAAATGATCGAGAACATATTGAAGGAAATACCAAATCTAAGTAA
GAAAATGCCGTTAAGGTTATCAAACATAAATAGCAATTCAGTGCAA
AGTGTAATATCGCCCAAAAAGCATGCAATTGAAGATGAAAACAAAT
CCAGTGAAAATGTGGACAATGAGGGCTCGAGAAAAATGTTAAAGA
TTGAATAG

2.4.3.2 Generation of centromeric plasmids carrying cin8-Motor-A or cin8-Tail-A sequences

For the creation of *cin8-Motor-A* (in which mutations fall into the motor domain) and *cin8-Tail-A* versions (in which mutations fall into the tail domain), a PstI enzymatic digestion of the centromeric plasmids containing the *CIN8* and *cin8-11A* genes was performed, and subsequently, the fragments obtained by cutting the different DNA fragment were ligated two-by-two to obtain the desired combinations. However, the PstI digestion did not allow us to clearly separate all the residues that fall into the motor from those present in the coil-tail domains and we obtained the following combinations:

- *cin8-6A* (T38A, S52A, S71A, T123A, S409A, S441A), which shows all the mutations in the phosphorylated sites that are in the motor domain except for T497A.

- *cin8-5A* (T497A, S564A, T761A, S820A, S859A), which presents all the mutations in the phosphorylated sites that are in the coil-tail domain, as well as the T497A mutation that falls into the motor domain.

The T497A mutation was successively reversed in *cin8-6A* and introduced into *cin8-5A* using the site-specific mutagenesis technique as described in section 2.3.8.2.

2.4.3.3 Generation of integrative plasmids carrying CIN8, cin8-S409A, cin8-S441A and cin8-2A

To generate the integrative plasmids, Rp173 plasmids Mp7, Cp7, Cp8, Cp9 containing *CIN8, cin8-S409A, cin8-S441A and cin8-2A* coding sequence, under the control of the endogenous *CIN8* promoter, were cut with a double enzymatic digestion using both KpnI and SalI. The fragments corresponding to *CIN8 cin8-S409A, cin8-S441A* and *cin8-2A* coding sequences were cloned into the Rp179 (YIplac204) plasmid to obtain Cp14, Cp15, Cp16 and Cp17 plasmids, respectively.

2.4.3.4 Generation of integrative plasmids carrying CIN8-3HA, cin8-S409A-3HA, cin8-S441A-3HA and cin8-2A-3HA

To insert the 3-HA tag at the C-terminus of the Cin8 sequences of interests, namely *CIN8, cin8-S409A, cin8-S441A and cin8-2A,* we designed overlapping oligos (FSM_55, FSM_56) bearing NotI-HindIII restriction sites on the ends and the 3-HA tag coding sequence between the restriction sites. The annealed oligos were directly cloned into the overhangs generated by restriction digest of NotI-HindIII sites of the Cp14, Cp15, Cp16 and Cp17 destination vectors to generate Cp16, Cp17, Cp18 and Cp19 plasmids, respectively.

2.4.4 Recombinant protein expression in *Baculovirus*

2.4.4.1 Generation of expression plasmids carrying CIN8-6HIS and cin8-2A-6HIS

To generate constructs for the Bac-to-Bac Baculovirus expression system (Thermo Fisher Scientific), we used the FSM_1 and FSM_18 oligos to amplify and concomitantly insert a 6-His tag to the coding sequence of both *CIN8* and *cin8-2A* from Mp7 and Cp9, using PCR. The resulting fragments were cloned in pFastBac vectors (Thermo Fisher Scientific), using BamHI-EcoRI sites. The recombinant plasmids obtained (Cp20 and Cp21) were confirmed by restriction enzyme digestion and sequencing.

2.4.4.2 Espression of Cin8-6His and cin8-2A-6His recombinant proteins

The crystallography unit in IEO produced all insect cell pellets according to the Bac-to-Bac Baculovirus expression system (Thermo Fischer Scientific), following the manufacturer's protocol.

2.4.4.3 Recombinant protein expression in E. Coli

Generation of the expression plasmids carrying *CIN8-MD-6HIS* and *cin8-2A-MD-6HIS*:

To generate truncated wild-type and 2A mutated constructs, we amplified the motor domain region (aa 1-485) from Mp7 and Cp9 using FSM_17 and FSM_15 oligos bearing NdeI and SalI restriction sites, respectively. A C-terminus 6-HIS tag was added by cloning the resulting fragments in a pET30a vector (Novagen) using NdeI-SalI sites generating the recombinant plasmids Cp22 and Cp23 that were then verified by sequencing.

2.4.4.4 Espression of Cin8-MD-6His and Cin8MD-2A-6His recombinant proteins

The expression plasmids Cp22 and Cp23 carrying *CIN8-MD-6HIS* and *cin8-MD-2A-6HIS* coding sequences were freshly transformed in Rosetta DE3 *E. coli* strain. Cells were inoculated in 10 ml LB and allowed to grow overnight at 37 °C. The day after, pre-cultures were diluted 1:500, grown at 37 °C, and the OD600 was monitored until it reached~0.6-0.8. Then, the temperature was lowered to 20°C and, once the bacterial broth was chilled, the protein expression was induced by adding 0.3 mM IPTG. The protein expression was allowed to proceed overnight. 16 hours after, the cells were harvested by centrifugation for 20 minutes at 5000g and washed in 30 ml 1X PBS. The harvested pellet was stored at -80 °C or further processed for protein purification.

2.4.5 His-tag protein purification

The cells pellet was resuspended in 25-30 ml ice cold Lysis Buffer. For insect cells, the presence of detergent is sufficient to induce the lysis. In the case of bacterial pellet, 1 mg/ml Lysozyme was added and after 30 minutes incubation on ice, the cells were lysed by sonication (6x30 seconds, 15 seconds rest, power 30%).

The lysate was clarified by centrifugation for 30-45 minutes. The supernatant was then incubated with Ni-NTA resin (previously equilibrated in lysis buffer, 1 ml slurry for 1l cultures) for at least 1 hour in the cold room and under very mild agitation.

The Ni-NTA resin was then harvested by centrifugation at 600 x*g* for 5 minutes. In order to clean the beads, the following washes were performed:

1x 10 bead volumes lysis buffer
2x 10 bead volumes washing buffer
1x 10 bead volumes lysis buffer

Finally, the beads were transferred to a disposable column (Thermo Fisher Scientific) and the elution was performed with 2-3 bead volumes of the Elution Buffer. The fractions were collected in a tube pre-filled with EDTA solution, in order to have 2 mM final EDTA in the eluate. The protein concentration and purity were evaluated by SDS-page gel separation. Selected fractions were pulled together, aliquoted, snap-frozen in liquid nitrogen and stored at -80°C.

Lysis buffer:	50 mM Hepes, pH 7.5
	300 mM NaCl
	2.5% glycerol
	EDTA 1 mM
	5 mM MgCl
	imidazole 20mM
	DNAase 1 ug/ml
	1 mM DTT
	protease inhibitors

Washing buffer: 50 mM Hepes, pH 7.5
500 mM NaCl
2.5% glycerol
EDTA 1 mM
5 mM MgCl
imidazole 30mM
1 mM DTT

Elution buffer: 50 mM Hepes, pH 7.5
150 mM NaCl
2.5% glycerol
EDTA 1 mM
5 mM MgCl
imidazole 250mM
1 mM DTT
protease inhibitors

2.4.6 SDS polyacrylamide gel electrophoresis

Appropriate amounts of proteins (50-100 μg of total extracts) were separated based on their molecular weight on 6%, 8% or 10% polyacrylamide gels. The gels were prepared from a 30% 30:0.8 acrylamide:bisacrylamide mixture (Sigma), 4X Separating buffer, 2X Stacking buffer and an appropriate amount of ddH_2O. As polymerization catalysis, ammonium persulphate (APS) and TEMED (BDH) were used. 1.5 mm thick polyacrylamide gels were run in 1X running buffer at 100-150 V for 2-3.5 hours.

4X Separating buffer: 1.5 M Tris base, bring to pH 8.8 with glacial acetic acid
0.4% SDS

2X Stacking buffer: 0.25 M Tris base, bring to pH 6.8 with glacial acetic acid
0.2% SDS

10X Running buffer: 2 M glycine
0.25 M Tris-HCl
0.02 M SDS
pH 8.3

2.4.7 Western blot hybridization

Proteins were transferred with the Trans-Blot Turbo Blotting System (BioRad), using the protocol for high molecular weight proteins. Ponceau S staining was used to roughly reveal the amount of proteins transferred onto the filters.

Membranes were blocked as follows:

- 1 hour at room temperature in 3% milk and 1X PBS-T for the anti-HA, anti-Myc, anti-Clb2, anti-Kar2, and anti-Pgk1 Western blots.
- 5 hours at room temperature in 5% ovalbumin and 1X PBS-T for the anti-Cdc5 Western blot.

After blocking, the membranes were incubated with the primary antibody as follows:

- 1:1000 mouse anti-HA (Covance), 1:1000 mouse anti-Myc (Covance, 9E10), 1:1000 rabbit anti-Clb2 (Santa Cruz), 1:200.000 rabbit anti-Kar2 (gifted from Dr. Kilmartin), 1:5000 mouse anti-Pgk1 (Invitrogen) diluted in 1% milk /1% BSA /1X PBS-T 1% or milk and 1% BSA / 1X TBS-T for 2 hours at RT or overnight at 4°C.
- 1:1000 goat anti-Cdc5 (Santa Cruz) diluted in 1% ovalbumin and 1X PBS-T overnight at 4°C.

The membranes were then washed 3 times for 5 minutes in 1X PBS-T or 1X TBS-T, after which they were incubated with the horseradish-peroxidase-conjugated secondary antibody as follows:

- 1:10.000 anti-mouse, 1:10.000 anti-rabbit in 1% milk and 1%BSA / 1X PBS-T for 1 hour.
- 1:5000 anti-goat in 1% ovalbumin and 1X PBS-T or 1X TBS-T for 1 hour.

After incubation with the secondary antibody, the membranes were washed 3 times for 15 minutes in 1X PBS-T or 1X TBS-T and the bound secondary antibody was revealed using ECL (Enhanced Chemiluminescence, Amersham) and imaged with Chemi Doc System (BioRad).

1X Transfer buffer:	0.2 M glycine
	0.025 M Tris base
	20% methanol
10X PBS buffer:	1.37 M NaCl
	27 mM KCl
	14.7 mM KH_2PO_4
	80 mM Na_2HPO_4
10X TBS buffer:	25mM Tris base
	150mM NaCl
	2 mM KCl
1X PBS-T buffer:	0.1% Tween
	1X PBS
1X TBS-T buffer:	0.1% Tween
	1X TBS

2.5 Cell biology procedures

2.5.1 Yeast tetrad dissection and analysis

MATa and *MATα* strains were mixed on solid medium, appropriate for the growth of both the haploids, and incubated overnight at permissive conditions. The next day, cells from the cross mixture were streaked to single colonies on selective medium and incubated at the appropriate temperature, allowing for selection of diploid cells. Single colonies grown under selective conditions were then amplified on rich media for 1 day. This step greatly increases the efficiency of sporulation. The following day, diploids were patched onto sporulation plates to induce sporulation by starvation. After 3-5 days, the diploids had efficiently sporulated and maturated and tetrads were dissected. In order to separate individual spores, the ascus was removed by enzymatic digestion. A toothpick full of tedrads was resuspended into the digestion mixture and incubated at 37°C for 3 minutes. Then, 1 ml ddH_2O was added to dilute the mixture and 20 µl of the mixture were dripped in a line onto the appropriate agar plate. Individual tetrads were dissected using the Nikon dissection microscope. The spores were left to grow at 23°C for 3-5 days. The colonies were plated in replicates onto selective media to define their genotype.

Digestion mixture: 198 µl ddH_2O
2 µl 10 mg/ml zymolase 100T (Seikagaka, Biobusiness)

Sporulation plates: 30 g K-Acetate
60 g Agar (DIFCO)
all amino acids at 1/4 of the normal concentration
up to 3 l with ddH_2O

2.5.2 Activation/inactivation of conditional mutants

2.5.2.1 Regulation of gene expression

To regulate the expression of specific proteins, yeast strains in which the encoding genes were cloned under the control of inducible promoters were used. The *PGAL1-10* promoter induces the expression at high levels of a downstream gene after the addition of galactose, while it shuts it off after the addition of glucose. To overexpress a gene of interest, 2% galactose was added at a specific time to cells growing in a media containing a poor carbon source such as raffinose.

2.5.2.2 Inactivation of temperature sensitive alleles

Temperature sensitive alleles were inactivated by shifting cells from a permissive (23°C) to a restrictive temperature (usually 37°C).

2.5.2.3 Inactivation of kinases with ATP-analogues

The *cdc5-as1* ATP-analogue sensitive allele was inactivated by the addition of 5μM CMK inhibitor (Accenda Tech; dissolved in DMSO) to the growth media.

2.5.3 Synchronization experiments

2.5.3.1 G1 phase arrest and release

Cells were grown overnight in the appropriate medium at 23°C in a water shaking bath. The following day, the cells were diluted to OD_{600} = 0.2 in fresh medium and left to grow for 2 hours. The cells were then diluted again to OD_{600} = 0.2 and added with 5 μg/ml α-mating factor synthetic peptide dissolved in ddH_2O (Primm). After 90 minutes incubation, 2.5 μg/ml α-factor was re-added to the culture. The G1 arrest was considered complete when more than 90% of the cells had shmoo, after which the cells were released from the G1 block. The α-factor was then washed out by filtration, using 5-10 volumes of medium

without the pheromone. The cells were then released into the appropriate fresh medium in the absence of the pheromone.

2.5.3.2 Nocodazole-mediated metaphase arrest

Cells were grown overnight in the appropriate medium at 23°C in a water shaking bath. The following day, the cells were diluted to OD_{600} = 0.2 in fresh medium and left to grow for 2 hours. The cells were then pre-synchronized in G1 by the addition of α-factor and then released in a medium containing 15 μg/ml nocodazole (NOC, Sigma) dissolved in DMSO. 7.5 μg/ml nocodazole was re-added to the culture after 90 minutes incubation. Once the arrest was complete, nocodazole was then washed out by filtration, using 5-10 volumes of medium containing 1% DMSO. The cells were then released into the appropriate fresh medium containing 1% DMSO.

2.5.4 Tubulin staining via *in situ* indirect immunofluorescence (IF)

1 ml of a cell culture at OD_{600} = 0.2-0.4 was collected by centrifugation for 1 minute at 13000 rpm at room temperature and incubated overnight at 4°C in 1 ml fixative solution. The cells were then pelleted and washed 3 times with 1 ml 0.1 M KPi pH 6.4, followed by a wash with 1 ml sorbitol-citrate solution. The cells were resuspended in 200 μl digestion solution and incubated at 35°C in order to enzymatically digest the cell wall, creating spheroplasts. Spheroplasts are osmotically fragile and lysed in a hypotonic solution; 1.2 M sorbitol maintains an isotonic environment in order to avoid cell lysis. The low pH helps slowing down the endogenous cell proteolytic activity. The digestion was assessed under an optical microscope by looking for burst spheroplasts when mixed with an equal volume of 1% SDS. When the digestion was complete, the spheroplasts were pelleted at 2000 rpm for 2 minutes and washed with 1 ml sorbitol-citrate solution. The pellet was then resuspended in an appropriate volume of sorbitol-citrate solution (10-50 μl, depending on the pellet size). 5 μl of the resuspended spheroplasts were then loaded on a 30-well slide

(ThermoScientific), previously coated with 0.1% polylysine (Sigma). To further fix the cells, the slide was then soaked in cold methanol for 3 minutes, followed by 10 seconds in cold acetone. Thereafter, the cells were incubated for 60-90 minutes in a humid dark incubation chamber with a rat anti-tubulin primary antibody (1:100 in PBS-BSA, Oxford-Biotechonology). After the incubation with the antibody, the cells were washed 5 times with PBS-BSA and incubated with a FITC-conjugated anti-rat secondary antibody (1:100 in PBS-BSA) for 60 minutes. The cells were then washed 5 times with PBS-BSA and then treated with a DAPI mounting solution. The slides were covered with a coverslip and sealed with nail polish. IF was analysis was performed with a Leica DMR HC BIOMED fluorescence microscope using a 100X immersion-oil objective.

0.1 M KPi buffer pH 6.4:	27.8 ml 1 M K_2HPO_4 72.2 ml 1 M KH_2PO_4 900 ml ddH_2O
Fixative solution:	3.7% formaldehyde in 0.1 M KPi, pH 6.4
Sorbitol-citrate 1.2 M:	17.4 g anhydrous KH_2PO_4 7 g citric acid 218.64 g sorbitol up to 1 l of ddH_2O
Digestion solution:	1.2 M sorbitol-citrate 10% glusulase 0.1 mg/ml zymolase 100T (Seikagaka Biobusiness)
PBS-BSA:	1% crude BSA (Sigma) 0.04 M K_2HPO_4 0.01 M KH_2PO_4 0.15 M NaCl 0.1% NaN_3

DAPI mount solution: 0.04 M K_2HPO_4
0.01 M KH_2PO_4
0.15 M NaCl
0.1% NaN_3
0.05 µg/ml DAPI
0.1% p-phenylenediamine
90% glycerol

2.5.5 Nuclei staining (DAPI staining)

1 ml of a cell culture at OD_{600} = 0.2-0.4 was collected by centrifugation and incubated for 10 minutes at room temperature in 1 ml 70% ETOH. The cells were pelleted and resuspended in 20 µl 0.001 mg/ml DAPI.

2.5.6 GFP-signals fixation

2 µl of a cell culture at OD_{600} = 0.2-0.4 were collected by centrifugation and then fixed via the addition of 100 µl paraformaldehyde (final concentration 2%). After 1.30 minute of incubation at room temperature, the cells were pelleted and washed twice with 500 µl 0.1 M K-phosphate buffer, pH 6.6, followed by resuspension in 500 µl 0.1 M K-phosphate buffer, pH 7.

0.1 M K-phosphate buffer pH 6.6: 62.5 ml 0.2 M mono-potassium salt
37.5 ml 0.2 M di-potassium salt

0.1 M K-phosphate buffer pH 7: 39 ml 0.2 M mono-potassium salt
61 ml 0.2 M di-potassium salt

0.2 M mono-potassium salt: 27.2 g KH_2PO_4
up to 1 l with ddH_2O

0.2 M di-potassium salt: 34.8 g K_2HPO_4
up to 1 l with ddH_2O

2.5.7 Scoring of indirect immunofluorescence samples

Cell cycle progression was scored by analyzing nulcear and spindle morphologies and dividing cells, using three categories:

1) Interphase cells (which includes cells in the G1, S and G2 phases of the cell cycle): these cells are typically unbudded (or cells with a small bud) with one nucleus, one single SPB (or two side-by-side SPBs) and 3-5 short cytoplasmic microtubules emanating from each SPB.

2) Metaphase cells: these cells are typically medium or large budded cells with an undivided nucleus closed to the bud-neck, two separated SPBs and a short and thick bipolar spindle.

3) Anaphase cells (including both anaphase and telophase cells): these cells are typically large budded cells with two nuclear masses (one in the mother cell and the other in the daughter cell), one SPB associated to each nucleus and an elongated spindle.

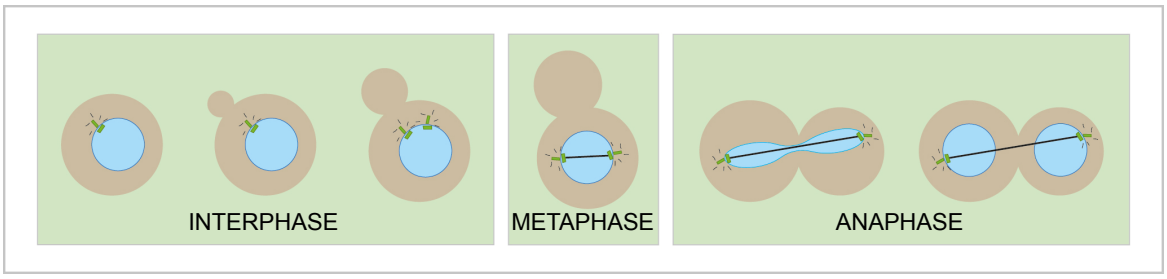

Figure 2.1 ***Cell morphological classification***
In yeast, cell cycle progression can be monitored by analyses of cell, nuclear and spindle morphologies.

2.5.8 Image acquisition and analysis

For spindle length measurements and nuclear morphology, representative images were acquired with a Leica DM6 B Multifluo microscope carrying a Hc Pl Apo 100X/1.40 oil objective and a Andor Zyla VSC-04470 sCMOS 16 bit camera using Las X software. The Fiji software was used to analyze the images. 100 cells were selected and analyzed from

each sample.

Fluorescence microscopy images were acquired with a Leica DM6 B Multifluo microscope carrying a Hc Pl Apo 100X/1.40 oil objective and a Andor Zyla VSC-04470 sCMOS 16 bit camera using Las X software with a z-stacks of 0.6 μm step from cells fixed as described in section 2.5.6. Stacks were deconvoluted by the Huygen program (Express deconvolution) and converted into maximal intensity projections using the Fiji software. No manipulations were performed other than adjustments in brightness and contrast.

2.5.9 Kinase assay

To be used in the kinase assay, Cdc5 and Cdc5-kinase dead mutant were purified by immunoprecipitation from yeast lysate. *CDC5* and *CDC5-KD* cells were arrested in metaphase as described in section 2.5.3.3. Cdc5 overexpression was induced in both strains by adding 2% galactose to the growth media. The cells were then harvested by 3 minutes centrifugation at 3000 rpm and the resulting pellet was transferred with 1 ml Tris-HCl pH 7.4 to a 2 ml Sarstedt tube. The tube was centrifuged at 4°C and the SN discarded. The pellet was frozen in liquid nitrogen in order to better preserve protein status. The pellet was then resuspended in 300 μl LLB lysis buffer. An equal volume of acid-washed glass beads (Sigma) was added (leaving a layer of SN over the beads) and the tubes were subjected to 3-5 rounds of Fast Prep (speed 6.5 for 45 minutes) at 4°C to break the cells. Cell breakage was verified under an optical microscope. The samples were centrifuged at maximum speed at 4°C for 30 minutes to clean up the extract. The SN was transferred to a new tube, leaving cellular debris on the bottom and the lipid layer on the top. In order to quantify the protein content, 10 μl of the lysate were diluted 1:3 with cold 50 mM Tris-HCl pH 7,5 / 0,3 M NaCl and 3 μl were used in the Biorad protein quantification assay. The absorbance was read at λ = 595 nm. 50 μl 3X SDS blue loading buffer was then added to each sample. Tipically, about 2 mg lysate (200 ug/reaction) were used for the immunoprecipitation (IP). A right volume of LLB buffer supplemented with HALT protease inhibitor cocktail

(Thermo Fisher Scientific) and phosphatases inhibitors (Roche) was added to each tube in order to perform the IP in the same condition (IP was usually performed in 250-300 ul). 25µl/mg lysate of slurry mouse Anti-HA Agarose beads (Thermo Fisher Scientific) were added to each sample and the samples were incubated on a rotating wheel for 3 hours at 4°C. After the incubation, the beads bound to the protein of interest were washed as follows:

2X 1ml of LLB with phosphatase/protease inhibitor
1X1ml of QA with phosphatase/protease inhibitor
1X 1ml of 5KB with phosphatase/protease inhibitor
2X in 1ml of KB with phosphatase/protease inhibitor

During each wash, samples were incubated for 1 minute at 4°C, centrifuged for 20 minutes at 13000 rpm at 4°C and the SN was removed.

Beads bound to the protein of interest were resuspended with 1ml KB buffer and incubated for at least 15 minutes at room temperature. The IP was then washed with 1 ml MOPS buffer and finally resuspended with 200 µl MOPS buffer.

2.5.9.1 Kinase assay sample preparation

Substrate proteins (previously quantified on gel) were diluted at the same concentration (0,5 µg/µl) in elution buffer. 5µg (10 µl) of substrate for each reaction were transferred in 1,5 ml tube. Radiolabelled γ-^{32}P-ATP was added to the kinase reaction mix and then aliquoted (15 ul/reaction) in the substrate tubes. Finally, the reaction was started by the addition of 10 µl immunoprecipitated Cdc5 or Cdc5-KD. The samples were incubated for 30 minutes at room temperature, tapping the tubes every 5 minutes to resuspend the beads. The reaction was then stopped with 8 µl 6X blue loading buffer and denaturated for 5 minutes at 95°C. The samples were spinned down at maximum speed and loaded on a 10% gel. The 1.5 mm thick polyacrylamide gel was run in 1X running buffer at 25mA for

1-2 hours. In order to fix the proteins, the gel was soaked in destaining solution for 20-30 minutes. The gel was stained with InstantBlue (Expedeon) for 15 minutes and then immersed for 10 minutes in 50% glycerole.

LLB buffer	HEPES 50mM (pH7.4 NaOH titratet)
	NP40 0.1%
	NaF 5mM
	2-glycerolphosphate 5mM
	MgCl2 1mM
	DTT 1mM
	KCl 75mM
	halt protease 1:100
	phosphatase Inhibitor 1:100
High-Salt QA buffer	Tris pH 7.6 20mM
	KCl final 250mM
	MgCl2 1mM
	DTT 1mM
	halt protease 1:100
	phosphatase inhibitor 1:100
5KB buffer	HEPES 50mM, Ph 7.4
	KAc 200mM
	MgCl2 10mM
	MnCl2 5mM
	DTT 1mM
	halt protease 1:100
	phosphatase inhibitor 1:100

KB buffer	HEPES 50mM, pH 7.4
	KAc 60mM
	MgCl2 10mM
	MnCl2 5mM
	halt protease 1:100
	phosphatase inhibitor 1:100
MOPS buffer:	MOPS 25 mM, pH 7.2
	MgCl2 15 mM
	EGTA 5 mM
	2-glycerophosphate 60 mM
	DTT 1mM
	halt protease 1:100
	phosphatase inhibitor 1:100
Kinase reaction mix:	MOPS buffer additioned with:
	0,18 mM ATP
	γ–^{32}P-ATP
Destaining solution:	75 ml acetic acid
	50 ml methanol
	875 ml ddH_2O

For mass spectrometry analysis, a similar protocol was used, omitting radioactive ATP addition in the reaction mixture. The samples were submitted for analysis to the Mass Spectrometry unit at the IFOM-IEO campus.

Table 2.1 Plasmid used in this study

Plasmid	Description	Origin
Cp12	Rp173 with *cin8- S424A* coding sequence cloned BamHI-SalI	This study
Cp13	Rp173 with *cin8- T75AS218A* coding sequence cloned BamHI-SalI	This study
Cp14	Rp179 with *CIN8* coding sequence cloned BamHI-SalI	This study
Cp15	Rp179 with *cin8- S409A* coding sequence cloned BamHI-SalI	This study
Cp15	Rp179 with *cin8- S441A* coding sequence cloned BamHI-SalI	This study
Cp15	Rp179 with *cin8-2A (S409AS441A)* coding sequence cloned BamHI-SalI	This study
Cp16	Rp179 with *CIN8-3HA* coding sequence cloned BamHI-SalI	This study
Cp17	Rp179 with *cin8- S409A-3HA* coding sequence cloned BamHI-SalI	This study
Cp18	Rp179 with *cin8- S441A-3HA* coding sequence cloned BamHI-SalI	This study
Cp19	Rp179 with *cin8-2A-3HA (S409AS441A)* coding sequence cloned BamHI-SalI	This study
Cp20	pFastBac *CIN8-6HIS* coding sequence cloned BamHI-EcoRI	*Baculovirus* expresssion
Cp21	pFastBac *cin8-2A-6HIS* coding sequence cloned BamHI- EcoRI	*Baculovirus* expresssion
Cp22	pET30a *CIN8-MD-6HIS*	*E.Coli* expresssion
Cp23	pET30a *cin8-2A-MD-6HIS*	*E.Coli* expresssion
Rp86	pFA6a-His3MX6	(Longtine, McKenzie et al. 1998)
Rp173	YCplac22	(Gietz R.D. et al., 1993)

Plasmid	Description	Origin
Mp1	pUC57 with WT *CIN8* coding sequence cloned BamHI-SalI	GenScript
Mp2	pUC57 with WT *cin8-4A* coding sequence cloned BamHI-SalI	Genscript
Mp3	pUC57 with *cin8-11A* coding sequence cloned BamHI-SalI	GenScript
Mp4	Rp173 with WT *CIN8* coding sequence cloned BamHI-SalI	This study
Mp5	Rp173 with *cin8-4A* coding sequence cloned BamHI-SalI	This study
Mp6	Rp173 with *cin8-11A* coding sequence cloned BamHI-SalI	This study
Mp7	Mp4 with 841bp CIN8 promoter cloned KpnI-BamHI	This study
Mp9	Mp6 with 841bp CIN8 promoter cloned KpnI-BamHI	This study
Cp1	Rp173 with *cin8-6A* coding sequence cloned BamHI-SalI	This study
Cp2	Rp173 with *cin8- 5A* coding sequence cloned BamHI-SalI	This study
Cp3	Rp173 with *cin8-Motor-A* (*T38A, S52A, S71A, T123A, S409A, S441A, T49A*) coding sequence cloned BamHI-SalI	This study
Cp4	Rp173 with *cin8-Tail A (S859AS820AT761AS564A*) coding sequence cloned BamHI-SalI	This study
Cp5	Rp173 with *cin8- T38A* coding sequence cloned BamHI-SalI	This study
Cp6	Rp173 with *cin8- T123A* coding sequence cloned BamHI-SalI	This study
Cp7	Rp173 with *cin8- S409A* coding sequence cloned BamHI-SalI	This study
Cp8	Rp173 with *cin8- S441A* coding sequence cloned BamHI-SalI	This study
Cp9	Rp173 with *cin8-S409AS441A* coding sequence cloned BamHI-SalI	This study
Cp10	Rp173 with *cin8- T412A* coding sequence cloned BamHI-SalI	This study
Cp11	Rp173 with *cin8- V421A* coding sequence cloned BamHI-SalI	This study

Table 2.2 Primers used in this study

Primer	Sequence (5'-3')	Purpose
T38A_F	GAGGAACTGAACATCGCTGTAGCTGTG CGATGCAGAGG	Mutagenesiss
T38A_R	CCTCTGCATCGCACAGCTACAGCGATGT TCAGTTCCTC	Mutagenesis
T123A_F	CATTAAAGGTTACAATTGCGCCGTACTG GTATATGGTATGACG	Mutagenesis
T123A_R	CGTCATACCATATACCAGTACGGCGCA ATTGTAACCTTTAATG	Mutagenesis
S409A_F	GCTGGTTCAATCAACCAAGCTCTATTGA CGCTGGGCAGGG	Mutagenesis
S409A_R	CCCTGCCCAGCGTCAATAGAGCTTGGTT GATTGAACCAGC	Mutagenesis
S441A_F	GCGGTTTTCGTATTACCACCCAGGGCAT CTTGAAGCAGGCGGG	Mutagenesis
S441A_R	CCCGCCTGCTTCAAGATGCCCTGGGTGG TAATACGAAAACCGC	Mutagenesis
T497A_F	GGTTAAAAATATAGCTATGGAATTAGC	Mutagenesis
T497A_R	GCTAATTCCATAGCTATATTTTTAACC	Mutagenesis
A497T_F	GGTTAAAAATATAACTATGGAATTAGC	Mutagenesis
A497T_R	GCTAATTCCATAGTTATATTTTTAACC	Mutagenesis
T75A_F	CCATTAACACGGCGGGAGATACCGG	Mutagenesis
T75A_R	CCGGTATCTCCCGCCGTGTTAATGG	Mutagenesis
S218A_F	GAGGATTTTTGATTCAGCCACAGCAAAT AATACCACTAGC	Mutagenesis
S218A_R	GCTAGTGGTATTATTTGCTGTGGCTGAA TCAAAAATCCTC	Mutagenesis
T224A_F	GCACAGCAAATAATACCGCTAGCAACA GTGCTAGTAGTTCC	Mutagenesis
T224A_R	GGAACTACTAGCACTGTTGCTAGCGGTA TTATTTGCTGTGC	Mutagenesis
3_F	GCCAGCGGAAAACCAAAATACGGG	Sequencing
273_F	GGACAAAGTCTTCGGTCCCGGC	Sequencing
748_F	GCTGCTCTATTAAGAAAAAGG	Sequencing/ Cin8 probe
1053_F	CGATTTTTCCAGTAGATCTCATACC	Sequencing
1394_F	GCAGTACATTAGAGTATGCTTCG	Sequencing
1824_F	GGTAATGCAAATGGCCCTACATG	Sequencing
2171_F	CCGAGAATCTTTCTGATATTAGCG	Sequencing
2355_F	CGAAAATAAAAAACTAATAATGC	Sequencing
2788_F	GGTAACAAGGAAAACGCTACC	Sequencing
478_R	GAACCCTCGGTATAATTCCTGC	Sequencing
923_R	GCCATCGAACTTCTTTGACCG	Sequencing

Primer	Sequence (5'-3')	Purpose
1759_R	CTAGTTGTGCCCTTAAATGATC	Sequecing/ Cin8 probe
2110_R	CATTGAAGAATTTAGGAGATTCG	Sequencing
2545_R	CAGTACTCTTGATTTGCGATAGCG	Sequencing
2731_R	GAGAGTGTGTTGATGTTATCG	Sequencing
3003_R	CTATTCAATCTTTAACATTTTTCTC	Sequencing
FSM_55	GGCCGCTACCCATACGATGTTCCTGACT ATGCGGGCTATCCCTATGACGTCCCGGA CTATGCAGGATCtTATCCATATGACGTTC CAGATTACGCTCCGTGA	3-HA tagging
FSM_56	AGCTTCACGGAGCGTAATCTGGAACGT CATATGGATAAGATCCTGCATAGTCCGG GACGTCATAGGGATAGCCCGCATAGTC AGGAACATCGTATGGGTAGC	3-HA tagging
FSM_15	CTAGGGTCGACTGAACCCAGTTGCGGCT T	CIN8-MD amplification
FSM_17	CGAACATATGCCAGCGGAAAACCAA	CIN8-MD amplification
PcinN_F	CGCCGGTACCTCAATGGCTTCCCC	*CIN8* promoter amplification (841bp)
PcinN_R	CGGCGGATCCCAAACAAATTCTTTCTTG TTGTATTTTTTGCGC	*CIN8* promoter amplification (841bp)
F4 pGAL	CTCGTTCAGAGCTTAAATTGGAAAGTAC GTCAAAACGTTTTTTAGGCAGAATTCGA GCTCGTTTAAAC	pGAL-DYN1-3HA introduction
R3 pGAL 3-HA	AACAAATTCTATCAGCTCATTAGCAAGT CTTGCCTCATTCTTGCACATGCACTGAG CAGCGTAATCTG	pGAL-DYN1-3HA introduction
Cc dyn F	CCCGAATTGATGCGCGGAAGGTCGC	Check pGAL-DYN1-3HA introduction
Cc dyn R	CGTGTCGAACTCTCTCCCATCCAATAAT CCC	Check pGAL-DYN1-3HA introduction

Table 2.3 Bacterial strains used in this study

Strain	Genotype
TOP10 *E. Coli*	F- mcrA Δ(mrr-hsdRMS-mcrBC) φ80lacZΔM15 ΔlacX74 nupG recA1 araD139 *E. coli* Δ(ara-leu)7697 galE15 galK16 rpsL(StrR) endA1 λ
Rosetta DE3 *E.Coli*	B F^- ompT gal dcm lon $hsdS_B(r_B^-m_B^-)$ λ (DE3 [lacI lacUV5-T7p07 ind1 sam7 nin5]) $[malB^+]_{K-12}(\lambda^S)$

Table 2.4 Yeast strains used in this study

Strain (Ry)	Genotype	Origin
1	*MATa, ade2-1, leu2-3, ura3, trp1-1, his3-11,15, can1-100, GAL, psi+*	Visintin lab
72	*MATa* (mating type tester)	Fink lab
73	*MAT* ✔ (mating type tester)	Fink lab
1574	*MATa, cdc14-1, ade2-1, leu2-3, ura3, trp1-1, his3-11,15, can1-100, GAL, psi+,*	Visintin lab
1602	*MATa, cdc14-1, cdc5-as1(L158G)*	Visintin lab
2446	*MATa, ade2-1, leu2-3, ura3, trp1-1, his3-11,15, can1-100, GAL, psi+, cdc5L158G*	Visintin lab
2725	*Ry 2725 MATa, cdc14-1, cdc5L158G, PDS1-HA -LEU2::pds1, SCC1myc18::TRP1*	Visintin Lab
4124	*MATa, ade2-1, leu2-3, ura3, trp1-1, his3-11,15, can1-100, GAL,psi+, cin8::cin8-F456A-3HA-LEU2*	Visintin Lab
4126	*MATa, cdc14-1, cin8::CIN8(F467A)-3HA::LEU2*	Visintin Lab
4128	*MATa, cdc14-1, cdc5-as1(L158G), cin8::CIN8(F467A)-3HA::LEU2*	Visintin Lab
4130	*MATa, cdc5-as1(L158G), cin8::CIN8(F467A)-3HA::LEU2*	Visintin Lab
4573	*MATa, cdc14-1, cdc5-as1(L158G), pGAL-3HA-STU2::KanMX6*	Visintin Lab
4596	*MATa, cdc14-1, cdc5-as1(L158G), pGAL-CIN8::TRP1*	Visintin Lab
4640	*MATa, cdc14-1, cdc5-as1(L158G), pGAL-3HA-KIP1::KanMX6*	Visintin Lab
4700	*MATa, cdc14-1, cdc5-as1(L158G), dyn1::URA3*	This thesis
4703	*MATa, cdc14-1, dyn1::URA3*	This thesis
4706	*MATa, cdc5-as1(L158G), dyn1::URA3*	This thesis
4997	*MATa, cin8::URA3*	Visintin lab

Strain (Ry)	Genotype	Origin
5005	*MATa, cin8::URA3, cin8-11A(S52A, S71A, S761A, S820A,+T38A,T123A, S409A, S441A, T497A, S654A, S859A) CEN-TRP1*	This thesis
5014	*MATa, cdc14-1, cin8::URA3*	Visintin lab
5028	*MATa, cin8::URA3, , cin8-Tail-A (S654A, S761A, S820A, S859A) CEN-TRP1*	This thesis
5029	*MATa, cin8::URA3, cin8-Motor-A (T38A,S52A, S71A, T123A, S409A*	This thesis
5030	*MATa, cdc14-1, cin8::URA3, CIN8-CEN-TRP1*	This thesis
5032	*MATa, cdc14-1, cin8::URA3, cin8-Tail-A (S654A, S761A, S820A, S859A) CEN-TRP1*	This thesis
5033	*MATa, cdc14-1 cin8::URA3, cin8-Motor-A (T38A,S52A, S71A, T123A, S409A, S441A,T497A) CEN-TRP1*	This thesis
5109	*MATa, cin8::URA3, cin8-S441A CEN-TRP1*	This thesis
5111	*MATa, cdc14-1, cin8::URA3, cin8-S441A CEN-TRP1*	This thesis
5140	*MATa, cdc14-1, cin8::URA3, cin8-S409A CEN-TRP1*	This thesis
5141	*MATa, cdc14-1, cin8::URA3, cin8-S409AS441A CEN-TRP1*	This thesis
5142	*MATa, cin8::URA3, cin8-S409A CEN-TRP1*	This thesis
5143	*MATa, cin8::URA3, cin8-S409AS441A CEN-TRP1*	This thesis
5567	*MATa, ade2-1, leu2-3, ura3, trp1-1, his3-11,15, can1-100, GAL,psi+, cin8::URA3, cin8-T412A-CEN-TRP1*	This thesis
5568	*MATa, ade2-1, leu2-3, ura3, trp1-1, his3-11,15, can1-100, GAL,psi+, cin8::URA3, cin8-V421A-CEN-TRP1*	This thesis
5569	*MATa, ade2-1, leu2-3, ura3, trp1-1, his3-11,15, can1-100, GAL,psi+, cin8::URA3, cin8-S424A-CEN-TRP1*	This thesis
5570	*MATa, cdc14-1, ade2-1, leu2-3, ura3, trp1-1, his3-11,15, can1-100, GAL,psi+, cin8::URA3, cin8-T412A-CEN-TRP1*	This thesis
5571	*MATa, cdc14-1, ade2-1, leu2-3, ura3, trp1-1, his3-11,15, can1-100, GAL,psi+, cin8::URA3, cin8-V421A-CEN-TRP1*	This thesis
5572	*MATa, cdc14-1, ade2-1, leu2-3, ura3, trp1-1, his3-11,15, can1-100, GAL,psi+, cin8::URA3, cin8-S424A-CEN-TRP1*	This thesis

Strain (Ry)	Genotype	Origin
6567	*MATa , ade2-1, leu2-3, ura3, trp1-1, his3-11,15, can1-100, GAL,psi+, cdc14-1 scc1::SCC1-GFP-KanMX6 Spc110-mcherry::hphMX3 cin8::cin8-F456A-3HA-LEU2*	This thesis
6571	*MATa, ade2-1, leu2-3, ura3, trp1-1, his3-11,15, can1-100, GAL,psi+, scc1::SCC1-GFP-KanMX6 Spc110-mcherry::hphMX3 cdc5-as1 (L158G) cin8::cin8-F456A-3HA-LEU2*	This thesis
6572	*MATa , ade2-1, leu2-3, ura3, trp1-1, his3-11,15, can1-100, GAL,psi+, scc1::SCC1-GFP-KanMX6 Spc110-mcherry::hphMX3 cin8::cin8-F456A-3HA-LEU2*	This thesis
7684	*MATa , ade2-1, leu2-3, ura3, trp1-1, his3-11,15, can1-100, GAL,psi+, cdc14-1 cdc5-as1 (L158G) dyn1::pGAL-3HA-DYN1::Kan-MX6*	This thesis
7809	*MATa, , ade2-1, leu2-3, ura3, trp1-1, his3-11,15, can1-100, GAL,psi+, cdc14-1, cin8::cin8-F456A-3HA-LEU2, psi+ PDS1-HA -LEU2::pds1, SCC1myc18::TRP1*	This thesis
7811	*MATa, cin8::cin8-F456A-3HA-LEU2, psi+ PDS1-HA -LEU2::pds1, SCC1myc18::TRP1*	This thesis
7868	*MATa, ade2-1, leu2-3, ura3, trp1-1, his3-11,15, can1-100, GAL,psi+, cdc14-1, cdc5L158G, cin8::cin8-F456A-3HA-LEU2, psi+ PDS1-HA -LEU2::pds1, SCC1myc18::TRP1*	This thesis
7897	*MATa, ade2-1, leu2-3, ura3, trp1-1, his3-11,15, can1-100, GAL,psi+, cdc14-1, cdc5L158G, ura::GAL-3Myc-CDC5::URA3, cin8::URA3, trp1::CIN8-3HA::TRP1*	This thesis
7917	*MATa, , ade2-1, leu2-3, ura3, trp1-1, his3-11,15, can1-100, GAL,psi+, cdc5L158G, cin8::cin8-F456A-3HA-LEU2, psi+ PDS1-HA -LEU2::pds1, SCC1myc18::TRP1*	This thesis
7928	*MATa, ade2-1, leu2-3, ura3, trp1-1, his3-11,15, can1-100, GAL,psi+, cdc14-1, cin8:: URA3, cin8-2A-3HA-TRP1, psi+, SCC1myc13::KAN*	This thesis
7929	*MATa, ade2-1, leu2-3, ura3, trp1-1, his3-11,15, can1-100, GAL,psi+, cdc14-1, cin8:: URA3, cin8-S409A-3HA-TRP1, psi+, SCC1myc13::KAN*	This thesis

Strain (Ry)	Genotype	Origin
7931	*MATa, ade2-1, leu2-3, ura3, trp1-1, his3-11,15, can1-100, GAL,psi+, cdc14-1, cin8:: URA3, cin8-S441A-3HA-TRP1, psi+, SCC1myc13::KAN*	This thesis
8028	*MATa, ade2-1, leu2-3, ura3, trp1-1, his3-11,15, can1-100, GAL,psi+, cdc14-1, cdc5L158G, ura::GAL-3Myc- CDC5::URA3, cin8::URA3, trp1::cin8-S409AS441A-3HA::TRP1*	This thesis
8042	*MATa, ade2-1, leu2-3, ura3, trp1-1, his3-11,15, can1-100, GAL,psi+, cdc14-1, cdc5L158G, ura::GAL-3Myc- CDC5::URA3, cin8::URA3, trp1::cin8-S409A-3HA::TRP1*	This thesis
8084	*MATa, ade2-1, leu2-3, ura3, trp1-1, his3-11,15, can1-100, GAL,psi+, cdc14-1, cdc5L158G, ura::GAL-3Myc- CDC5::URA3, cin8::URA3, trp1::cin8-S441A-3HA::TRP1*	This thesis

3 Results

The combination of the loss of function alleles of the Cdc5 kinase and the Cdc14 phosphatase (*cdc5 cdc14*) results in cell cycle arrest in *mini-anaphase*, namely after cohesin cleavage but before chromosome segregation (Roccuzzo *et al.*, 2015). Indeed, although cohesin is properly cleaved and, hence, the cells have passed through the metaphase to anaphase transition, *cdc5 cdc14* cells retain at their terminal arrest a short bipolar spindle with a length of 2-4 μm, typical of metaphase cells. Previous work from our laboratory established that anaphase spindle elongation represents the primary defect of the double mutant phenotype. This observation suggests that, after cohesin cleavage, an active mechanism controlled by Cdc5 and Cdc14 is required to segregate chromosomes. Thus, the main aim of this work is to understand the molecular mechanism by which the two proteins drive anaphase spindle elongation.

3.1 The motor protein Cin8 is a key target of the Cdc14-Cdc5 pathway controlling anaphase spindle elongation

The *cdc14 cdc5* impairment in anaphase spindle elongation could reflect defects in the regulation of microtubule motors and/or of microtubule-associated proteins (MAPs).

In yeast, the spindle elongates in anaphase as a result of the pushing force generated at the midzone by the interpolar microtubules, stabilized by the MAP Stu2 (Severin *et al.*, 2001) and slid by the two members of the Kinesin-5 family: Cin8 and Kip1 (M Andrew Hoyt *et al.*, 1992) (Gardner *et al.*, 2009).

In order to identify novel components and/or targets of the spindle elongation pathway controlled by Cdc14 and Cdc5, we began by testing the consequences of the overexpression of motor proteins and MAPs, known to be required for this process.

To test the hypothesis that behind the spindle elongation defect of *cdc5 cdc14* cells **(Figure 3.1A)** there is a mis-regulation of kinesins-5 activities and/or of the MAP Stu2, we asked whether ectopic expression of the proteins, thus increasing their levels, would rescue the spindle elongation defects of *cdc5 cdc14* double mutant cells. To overexpress Cin8, Kip1 and Stu2 proteins, we placed the encoding genes under the galactose inducible promoter *GAL1-10.* The fusion constructs were then introduced in the *cdc5 cdc14* background. For the experiment, *cdc5-as1, cdc14-1, cdc5-as1 cdc14-1, cdc5-as1 cdc14-1 pGAL-CIN8* and *cdc5-as1 cdc14-1 pGAL-KIP1* cells were arrested in G1 phase in raffinose-containing media. When about 90% of the cells reached the arrest, the cells were synchronously released into the next cell cycle in galactose-containing cell growth medium, to induce the overexpression of the proteins, in the presence of the CMK inhibitor and incubated at 37°C to inactivate *cdc5-as1* and *cdc14-1* mutants, respectively (**Figure 3.1 A and C**). Since *STU2* is an essential gene, to avoid the lethal phenotype of *stu2Δ* cells, *cdc5-as1 cdc14-1 pGAL-STU2* cells were grown in growth media supplemented with galactose throughout

the entire experiment (**Figure 3.1B**). After the release of the cells, cycle progression was assessed by scoring for the presence of metaphase and anaphase spindles. To properly evaluate the contribution of Stu2, Cin8 and Kip1 proteins in anaphase spindle elongation, starting from the establishment of a bipolar spindle (120 minutes from the cell release, corresponding to metaphase), we measured spindle length every 30 minutes for four hours. We found that neither the overexpression of Kip1 nor of Stu2 rescues the spindle elongation defect of *cdc14 cdc5* double mutant cells, suggesting that the two proteins are not components of the Cdc14-Cdc5 pathway (**Figure 3.1**). On the contrary, enhancement of the levels of *CIN8* allowed the majority of *cdc14 cdc5* cells to divide their nuclei and to elongate their spindles. Indeed, about 60% of the cells reached a spindle length greater than 4 μm (corresponding to early anaphase), of which 40% had a spindle length between 4-6 μm and about 20% had spindles that were more than 6 μm long (**Figure 3.1C-D**). The observation that high levels of the conserved kinesin-5 Cin8 were sufficient to allow spindle elongation and nuclear division in the *cdc14 cdc5* double mutant indicates that Cin8 may act downstream of or in parallel with one or both enzymes.

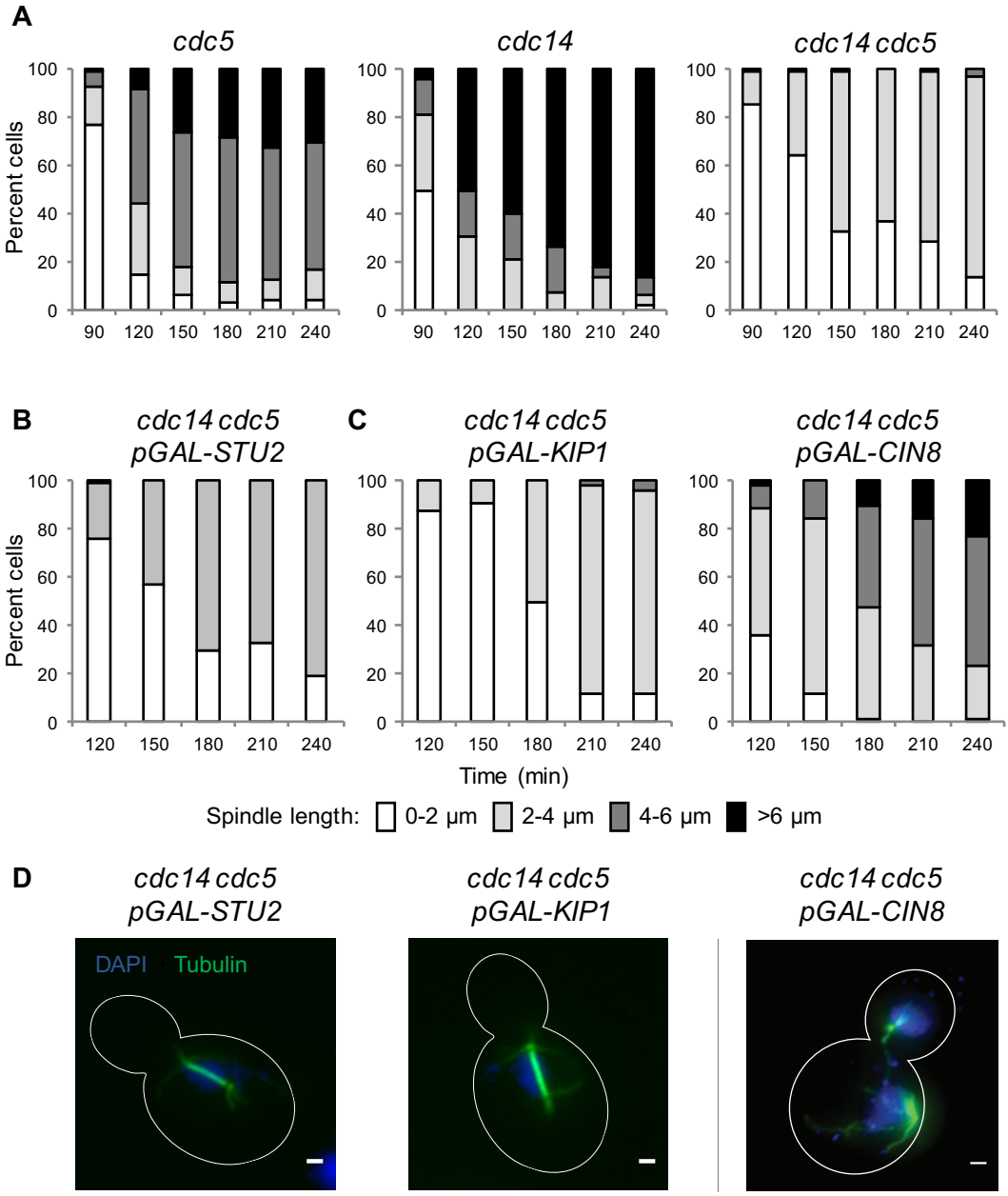

Figure 3.1: The motor protein Cin8 is a key target of the Cdc14-Cdc5 pathway controlling anaphase spindle elongation

Cells were arrested in G1 phase and synchronously released into the next cell cycle. The spindles length was determined for 100 cells from 120 minutes to 240 minutes; spindle length distribution is shown in histogram graphs, indicated as different shades of grey. (A) cdc5-as1 (Ry 2446), cdc14-1 (Ry 1574) and cdc14-1 cdc5-as1 (Ry 1602) cells. (B) cdc14-1 cdc5-as1 pGAL-STU2 cells (Ry 4573). (C) cdc14-1 cdc5-as1 pGAL-KIP1 (Ry 4640) and cdc14-1 cdc5-as1 pGAL-CIN8 cells (Ry 4596).

(D) Representative images of cdc14-1 cdc5-as1 pGAL-STU2, cdc14-1 cdc5-as1 pGAL-KIP1 and cdc14-1 cdc5-as1 pGAL-CIN8 cells at the terminal phenotype (240 minutes) are shown.

Blue: DAPI; green: tubulin. Bars: 2 µm.

3.2 Modulating dynein 1 levels does not rescue the spindle elongation defect of *cdc5 cdc14* cells

In several organisms, besides the pushing force generated at the midzone by the interpolar microtubules, a pulling force exerted by the dynein motor at the cell cortex is also required for proper anaphase spindle elongation. The relevance of this pulling force varies among organisms and in yeast it seems to be dispensable during a wild type anaphase spindle elongation (Sullivan and Huffaker, 1992). Since it was observed that combining the deletion of the *DYN1* gene, *dyn1Δ*, with a mutant of Cin8, *cin8-3* (Gheber, Kuo and Hoyt, 1999), which affects its microtubule binding, resulted in cells defective in the slow phase of anaphase spindle elongation (M A Hoyt *et al.*, 1992b) (Saunders *et al.*, 1995) (Gerson-Gurwitz *et al.*, 2009), we wondered whether the contribution of Dyn1 to spindle elongation may become essential in cells defective for other motors. If true, this hypothesis would imply that dynein-mediated pulling force could compensate for the absence of the pushing force applied by kinesins at the midzone. To test this possibility, we modulated dynein levels, both by raising and lowering its expression levels, in the *cdc5* and *cdc14* single and double mutant backgrounds.

In yeast, Dyn1 is the sole member of the dynein family and it localizes at the cell cortex by associating with dynactin and binds astral microtubules, hence the connected spindle pole bodies (SPBs) (Yeh *et al.*, 1995), thereby guiding spindle and nuclear positioning. To overexpress dynein 1, we cloned the *DYN1* gene under the control of the galactose inducible promoter *GAL1-10*. For the experiment, *cdc5-as1 cdc14-1* and *cdc5-as1 cdc14-1 pGAL-DYN1* cells were arrested in G1 phase and in metaphase in raffinose-containing cell growth medium. When about 90% of the cells reached the arrests, as assessed by looking at nuclear morphology, the cells were synchronously released into the next cell cycle in restrictive conditions for both Cdc14-1 and Cdc5-as1 mutant proteins. At the time of cell

release, each of the arrested culture (G1 and metaphase) was split into two: to one half, galactose was added at the time of release, and to the other half, galactose was added once *cdc5 cdc14* cells reached their terminal phenotype, (about 210 minutes after the cell release). Cell cycle progression and spindle elongation were assessed by measuring spindle length every 30 minutes for three hours after the induction. We found that, in all conditions tested, the overexpression of *DYN1* does not rescue the spindle elongation defect of the *cdc5 cdc14* double mutant cells, which retain a spindle length of 2-4 µm at their terminal arrest (**Figure 3.2** and data not shown).

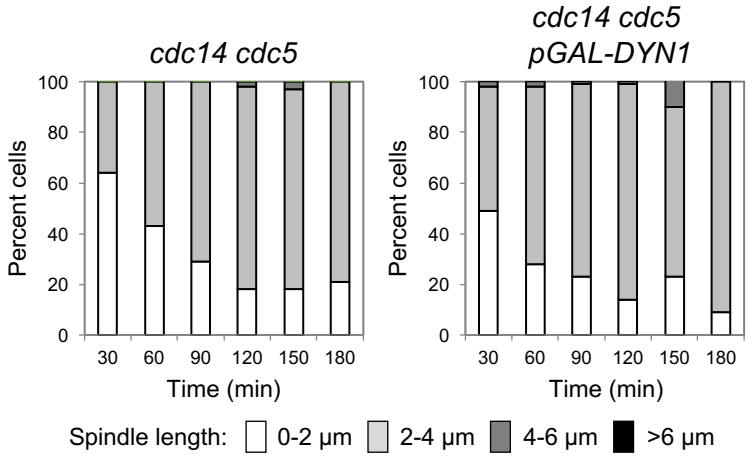

Figure 3.2: Dyn1 overexpression does not affect cdc5 cdc14 spindle elongation defect
cdc14-1 cdc5-as1 (Ry 1602) and cdc5-as1 cdc14-1 PGAL-DYN1 (Ry 7684) cells were arrested in G1 phase in YPR cell growth medium at 23°C and then synchronously released into the next cell cycle in YPR supplemented with 2% galactose to induce Dyn1 overexpression and in presence of the CMK inhibitor at 37°C to inactivate cdc5-as1 and cdc14-1.
Samples were collected every 30 minutes after galactose induction up to 3 hours. The spindle length was determined for 100 cells. Spindle length distribution is shown in histogram graphs, indicated as different shades of grey.

Viceversa, to evaluate whether the absence of Dyn1 activity impacts on the spindle elongation dynamics of our mutants, *cdc5-as1, cdc14-1 and cdc5-as1 cdc14-1* cells deleted in *DYN1* (*dyn1Δ*) were arrested in G1 phase and synchronously released into the next cell cycle in conditions restrictive for both Cdc14-1 and Cdc5-as1 mutant proteins (**Figure**

3.3). We found that the lack of dynein 1 does not alter the spindle elongation kinetics of either the single or the double *cdc14 cdc5* mutants. Taken together, these results suggest that Dyn1 is not a component/target of the Cdc14-Cdc5 pathway.

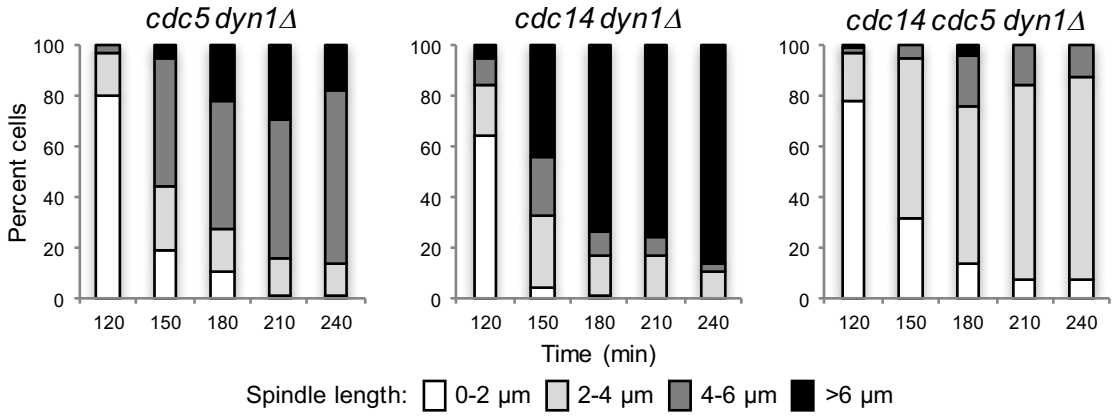

Figure 3.3: DYN1 deletion does not affect cdc5, cdc14 or cdc14 cdc5 terminal phenotypes
cdc5-as1 dyn1Δ (Ry 4706), cdc14-1 dyn1Δ (Ry 4703) and cdc14-1 cdc5-as1 dyn1Δ (Ry 4700) cells were arrested in G1 phase by adding α-factor in YEPD cell growth medium at 23°C and the cells were then released at 37°C in YEPD cell growth medium lacking the pheromone, but supplemented with the CMK inhibitor to inactivate cdc14-1 and cdc5-as1. Cells were collected and the spindle length was determined for 100 cells at the indicated time points. Spindle length distribution is shown in histogram graphs, indicated as different shades of grey.

3.3 *cdc14 cin8-F429(467)A* cells arrest with short bipolar spindles

Our data highlight Cin8 as an essential target of the Cdc5-Cdc14 spindle elongation pathway. Cin8 is a known substrate for Cdc14 (R. Avunie-Masala *et al.*, 2011). Cdc14 removes CDK-mediated phosphorylation on residues S239, T247 and S455 in Cin8 and this dephosphorylation is required for proper Cin8 localization to the spindle midzone (Goldstein *et al.*, 2017). Consistent with this role of Cdc14 in the regulation of Cin8 localization, introducing the *cin8-3^{CDK}A* allele into the *cdc14 cdc5* double mutant background rescues the spindle elongation defect of this strain (Roccuzzo *et al.*, 2015).

Several observations prompted us to test whether the motor protein could also be a target of the Cdc5 branch. Namely, i) a role for Plk1 (orthologue of Cdc5) in the regulation of Eg5 (orthologue of Cin8) has been proposed in centrosome separation in human cells, where both Plk1 and Cdk1/2 trigger Eg5 centrosome localization (Smith *et al.*, 2011). However, while Cdk1/2 regulate this process by phosphorylating Eg5 C-terminal domain (Thr927) and promoting the kinesin-5 binding on MTs, a direct role for Plk1 regulation of Eg5 has not been observed yet; ii) the polo-like kinase is known to be necessary for spindle elongation in vertebrate cells (Brennan *et al.*, 2007a) and to bind several spindle proteins, including kinesins in yeast (Snead *et al.*, 2007), and, finally, iii) Eg5 was identified as a Plk1 substrate in a proteomic study of the early mitotic spindle (Santamaria *et al.*, 2011).

To assess if Cin8 belongs also to the Cdc5 branch of the Cdc14-Cdc5 spindle elongation pathway, we performed a genetic epistasis analysis by combining allelic variants of Cin8 with *cdc14*, *cdc5* and *cdc14 cdc5* mutants. We reasoned that, if Cin8 belongs also to the Cdc5 branch of the pathway, then at least one of its alleles in combination with the *cdc14-1* mutation should lead to cells arresting with short "metaphase-like" bipolar spindles and recapitulate the mini-anaphase phenotype typical of *cdc14 cdc5* cells. In this analysis, we included also the double mutant to assess whether in the so far named Cdc14-Cdc5 pathway a third branch including Cin8 would exist.

Available Cin8 mutants that impair or weaken the kinesin activity include: *i) cin8Δ, ii) cin8-3^{CDK}D,* in which the three CDK sites are mutated into aspartic acid (phospho-mimetic), and *iii) cin8-F429(467)A* (Movshovich *et al.*, 2008), in which a mutation within the motor domain weakens the interaction between the kinesin and the spindle microtubules. Knowing that, besides its role in spindle elongation, Cin8 is also involved in spindle pole body (SPB) separation (Lim, Goh and Surana, 1996) and bipolar spindle formation (Mark Winey and Bloom, 2012), we tested cell cycle progression in the mutants of interest both at permissive and restrictive temperatures. We found that while *cin8-F429(467)A* mutant cells grew like wild type at all of the temperatures tested (**Figure 3.4**),

in agreement with what is reported in the literature, both *cin8Δ* and *cin8-3^{CDK}D* mutants died at 37°C with mono-astral spindles due to defects in SPBs separation.

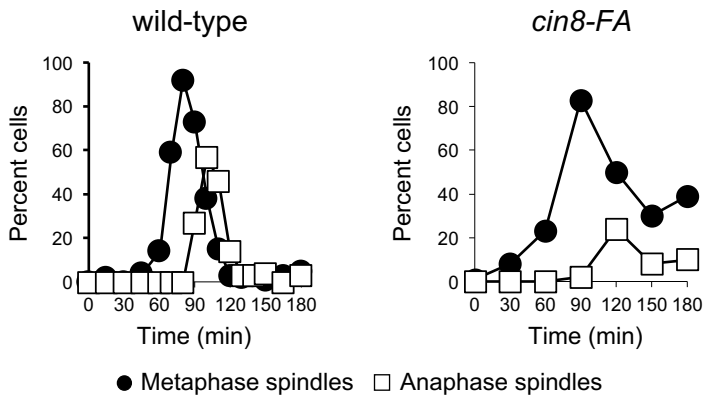

Figure 3.4: cin8-FA mutant cells are viable at 37°C
Wild type (Ry 1) and cin8-F429(467)A (Ry 4124) cells were grown in YEPD cell growth medium and arrested in G1 phase by adding the α-factor pheromone. Cells were then released into fresh YEPD cell growth medium lacking the pheromone and incubated at 37°C. Cells were collected at the indicated time points to determine the percentage of cells with metaphase spindles (closed circles) and anaphase spindles (open squares). N=100 cells were counted at each time point.

As we were searching for a mutant specifically defective in spindle elongation, we limited our analysis to the cells carrying the *cin8-F429(467)A* mutation. Indeed, the *cin8-F429(467)A* mutant fulfilled the motor function in SPBs separation and caused the cells to grow at both permissive and non-permissive temperatures. For the epistatic analysis, we initially assessed the spindle length phenotype of *cin8-F429(467)A* mutant in *cdc5*, *cdc14* and *cdc5 cdc14* mutant backgrounds.

The *cdc5-as1 cin8-F429(467)A*, *cdc14-1 cin8-F429(467)A* and *cdc5-as1 cdc14-1 cin8-F429(467)A* cells were arrested in G1 phase and then synchronously released in restrictive conditions for both *cdc14-1* and *cdc5-as1* mutants (**Figure 3.5**). A possible genetic interaction between the mutants was investigated by measuring spindle length for three hours every 15 minutes starting from the establishment of a bipolar spindle (90 minutes, corresponding to metaphase). We found no genetic interaction between the *cin8-F429(467)A* and *cdc5* mutants, as the *cdc5-as1 cin8-F429(467)A* cells undergo a cell cycle

arrest, maintaining a spindle with a length resembling the one showed by the single *cdc5* mutant. However, combining *cin8-F429(467)A* with *cdc14,* exacerbates the spindle elongation defect of the single *cdc14* mutant, causing 60% of the *cdc14-1 cin8-F429(467)A* cells to terminally arrest with spindles shorter than 2 μm, and 30% of the *cdc14-1 cin8-F429(467)A* cells to arrest with metaphase-like short bipolar spindles. Interestingly, an additive effect was observed also when the *cin8-F429(467)A* mutation was introduced in the *cdc5 cdc14* mutant background.

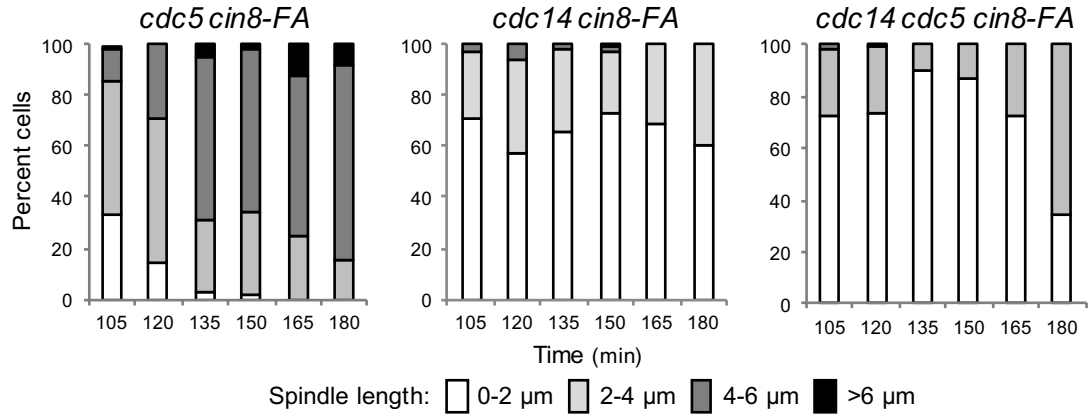

Figure 3.5: cdc14 cin8F429(467)A cells arrest with short bipolar spindles
cdc5-as1 cin8-F429(467)A (Ry 4130), cdc14-1 cin8-F429(467)A (Ry 4126) and cdc5-as1 cdc14-1 cin8-F429(467)A cells (Ry 4128) were arrested in G1 phase and released into cell cycle at cdc14-1 and cdc5-as1 restrictive conditions (YEPD cell growth medium at 37°C in the presence of the cdc5-as1 inhibitor CMK).
Mitotic spindle length was measured (μm) for 100 cells for each time point between 105 minutes and 180 minutes. Spindle length distribution is shown in histogram graphs as different shades of grey.

3.4 *cdc14 cin8-F429(467)A* cells arrest in mini-anaphase

The observation that *cdc14-1 cin8-F429(467)A* cells arrest with short bipolar spindles supports our hypothesis that Cin8 could be a relevant target of Cdc5 in the spindle elongation process. To assess whether this mutant reaches the mini-anaphase arrest, typical for *cdc5-as1 cdc14-1* double mutant cells, we probed for the occurrence of cohesin

cleavage in *cdc14-1 cin8-F429(467)A* cells, both at the population and the single cell level. For the population studies, *cdc5-as1 cin8-F429(467)A*, *cdc14-1 cin8-F429(467)A* and *cdc5-as1 cdc14-1 cin8-F429(467)A* cells, carrying the cohesin subunit Scc1 tagged with 18 copies of a *MYC* tag derived from the c-myc protein, *SCC1-18MYC*, and the Securin Pds1 tagged with 3 copies of the *HA* tag derived from the human influenza hemagglutinin (HA) molecule, *PDS1-3HA*, were arrested in G1 phase and then synchronously released into the next cell cycle at 37°C in the presence of the CMK inhibitor to inactivate Cdc14-1 and Cdc5-as1. Cell cycle progression was scored by measuring spindle length and by probing the accumulation and degradation kinetics of key cell cycle proteins, including securin Pds1 and mitotic cyclin Clb2 by Western blot analysis. Scc1 levels and cleavage were monitored by Western blot analysis as well (**Figure 3.6**). As expected, we found that Clb2 levels are reduced by 50% in cells bearing the *cdc14* mutation, while the levels remain high in cells carrying the *cdc5* mutation (Visintin *et al.*, 1998) (Jaspersen *et al.*, 1998). The presence of the *cin8-F429(467)A* allele does not alter this pattern (**Figure 3.6B**). In respect to the degradation of the Securin Pds1 and the cleavage of the cohesion subunit Scc1, the three mutants are proficient in both processes and are very similar in the kinetics of the events (**Figure 3.6B**). However, while the *cdc5-as1 cin8-F429(467)A* mutant is able to fully elongate its spindle, arresting with the spindle length typical of the *cdc5-as1* single mutant (compare **Figure 3.6A** with **Figure 3.1A**), the *cdc14-1 cin8-F429(467)A* cells maintain the short bipolar spindle that is typical of metaphase, perfectly pheno-copying the mini-anaphase arrest of *cdc5 cdc14* cells (compare **Figure 3.6A** with **Figure 3.1A**). The observation that *cdc5-as1 cdc14-1 cin8-F429(467)A* cells showed a slight delay in Pds1 degradation and Scc1 cleavage, hence in cell cycle progression, could provide an explanation for the additive effect observed in the triple mutant when probing spindle elongation.

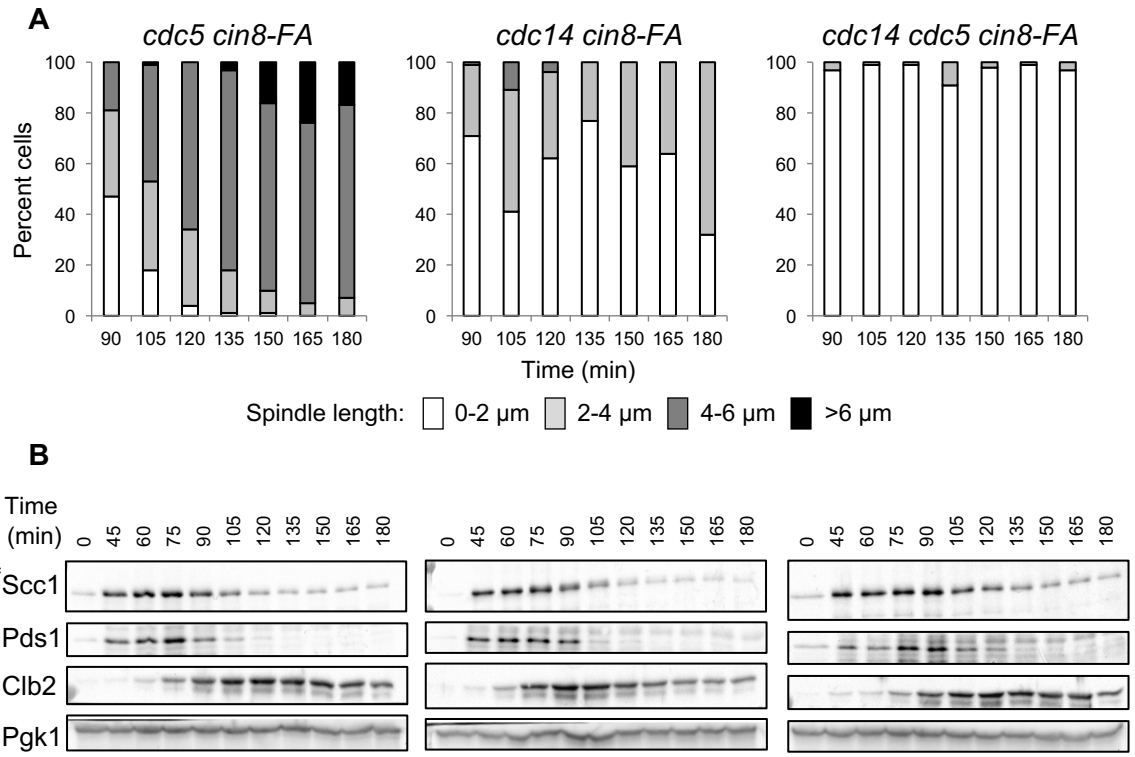

Figure 3.6: cdc14 cin8F429(467)A cells arrest in mini-anaphase
cdc5-as1 cin8-F429(467)A (Ry 7917), cdc14-1 cin8-F429(467)A (Ry 7809) and cdc5-as1 cdc14-1 cin8-F429(467)A (Ry 7868) cells were arrested in G1 phase and released into cdc5-as1 and cdc14-1 restrictive conditions (YEPD cell growth medium at 37°C in the presence of the cdc5-as1 inhibitor CMK). Samples were collected at the indicated time points to measure spindle length (µm) (A), as well as to analyze Scc1, Securin (Pds1) and Clb2 protein levels by Western blot analysis (B). The spindles length was determined for 100 cells from 90 minutes to 180 minutes; spindle length distribution is shown in histogram graphs, indicated as different shades of grey. Pgk1 protein was used as an internal loading control.
** Note: Scc1 cleavage was followed by monitoring the reduction of the full-length protein levels.*

To exclude that the persistence of residual cohesin in *cdc14-1 cin8-F429(467)A* cells could account for the spindle elongation defect of this strain, we directly examined the presence of cohesin at the single cell level by imaging techniques. To this aim, the cohesin subunit Scc1 was tagged with the green fluorescent protein (GFP), Scc1-GFP, and introduced in *cdc5-as1 cin8-F429(467)A*, *cdc14-1 cin8-F429(467)A* and *cdc5-as1 cdc14-1 cin8-F429(467)A* cells endogenously expressing mCherry-labeled spindle pole body protein Spc110 (Spc110-mCherry). The three strains were arrested in G1 phase and then synchronously released into the next cell cycle at the restrictive conditions for Cdc14-1 and Cdc5-as1 mutant proteins. Cell cycle progression was monitored in real time by probing

nuclear positioning (not shown). Cells were collected for imaging analyses in metaphase (80 minutes after the G1 release) and at their terminal arrest (240 minutes after the G1 release). Our data show that, in metaphase, all strains had accumulated cohesin on the chromatin, whereas at the terminal arrest all strains had released the cohesin from the DNA. However, whereas *cdc5-as1 cin8-F429(467)A* cells progress through mitosis and arrest in late anaphase (arrest with elongated spindles), the *cdc14-1 cin8-F429(467)A* and *cdc14-1 cdc5-as1* double mutants fail to progress through anaphase, maintain the short bipolar spindle characteristic of metaphase cells, as judged by the interpolar distance between the two Spc110 signals, and are proficient in cohesin cleavage (**Figure 3.7**). These results suggest that Cin8, in addition to being a substrate of Cdc14, belongs to the Cdc5 branch of the Cdc14/Cdc5 pathway.

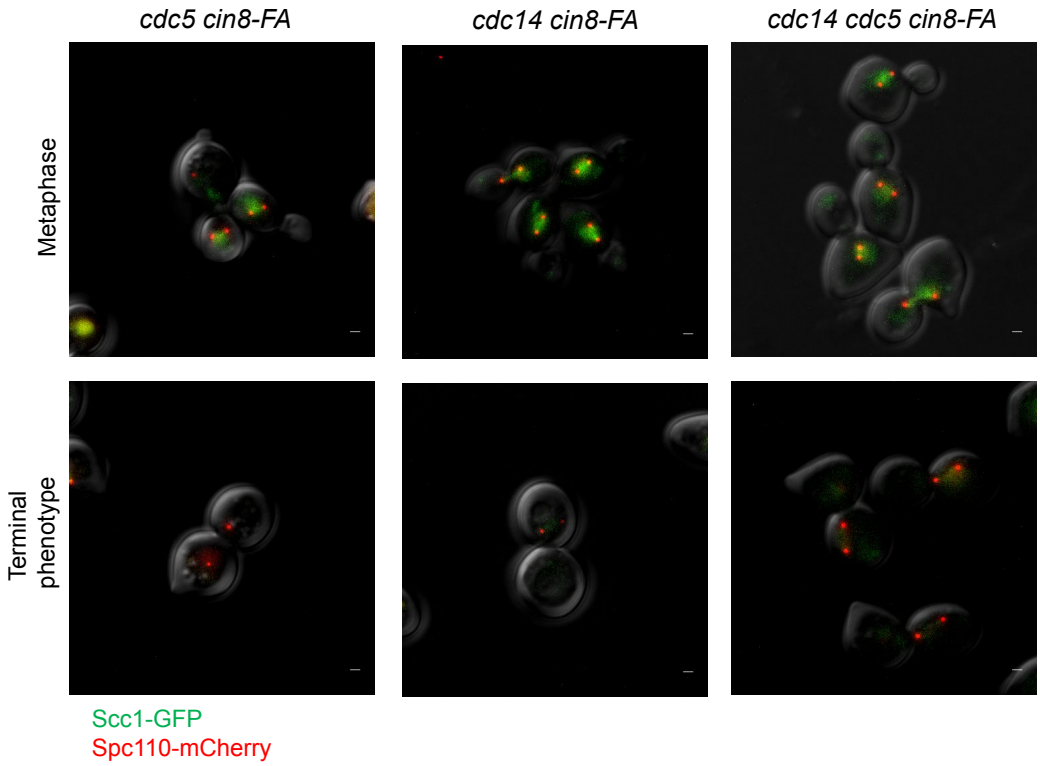

Figure 3.7: cdc14 cin8-F429(467)A cells are proficient in cohesin cleavage
cdc5-as1 cin8-F429(467)A (Ry 6571), cdc14-1 cin8-F429(467)A (Ry 6567) and cdc5-as1 cdc14-1 cin8-F429(467)A cells (Ry 6566) carrying SCC1-GFP and SPC110-mCherry fusion proteins were arrested in G1 in YEPD cell growth medium at 23°C. Next, cells were released into fresh YEPD supplemented with the CMK inhibitor and incubated at 37°C to inactivate the cdc5-as1 and cdc14-1 alleles. When the cells were in metaphase (80 minutes after the G1 release) and at their terminal arrest (240 minutes after the G1 release), samples were collected and prepared for microscopy analyses (see materials and methods). Red: Spc110; green: Scc1.

3.5 Cin8 contains 11 putative Cdc5 phosphorylation sites

The observation that Cin8 overexpression recovers the spindle elongation defect of *cdc5 cdc14* cells, places Cin8 activity downstream of the Cdc5/Cdc14 pathway. The genetic interaction observed in *cdc14 cin8-F429(467)A* cells indicates that Cin8, in addition to being a substrate of Cdc14, belongs to the Cdc5 branch of the pathway. To understand if Cdc5 regulates Cin8 in a direct or indirect manner, we first asked if Cdc5 could phosphorylate Cin8 *in vitro*. To this aim, we performed a preliminary experiment in collaboration with Dr. Schiebel's laboratory, which showed that Cdc5 phosphorylates Cin8 *in vitro* (not shown). Building on this information, we set out to identify the residues of Cin8 that are phosphorylated by Cdc5, with the ultimate goal of understanding whether and how this modification affects the kinesin function in spindle elongation. To this aim, we pursued two strategies in parallel: 1) mass spectrometry analysis and 2) Cin8 sequence scanning for the Cdc5 recognition motif. Concerning the mass spectrometric analysis, in collaboration with the biochemistry facility, we set to produce recombinant full-length Cin8 in *Baculovirus*. So far, the purification of full-length Cin8 turned out to be very challenging and we managed to obtain only small, diluted amounts of the protein, insufficient for a proper kinase assay. For this reason, in parallel, we decided to scan the Cin8 protein sequence for two reported Cdc5-consensus motives: [E/D]-X-[S/T]-[F/L/I/Y/V/W/M] (Nakojima *et al.*, 2003) and [E/N/D/Q]-X-[S/T]-[F/L/I/Y/V/W/M] (Santamaria *et al.*, 2011). We identified 11 putative Cdc5 sites, of which only four were common between the two sequences (S52, S71, T761 and S820). Other putative sites include T38, S52, S71, T123, S409, S441, T497, S654, T761, S820 and S859. These 11 sites are distributed along the entire Cin8 protein sequence, and, precisely, 3 are in the N-terminal domain, 4 are in the motor domain and 4 are in the tail domain (Figure 3.8).

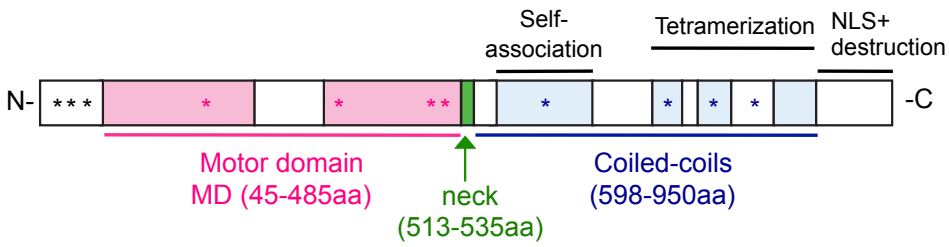

[E/D]-X-[S/T]-[F/L/I/Y/V/W/M]	**S52, S71, T761 e S820**
[E/N/D/Q]-X-[**S**/**T**]-[F/L/I/Y/V/W/M]	**T38, S52, S71, T123, S409, S441, T497, S654, T761, S820, S859.**

Figure 3.8: Cdc5 putative phosphorylation residues on the Cin8 protein
Graphical representation of the Cin8 protein, subdivided according to the main protein domains: motor domain (red), neck (green) and Coiled-coil (blue). Asterisks indicate Cdc5 putative phosphorylation sites.

3.6 Preventing phosphorylation of the putative Cdc5 residues within the tail domain of Cin8 does not impact on spindle elongation

To assess whether Cdc5 phosphorylation of Cin8 is relevant for spindle elongation, we decided to mutate the identified putative sites alone or in combination to alanine (non-phosphorylatable) and to search for a Cin8 "alanine" mutant (henceforth *cin8-A*) that behaves as the *cin8-F429(467)A*. Namely, a mutant that *i)* fulfills the early mitotic functions of Cin8 (SPBs separation, hence bipolar spindle formation) and *ii)* in combination with the *cdc14-1* allele arrests in mini-anaphase (short bipolar spindles, undivided nuclei, cleaved cohesin).

To this aim, all the allelic variants of Cin8, including the wild type counterpart, were first tested for their ability to rescue *cin8Δ* lethality at 37°C. The variants that allowed *cin8Δ* cells to grow as wild type at 37°C were then combined with the *cdc14-1* mutation, and the

obtained terminal phenotype of the double mutant probed for anaphase spindle elongation (**Figure 3.9A**).

We began by mutating the 11 and 4 putative sites identified with the two consensus motifs (*cin8-11A* and *cin8-4A*). The *cin8-11A, cin8-4A* and *CIN8* wild type sequences were *in vitro* synthesized by GenScript. The obtained wild type and mutated constructs were then sub-cloned into yeast vectors (both centromerics and integratives) and transformed into yeast cells deleted for the endogenous *CIN8* gene (*cin8Δ*). We found that while *cin8Δ* cells carrying the Cin8-11A mutant protein die at 37°C, the strain with Cin8-4A was viable and could be probed for genetic interaction with *cdc14-1.* Since we did not detect any genetic interaction, we can conclude that phosphorylation of the putative residues S52, S71, T761 and S820 is not essential for the kinesin function in spindle elongation (**Figure 3.9B**).

On the other hand, the inability of the *cin8-11A* mutant to rescue the lethality of *cin8Δ* at the restrictive temperature indicates that the mutation of all 11 residues to alanine severely affected the protein activity. To identify Cin8 sites that are regulated by Cdc5, we next decided to "cluster" the mutations according to their position along the protein sequence. We obtained two *cin8-A* allelic variants: *cin8-Motor-A* and *cin8-Tail-A*. We mutated all residues in the N-terminal domain (T38, S52, S71, T123, S409, S441 and T497), including the motor domain, in *cin8-Motor-A*, and all residues in the C-terminal domain (S654, T761, S820 and S859), including the coiled-coil domain, in *cin8-Tail-A* (**Figure 3.9B**). While the *cin8-Motor-A* mutant variant was not able to rescue the *cin8Δ* phenotype at 37°C, the *cin8-Tail-A* variant was capable of doing so, thus, suggesting that the mutation of all residues within the N-terminal domain was still compromising the protein activity too much, whereas the mutation of the residues in the tail domain was preserving Cin8 functions. Based on these results, we decided to proceed with the second step of our analysis by analyzing the *cin8-Tail-A.* When the *cin8-Tail-A* mutant was combined with a *cdc14-1* mutant, no synergistic effect was observed and the cells could reach the spindle length characteristics of the *cdc14-1* single mutant. Taken together, these data allow us to

conclude that phosphorylation of the residues lying in the tail domain is not relevant for Cin8 function in the spindle elongation process.

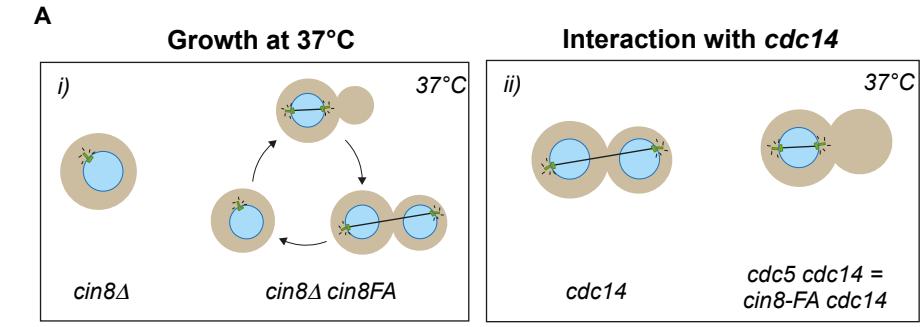

B

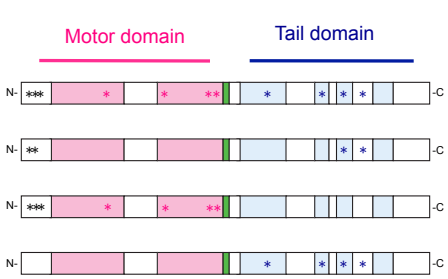

Mutant	Growth at 37°C	Interaction with *cdc14*
Cin8-11A	NO	n.d.
Cin8-4A	YES	NO
Cin8-Motor-A	NO	n.d.
Cin8-Tail-A	YES	NO

*n.d.: not determined

Figure 3.9: Graphical representations of Cin8 proteins. Putative phosphorylation residues and their relative position and nomenclature are indicated.
(A) Graphical representation of the analyses of the Cin8 mutated protein: each mutant was tested for two parameters: i) capability of growth at 37°C and ii) genetic interaction with the cdc14 mutant. (B) On the left a graphical representation of Cin8 protein shows the position (asterisks) of the mutated residues in the different constructs. The table to the right shows the results obtained from the analyses of Cin811A, Cin8-4A Cin8-Motor-A and Cin8-Tail-A mutated protein phenotypes.

3.7 Cdc5 phosphorylation of residues S409 and S441 in Cin8 is relevant for the kinesin function in anaphase spindle elongation

To test whether any of the residues within the N-terminal domain in Cin8-Motor-A is important for the kinesin function in anaphase spindle elongation process, we further dissected the *cin8-Motor-A* construct and created single mutant proteins, each carrying only one residue mutated to alanine with the exception of S52 that was already present in

the *cin8-4A* construct. We found that all of the single mutants recovered the *CIN8* deletion phenotype but only strains carrying the S409A and S441A mutated residues gave an additive phenotype when combined with the *cdc14-1* allele. In fact, both *cdc14-1 cin8-S409A* and *cdc14-1 cin8-S441A* mutant cells arrested with short bipolar spindles and undivided nuclei (**Figure 3.10**).

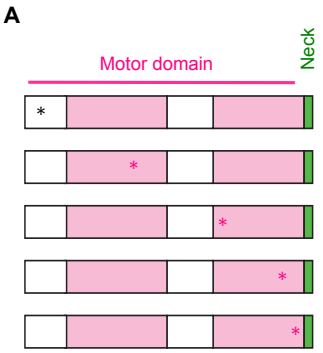

Mutant	Growth at 37°C	Interaction with *cdc14*
Cin8-T38A	YES	NO
Cin8-T123A	YES	NO
Cin8-S409A	**YES**	**YES**
Cin8-S441A	**YES**	**YES**
Cin8-T497A	YES	NO

Figure 3.10: Cdc5 phoshorylation of Cin8 residues S409 and S441 impacts on anaphase spindle elongation
(A) On the left a graphical representation of Cin8 motor domain shows the position (asterisks) of the mutated residues in the different constructs. The table to the right shows the results obtained from the analyses of Cin8-T38A, Cin8-T123A, Cin8-S409A, Cin8-S441A and Cin8-T497A mutated protein phenotypes.
(B) Representative images of cdc14-1 CIN8, cdc14-1 cin8-S409A and cdc14-1 cin8-S441A cells at the terminal phenotype (at 240 minutes) are shown. Blue: DAPI; green: tubulin. Bars: 1μm.

Since the S409 and S441 residues, in sequence, are in close proximity to the F429(467) (*cin8-F429(467)A*) residue, we wondered whether they are: i) in close proximity also in the tertiary structure and/or ii) part of a conserved stretch of amino acids. To address these possibilities, in collaboration with Sebastiano Pasqualato (head of the Biochemistry facility), we analysed a sequence alignment of Cin8 from different species and performed homology modelling of the three-dimensional structure of the protein, using the Phyre2 (Kelley *et al.*, 2015) program. Having found that, i) the S409 and S441 residues are in

close proximity to F429(467) both in the sequence and in the tertiary structure, and ii) that the three residues are contained in a highly conserved stretch of Cin8 residues (all three residues are conserved across different species) (**Figure 3.11**), we were concerned that the synthetic interaction observed in *cdc14-1 cin8-S409A* and *cdc14-1 cin8-S441A* mutant cells was not caused by the lack of phosphorylation of the residues of interest, but a consequence of hampering a critical motif within the motor domain.

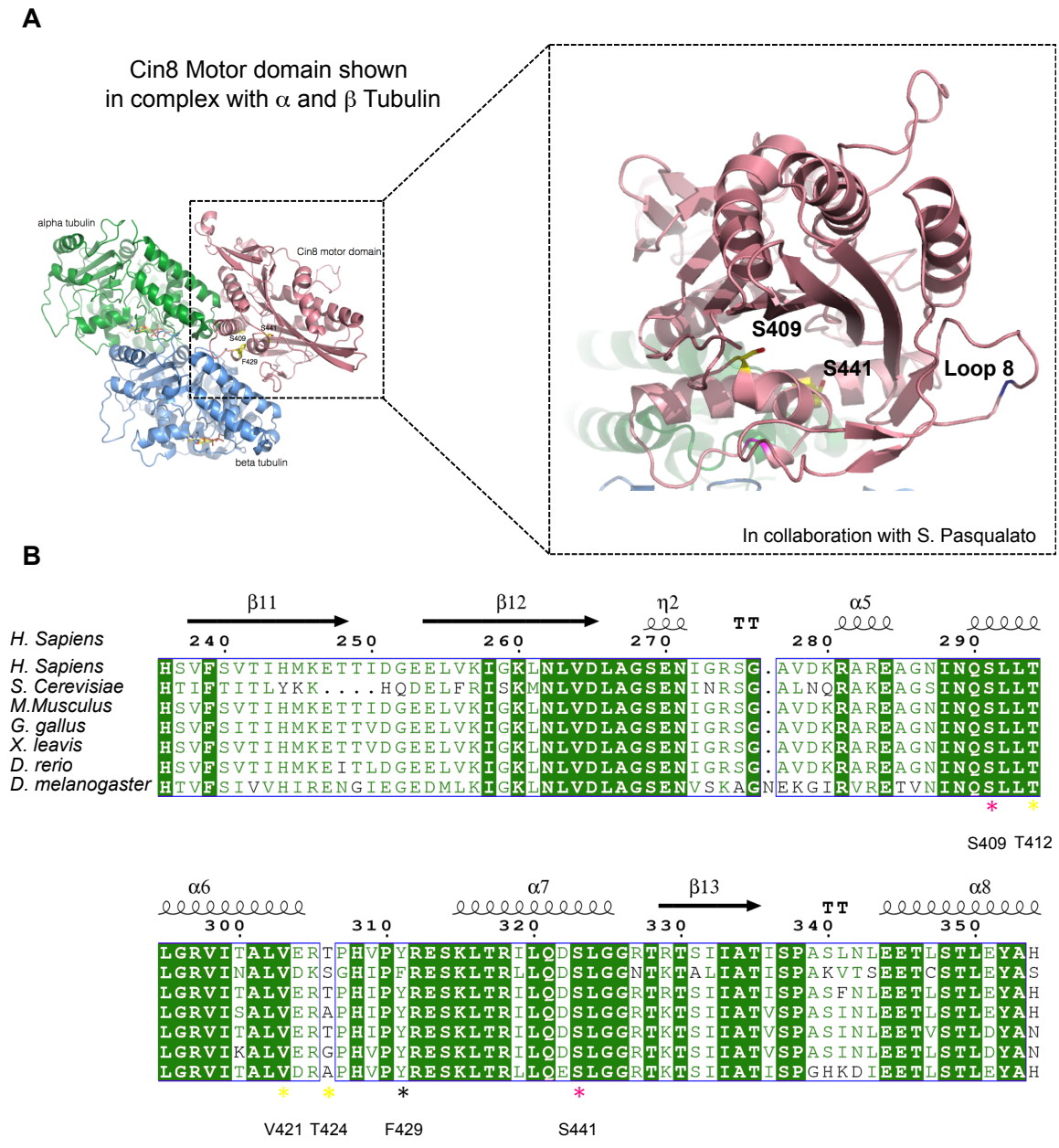

Figure 3.11: Cin8 residues S409, S441 and F429 are highly conserved and lay close to each other in the predicted tertiary structure of the protein

(A) Cin8 motor domain structure (shown in complex with α-tubulin), modeled over its ortholog Eg5; (B) Cin8 gene orthologue multiple alignment (Clustal W) visualized with ESPript 3.

It is worth noting that the *cin8-F429(467)A* mutant employed in our analysis is not phospho-deficient but, nevertheless, leads to a mutant motor protein with a reduced affinity for microtubules. To address this concern, we mutated random residues within the conserved stretch, including putative sites for phosphorylation, and analyzed them according to our strategy. For this analysis, we chose residues T412, V421 and S424. In all cases (*cin8-T412A, cin8-V421A* and *cin8-S424A*), we obtained functional proteins capable of recovering the *cin8Δ* lethality at 37°C, and none of them resulted in a synthetic interaction with *cdc14-1* (**Figure 3.12**), thus suggesting that random interference within the conserved sequence does not impact on spindle elongation. These findings highlight the potential relevance of Cdc5-mediated phospho-regulation of residues S409 and S441 in the motor protein Cin8.

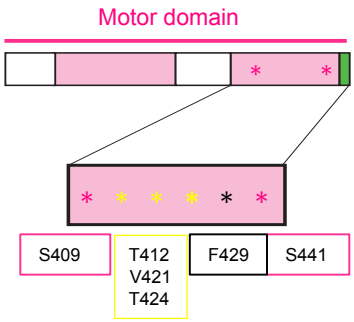

Mutant	Growth at 37°C	Interaction with *cdc14*
Cin8-T412A	NO	NO
Cin8-V421A	NO	NO
Cin8-T424A	NO	NO

Figure 3.12: Cdc5 phosphorylates Cin8-MD on multiple sites, including the S409 and S441 residues.
On the left a graphical representation of Cin8 motor domain shows the position (asterisks) of the mutated residues in the different constructs. The table to the right shows the results obtained from the analyses of Cin8-T412A, Cin8-V421A and Cin8- mutated protein phenotypes.

3.8 Cdc5 phosphorylates the Cin8 motor domain on residues S409 and S441 *in vitro*

Having identified residues S409 and S441 in Cin8 as putative phosphorylation sites for Cdc5 solely by scanning the motor sequence for the kinase consensus motif, before moving into the molecular characterization of the mutant, in collaboration with Francesca Senic-Matuglia, a post doc in the laboratory, we tested whether these sites were direct targets of Cdc5. We first asked whether Cdc5 phosphorylates these residues *in vitro*. To overcome the problems associated with the purification of full-length Cin8, given that the residues of interest lie in the motor domain, we changed strategy and produced truncated recombinant proteins containing the motor domain to use in an *in vitro* kinase assay.

To define the boundaries of the motor domain, we performed homology modelling of the three-dimensional structure of the protein, using the Phyre2 (Kelley *et al.*, 2015) program. The motor domain, modelled on the structure of Cin8 human homologue Eg5, encompasses residues 1-485. This domain, preceding the neck and coiled-coil region, required for dimerization, was cloned and used for further studies (Cin8MD) (**Figure 3.13**).

Figure 3.13: Cin8 motor domain.
(A) Cin8 motor domain structure (shown in complex with α-tubulin), modeled over its ortholog Eg5. The relative position of residues S409 and S441, and of Loop8 are indicated. (B) Cin8 motor domain sequence. Motor and neck domains, unstructured stretches and loop8 are highlighted in different colors.

Recombinant wild type (Cin8MD) and double alanine mutant (Cin8MD-S409AS441A, henceforth Cin8MD-2A) proteins, produced in *E. coli*, were used as substrates for an *in vitro* Cdc5 kinase assay using both wild type and kinase-dead (KD) Cdc5 (**Figure 3.14**). To this purpose, yeast cells carrying the *GAL-CDC5* and *GAL-CDC5KD* fusion constructs were arrested in metaphase by adding the microtubule (MT) depolymerizing drug nocodazole. When about 90% of cells reached the arrest, galactose was added to the growth media to induce the overexpression of wild type and kinase dead Cdc5. Three hours after the induction with galactose, the cells were collected and prepared to immunoprecipitate the kinase. For the *in vitro* kinase assay, the Cin8 recombinant motor domain (Cin8MD and Cin8MD-2A) was incubated with immunoprecipitated Cdc5 from both wild type and kinase dead strains. Casein was used as a control substrate. We found that wild type Cdc5 but not its kinase dead counterpart phosphorylated both Cin8 motor domains i*n vitro* (**Figure 3.14A**). If these data support our preliminary finding that Cin8 is a substrate for Cdc5, they call into question whether the S409 and S441 residues are real Cdc5 substrates. Therefore, in order to identify the *in vitro* phosphorylated residues in Cin8 by Cdc5, we performed a mass spectrometry analysis. Besides the S409 and S441 residues, additional phosphorylated sites were identified in Cin8 (**Figure 3.14B** and data not shown). The remaining phospho-residues were located within loop 8, a non-conserved, uncharacterized insertion of about 100 amino acids within the Cin8 motor domain. Interestingly, none of these additional residues contains a Cdc5 consensus motif, explaining why they were not identified in our sequence scanning analysis. Taken together, these data suggest that Cdc5 phosphorylation of the S409 and S441 residues in Cin8 may be relevant for its motor regulation *in vivo.* The significance of Cdc5-mediated phosphorylation of the residues within the loop8 is unclear but is worth exploring in the future. Of note, loop8 is present only in budding yeast.

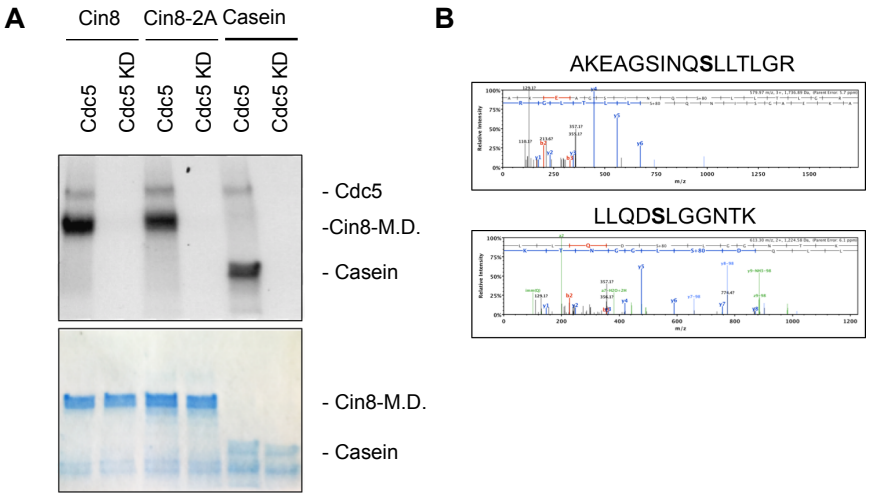

Figure 3.14: Cdc5 phosphorylates Cin8 motor domain on multiple residues, including S409 and S441.
(A) Cin8 and Cin8-2A recombinant proteins (yield in E. coli) were used as substrates in an in vitro kinase assay: proteins were incubated in the presence of Cdc5 active kinase or Cdc5 kinase dead (KD). Casein was used as control. The radioactive signal associated with the phosphorylation of Cin8 and Cin8-2A by Cdc5 active kinase is shown in the upper panel. In the lower panel, the kinase gel (SDS-PAGE) stained with blue Comassie. (B) Recombinants Cin8-MD was phosphorylated by Cdc5 and analyzed by mass spectrometry.

3.9 Cdc5 phosphorylates the Cin8 protein *in vivo*

Our *in vitro* results indicate that Cdc5 phosphorylates multiple residues within the Cin8 motor domain, including S409A and S441A. The question is whether these sites are Cdc5 substrates also *in vivo.*

To answer this question, *cdc14-1* cells carrying the *GAL-CDC5* construct and an allelic variant of *CIN8* fused to 3 copies of the HA, *CIN8-3HA* were arrested in metaphase by the addition of nocodazole to the growth medium at 33°C to inactivate Cdc14-1 mutant. When most of the cells reached the arrest, the culture was split in two parts: one-half was maintained in raffinose-based medium (-GAL) at 33°C, and the second half was supplemented with 2% galactose (+GAL) to induce *CDC5* expression at 33°C. The cells

were then collected at different time points for 2 hours after *CDC5* induction (**Figure 3.15**) for protein analyses.

By looking at Cin8 migration pattern, we observed a lower migration mobility shift that progressively accumulated (starting from the 60 minutes time point after the induction), correlating with cells ectopically expressing *CDC5* (**Figure 3.15**). This result suggests that, at least when overexpressed, Cdc5 can directly phosphorylate Cin8 *in vivo*.

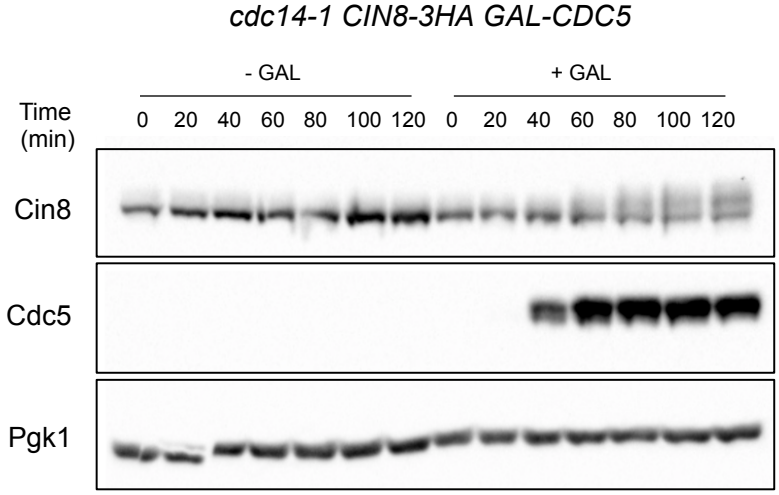

Figure 3.15: Cdc5 phosphorylates Cin8 in vivo.
cdc14-1 CIN8-3HA GAL-CDC5 (Ry 7897) cells were arrested in metaphase. Once 90% of the cells were arrested, 2% galactose was added to the growth medium to induce the expression of CDC5 at 33°C. Cells were collected at the indicated time points for protein analyses by Western blot.

Once Cdc5 was validated as a direct regulator of Cin8 *in vivo*, we moved on to test whether the identified S409 and S441 residues are actually phosphorylation sites. Thus, we repeated the experiment and included *cdc14-1 cin8-S409A-3HA GAL-CDC5, cdc14-1 cin8-S441A-3HA GAL-CDC5* and *cdc14-1 cin8-2A-3HA GAL-CDC5* cells in the analysis. As expected, we confirmed that wild type Cin8 exhibits the progressive Cdc5-dependent phosphorylation, which, instead, is reduced in the *cin8-2A* double mutant strain (**Figure 3.16A-B**). The persistence of some phosphorylation levels in *cin8-S409A*, *cin8-S441A* and *cin8-2A* mutant cells is consistent with the finding that additional sites, namely the ones

within loop 8, are targets for the kinase. Nevertheless, the decrease in phosphorylation observed in cells mutated for residues S409 and S441 further supports a role for the kinase in the regulation these sites.

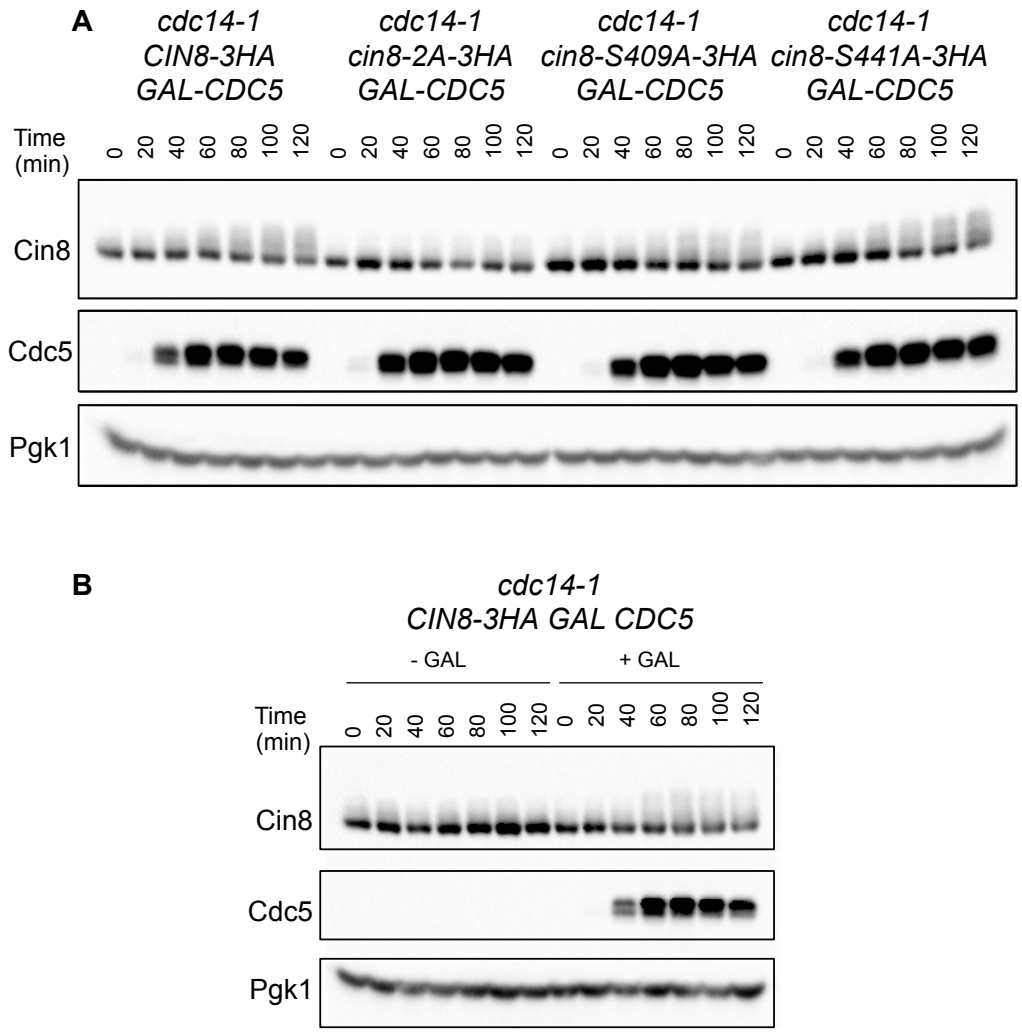

Figure 3.16: Cdc5 phosphorylates the S409 and S441 residues in vivo.
(A) cdc14-1 CIN8-3HA GAL-CDC5 (Ry 7897),cdc14-1 cin8-S409A-3HA GAL-CDC5(Ry 8042), cdc14-1 cin8-S441A-3HA GAL-CDC5 (Ry 8084) and cdc14-1 cin8-2A-3HA GAL-CDC5 (Ry 8028) cells were arrested in metaphase. Once 90% of the cells were arrested, 2% galactose was added to the growth medium to induce the expression of CDC5 at 33°C. The cells were collected at the indicated time points for protein analyses by Western blot. (B) CIN8-3HA GAL-CDC5 (Ry 7897) cells were arrested in metaphase and maintained in medium lacking galactose (-GAL) for the entire length of the experiment to serve as a control for the experiment in (A). Samples were loaded with the corresponding "+GAL" (Cdc5 overexpression) from (A)

3.10 Cdc5 phosphorylation of Cin8 residues S409 and S441 is cell cycle-regulated

Having established that, when overexpressed, Cdc5 can phosphorylate Cin8 *in vivo*, we next tested whether this regulation is appreciable also in physiological conditions and, more importantly, whether *cdc14 cin8* double mutant cells arrest in mini-anaphase. To this aim, *cdc14* yeast strains bearing *CIN8*, *cin8-S409A*, *cin8-S441A* or *cin8-2A* mutants were synchronized in G1 phase, released at the restrictive conditions for the *cdc14-1* mutant and collected at different time points for protein and spindle length analyses.

We found that all Cin8 protein variants (wild type and mutants), in terms of protein levels, are almost absent in the G1 phase, as reported by Qiao and colleagues (Qiao *et al.*, 2010), and that they begin to accumulate in S phase, 60 minutes after the G1 release. In terms of migration, we observed that wild type Cin8 migrates sharply in the early time points, and then becomes progressively phosphorylated (first, a doublet band appears at 105 minutes after the G1 release, which then shifts to a whole band, indicating the complete phosphorylation of the protein in the later time points). Instead, a slight reduction in the phosphorylation-dependent shift of Cin8-S409A and Cin8-S441 mutant proteins was scored, which was almost abolished in the Cin8-2A variant. Taken together, these results suggest that Cdc5 phosphorylates the S409 and S441 residues *in vivo* under physiological conditions (**Figure 3.17**).

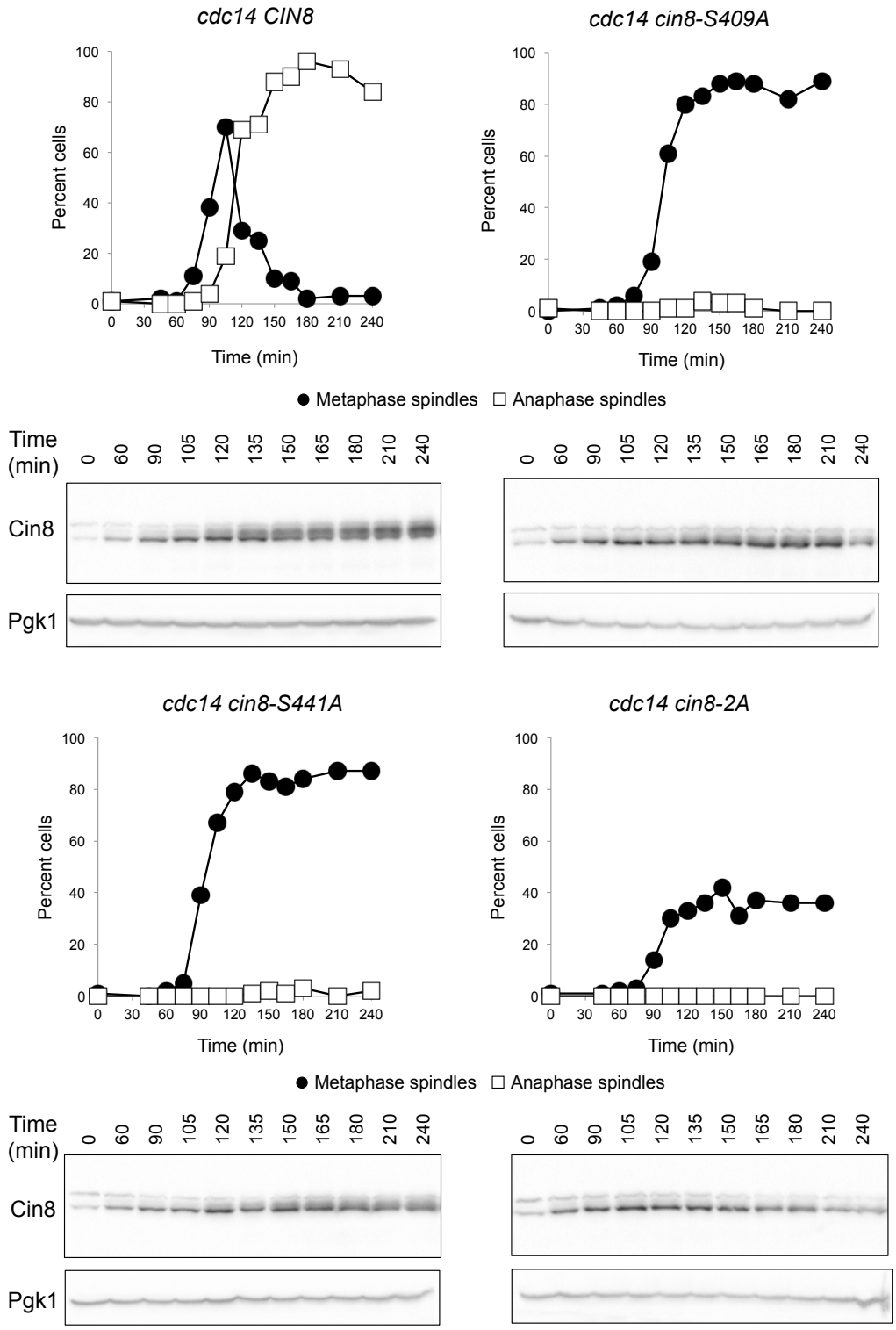

Figure 3.17: cdc14 CIN8-3HA cdc14 cin8-S409A, cdc14 cin8-S441A and cdc14 cin8-2A
cdc14-1 CIN8-3HA cdc14-1 cin8-S409A-3HA, cdc14-1 cin8-S441A-3HA and cdc14-1 cin8-S409S441A-3HA cells were arrested in G1 phase and released in cdc14-1 restrictive condition (YEPD cell growth medium at 37°C).
Cells were collected at the indicated time points to determine the percentage of cells with metaphase spindles (closed circles) and anaphase spindles (open squares) N=100 cells were counted at each time poin as well as to analyze Cin8 protein levels by Western blot.
Pgk1 protein was used as an internal loading control.

To assess how Cdc5 phosphorylation impacts on Cin8 activity, we next characterized the cell cycle progression and the terminal phenotype of *cin8-S441A cdc14-1* and *cin8-S409A cdc14-1* double mutant cells. We earlier observed that these mutants arrest with short bipolar spindles, yet we did not know whether they were arrested in mini-anaphase, namely after cohesin cleavage. Therefore, *cin8-S409A cdc14-1, cin8-S441A cdc14-1* and *cin8-S409AS441A* (*cin8-2A*) *cdc14-1* mutants were synchronized in G1 phase and released at the restrictive conditions for the *cdc14-1* mutant. We found that 40% of the *cin8-S409A cdc14-1* mutant arrested cells had a spindle shorter than 2 μm and that more than 60% of the cells had a spindle length of 2-4 μm. Similarly, about 55% of the *cin8-S441A cdc14-1* arrested cells had a spindle length of 2-4 μm. The *cin8-2A cdc14-1* mutant had the most severe phenotype as 100% of the cells arrested with spindles shorter than 2 μm (**Figure 3.18**). All of the mutant strains were proficient in Pds1 degradation and cohesin cleavage (**Figure 3.18**). Taken together, these data suggest that Cdc5-mediated phosphorylation of the S409 and S441 residues is critical for Cin8 function in promoting anaphase spindle elongation.

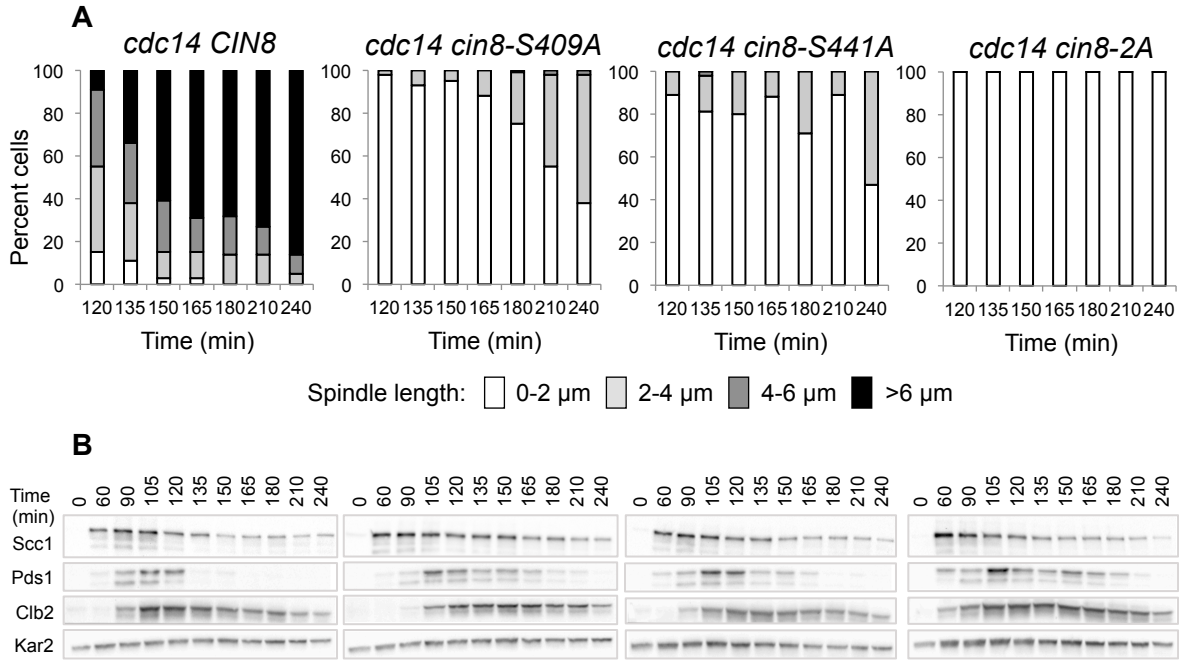

Figure 3.18: CIN8-3HA cdc14-1, cin8-S409A-3HA, cdc14-1 cin8-S441A-3HA, and cdc14-1 cin8-S409S441A-3HA cells arrest in mini-anaphase.

cdc14-1 CIN8-3HA cdc14-1 cin8-S409A-3HA, cdc14-1 cin8-S441A-3HA and cdc14-1 cin8-S409S441A-3HA cells carrying a SCC1-13myc fusion were arrested in G1 phase and released in cdc14-1 restrictive condition (YEPD cell growth medium at 37°).

Samples were collected at the indicated time points to measure spindle length (µm) (A), as well as to analyze Scc1, Securin (Pds1) and Clb2 protein levels by Western blot (B). The spindles length was determined for 100 cells from 90 minutes to 180 minutes; spindle length distribution is shown in histogram graphs, indicated as different shades of grey. Kar2 protein was used as an internal loading control.

** note: Scc1 cleavage was followed by monitoring the reduction of the full-length protein levels.*

4 Discussion and future directions

During mitosis, the replicated chromosomes (sister chromatids) are equally distributed into the daughter cells through a fine-regulated process called chromosome segregation. Defects in this process can cause chromosome instability and aneuploidy, two key events in tumorigenesis (Gordon, Resio and Pellman, 2012). Chromosome segregation begins at the onset of anaphase when the separase (Esp1 in buddying yeast) triggers the cleavage of cohesin, a protein complex that holds sister chromatids together. Next, chromatids are segregated into the daughter cells by the pulling force of the mitotic spindle (Nasmyth, 2002). The mitotic spindle is a sophisticated and complex machinery built of microtubules, arbitrarily defined as astral, kinetochore and interpolar spindle microtubules. This view of spindle organization holds true for most spindles, including that of the budding yeast *Saccharomyces cerevisiae.*

Proper chromosome segregation requires an orderly sequence of events whereby spindle elongation follows the dissolution of sister chromatid cohesion. The molecular mechanism that guarantees this chain of events remains elusive. Although cohesin is thought to provide the main force that counteracts the pulling force of the mitotic spindle, also cohesin-independent mechanisms may contribute to control the timing of spindle elongation (Yanagida, 2009), which was suggested already by the initial observation that yeast cells lacking either securin (Pds1 in buddying yeast) or cohesin do not elongate their spindles prematurely (Baskerville, Segal and Reed, 2008) (Severin, Hyman and Piatti, 2001). Liang and colleagues propose that the timely control of spindle elongation is based on a balance of mitotic (positive effect) versus S phase (negative effect) cyclin-dependent kinase (CDK) activity (Liang, Richmond and Wang, 2013). This explanation perfectly fits into the current knowledge that a global kinase to phosphatase shift is required for the timely progression through anaphase (Uhlmann, Bouchoux and López-Avilés, 2011). However, the recent finding that cells simultaneously lacking the polo-like kinase Cdc5

and the phosphatase Cdc14 arrest in "mini anaphase" due to defects in spindle elongation, calls this view into question. In fact, what these data suggest that the two antagonistic enzymatic activities have overlapping roles in controlling an active mechanism during anaphase and provide a glimpse to a more sophisticated picture. The main aim of my work is to understand the molecular mechanism by which the two proteins, Cdc5 and Cdc14, contribute to anaphase spindle elongation, with a particular focus on the role of Cdc5.

How does Cdc5 fit in the kinase/phosphatase threshold model?

The general mechanism via which eukaryotes ensure faithful chromosome segregation, that relies on a global kinase to phosphatase shift setting proper kinase/phosphatase thresholds, foresees two key processes: a constant rise in mitotic CDK activity to guide and order the sequence of events during early mitosis, with a lower mitotic CDK activity threshold that triggers the entry into mitosis and a higher one that triggers the entry into anaphase, (Rahal and Amon, 2008)followed by a gradual decrease in mitotic CDK activity associated with a gradual increase in the activity of their counteracting phosphatase(s).

In budding yeast, the main CDK-counteracting phosphatase is Cdc14. Both CDK inactivation and Cdc14 activation are necessary for cells to exit from mitosis (Yeong *et al.*, 2000) (Bäumer, Braus and Irniger, 2000). The two events are coupled through the activity of the anaphase promoting complex or Cyclosome bound to its activator Cdc20 (APC/C^{Cdc20}). The APC/C^{Cdc20} accomplishes these tasks by targeting for degradation the mitotic cyclin Clb2 and the anaphase inhibitor Pds1. Given that Cdc14 has different affinities toward its substrates, being higher toward its early anaphase substrates and lower versus its late ones (Bouchoux and Uhlmann, 2011). This tightly regulated activity of CDK and phosphatases enables unique temporal phosphorylation kinetics of each CDK substrate during the cell cycle (Bouchoux and Uhlmann, 2011). In agreement with this, the

modulation of mitotic CDKs activity during anaphase impacts on the kinetics of anaphase spindle elongation (Roccuzzo *et al.*, 2015). Indeed, ectopically increasing the levels of mitotic CDK activity causes spindle elongation defects in cells harboring the hypomorphic *cdc14-1* allele, suggesting that high CDK activity in a phosphatase defective background is detrimental for anaphase spindle elongation. Since the phenotype of these cells is reminiscent of the one of *cdc5 cdc14* double mutant cells, it was proposed that one possible role for the polo-like kinase at anaphase is to contribute to the decline in CDK activity (Roccuzzo *et al.*, 2015), which is further supported by the observation that *cdc5* mutant cells are defective in CDK inactivation and arrest with high levels of CDK activity. However, the observations that i) ectopically lowering CDK activity in *cdc5 cdc14* cells only partially rescues the defect in spindle elongation of the mutant and ii) the spindle elongation defect of *GAL-CLB2 cdc14-1* (high levels of CDK activity independent from Cdc5) cells is milder than the one of *cdc5 cdc14* cells calls for additional roles of the kinase in the process.

Microtubules enter the scene

The model foreseeing the transient down-regulation of mitotic CDK activity and the gradual activation of the counteracting phosphatase(s) at the onset of anaphase provides an explanation for the decrease in microtubule dynamics observed in this cell cycle phase that turned out to be critical for chromosome movement during anaphase. In support of this model is the observation that, similarly to CDK and Cdc14 activities, microtubule turnover changes throughout mitosis.

Microtubules are characterized by dynamic instability, a behavior involving repeated cycles of growth and shrinkage. In agreement with the global requirement for changes in kinase and phosphatase thresholds is the finding that microtubule turnover changes as cells progress into mitosis. A fast turnover of spindle microtubules up to metaphase, promoted

by the rise in CDK activity (Rees *et al.*, 1990) (Belmont *et al.*, 1990), is followed by the stabilization of microtubule dynamics (D J Sharp, Rogers and Scholey, 2000) in anaphase mediated by phosphatases. The fast turnover is thought to help correct erroneous attachments that occur during bipolar chromosome alignment, whereas microtubule stabilization is necessary for spindle elongation. Although the mechanisms that coordinate these activities are not known (Mark Winey and Bloom, 2012), stabilization of microtubule dynamics seems to be mediated by a shift from a phosphorylated to a dephosphorylated status of multiple proteins (Mallavarapu, Sawin and Mitchison, 1999), (Higuchi and Uhlmann, 2005b) , dictated by the concomitant down-regulation of CDK and the activation of CDK-counteracting phosphatases. Data in favor of this hypothesis include the observation that in Drosophila embryos, high levels of non-degradable cyclin B maintain high levels of CDK1 activity in anaphase and prevent spindle elongation, even though sister chromatids have been disjoined. Similar defects were reported for cultured mammalian cells after microinjection of a stable version of cyclin B (Roostalu, Schiebel and Khmelinskii, 2010). The identity of the phosphatases that counteract CDK1 activity remains unclear. While fission yeast and *C. elegans* rely in part on Cdc14 homologues [19], the majority of eukaryotes do not need Cdc14 for mitotic exit (Roostalu, Schiebel and Khmelinskii, 2010). Nevertheless, a systematic RNAi screen in Drosophila S2 cells revealed that several phosphatases are required to progress through and exit from mitosis (Roostalu, Schiebel and Khmelinskii, 2010). In *Xenopus* egg extracts, PP1, PP2A and calcineurin have been shown to oppose CDK1 activity (Roostalu, Schiebel and Khmelinskii, 2010). The best-characterized CDK-counteracting phosphatase remains the budding yeast Cdc14 (Bouchoux and Uhlmann, 2011). The activity of Cdc14 is regulated by changes in its subcellular localization and an essential role in this process is played by the conserved polo kinase Cdc5 (Bouchoux and Uhlmann, 2011). Consistent with the central role played by Cdc5 in the regulation of Cdc14, budding yeast cells carrying mutations in either Cdc14 or Cdc5 arrest in telophase (Hartwell *et al.*, 1974). In both cases

the arrest is caused by the lack of Cdc14 activity (Stegmeier and Amon, 2004). However, the synthetic interaction observed between Cdc14 and Cdc5 suggests that a pool of active Cdc14, independent from Cdc5, exists and thereby explains the redundant role of Cdc5 and Cdc14 in controlling spindle elongation. Therefore, additional roles for Cdc5 have to be envisioned besides its contribution to decreasing the activity of CDK and increasing the activity of Cdc14 (Roccuzzo *et al.*, 2015).

Building on the knowledge that Cdc14 contributes to spindle elongation by dephosphorylating several motor proteins and spindle midzone components, to explain its overlapping role with Cdc5 and to unveil the molecular mechanism regulating what we define as the two-branched spindle elongation pathway, we searched for downstream component of the pathway, hence possible targets for Cdc14 and Cdc5, among proteins known to be involved in the process. Of all the proteins tested only the kinesin 5 motor protein Cin8 proved to be a key target. It has been reported that Cin8 is phosphorylated and dephosphorylated by CDK and Cdc14, respectively (Chee and Haase, 2010a). (R. Avunie-Masala *et al.*, 2011) Consistent with this finding, inserting a non-phosphorylatable allele of Cin8 in *cdc14 cdc5* cells, *cin8-3*^{CDK}*A,* entirely rescues the double-mutant arrest, causing the cells to completely elongate their spindles (Roccuzzo *et al.*, 2015). Here, we show that Cdc5 controls spindle elongation by directly phosphorylating the kinesin-5 motor protein Cin8. The conserved relevance for this regulation is underscored by the identification of Eg5/Kif11 (the vertebrate homolog of Cin8) as a substrate of Plk1 (the vertebrate homolog of Cdc5) in a Plk1-dependent phospho-proteome analysis of the early mitotic spindle (Santamaria *et al.*, 2011). We identified two conserved Cin8 residues, S409 and S441, as critical for the kinesin function in spindle elongation. These residues lie in close proximity of F429(467) and the three residues are positioned within a highly conserved motif of the motor domain. As mutating the F429(467) into alanine interferes with the ability of the kinesin to interact with spindle microtubules, we speculate that this region is also involved in microtubule interaction. Since phosphorylation adds negative charges and microtubules

are negatively charged, to imagine that phosphorylation facilitates microtubule binding is somewhat counterintuitive. However, recent works provide a plausible explanation to this hypothesis. Several studies propose that auto-inhibition of kinesin motor proteins may be a general mechanism for regulating their activity (Hammond *et al.*, 2010) (Kaan, Hackney and Kozielski, 2011) (Verhey and Hammond, 2009) (Imanishi *et al.*, 2006). According to this model, motors adopt a folded, compact active conformation and an extended, almost linear, inactive conformation. The switch between the two conformations is proposed to require 1) cargo binding, 2) protein oligomerization and/or 3) post translational modifications such as phosphorylation. In agreement with the auto-inhibition model, we speculate that Cdc5-mediated phosphorylation of residues S409 and S441 is required for relieving the auto-inhibition of Cin8, thereby allowing the protein to fulfill its role in spindle elongation. Whether the residues within the loop 8 (a 99-residues insert (222-313) in the motor domain) that we found phosphorylated by Cdc5 contribute to this process is beyond the purpose of this thesis but, nevertheless, remains an interesting question for the future.

How does Cdc5-mediated phosphorylation affect the function of Cin8?

So far, we assumed that Cdc5-mediated phosphorylation affects Cin8-microtubule binding based on data concerning the *cin8FA* mutant but no experimental data were acquired. To elucidate the mechanism by which Cdc5-mediated phosphorylation affects the function of Cin8, we are currently testing i) the interaction of Cin8 with microtubules; ii) the motility of Cin8 on microtubules and/or iii) the localization of Cin8 variants in several mutant backgrounds. In detail, i) to evaluate if Cdc5-mediated phosphorylation is relevant for the ability of Cin8 to interact with microtubules, we will perform microtubule-binding assays using Cin8 wild-type and mutant variants, including phospho-mimicking (containing or lacking loop 8) both *in vitro* and *in vivo*; ii) to evaluate if Cdc5-mediated phosphorylation

affects the motility of Cin8 on microtubules we will reconstitute kinesin movement in an *in vitro* system and directly observe the motility of wild type and mutants using microscope-based techniques (e.g., kymograph analysis to track individual proteins positioned on microtubules through time; or gliding motility assays to observe microtubules that are captured and transported along the surface of immobilized kinesin proteins) and, finally, iii) to evaluate whether Cdc5-mediated phosphorylation regulates the subcellular localization of Cin8, we will employ two strategies: (1) through indirect immunofluorescence on fixed cells, we will track the localization of Cin8 mutants using specific antibodies and compare it to that of its wild-type counterpart; (2) via live cell imaging, we will track GFP-tagged-Cin8-mutant variants in cells expressing mCherry-labeled-Tubulin. Live cell imaging will allow us to examine and correlate changes in the distribution of Cin8 variant proteins with mitotic spindle morphology. By this set of experiments, we expect to unambiguously identify the impact of Cdc5-mediated phosphorylation of residues S409 and S441 on Cin8 activity.

Final remarks: the Cin8 conundrum and the two-branched spindle elongation pathway

Overall, our work sheds light on our understanding of the intricate and poorly understood regulation of the mitotic spindle, a complex molecular machinery that coordinates chromosome segregation with the completion of previous cell cycle events to guarantee genomic stability. Given the conserved nature of the proteins involved and reinforced by the observation that polo mutants of Drosophila exhibit a phenotype similar to the one observed in our *cdc14 cdc5* double mutant strain (Donaldson *et al.*, 2001), we speculate that elucidating the role of budding yeast Cdc14 and Cdc5 activities in the spindle process will also be instrumental to understand spindle dynamics in higher eukaryotes, including humans, with the ultimate goal of identifying new "druggable" targets in cancer therapies.

On a more controversial issue, it is surprising that the function of Cin8 is essential for mitotic spindle elongation, given that the protein *per se* is dispensable for viability at least at permissive temperatures. Kinesins, in general, are redundant proteins, yet the overexpression of Kip1, the yeast homolog of Cin8, did not rescue the spindle elongation defect of *cdc5 cdc14* double mutant cells, but which was recovered solely by high levels of Cin8. Can it be that the two kinesin 5 motor proteins are mutually exclusive and compensate for each other only if one of them is missing? Or are there other proteins able to compensate the function of Cin8 in spindle elongation? To address this issue, it will be interesting to search for proteins capable of rescuing the spindle elongation defect of *cdc5 cdc14 cin8Δ* cells by a genome-wide approach and to test our proposed model that foresees the kinase and the phosphatase that regulate anaphase spindle elongation by acting on the same substrate.

On a different note, the finding that Cin8 is simultaneously a substrate of a kinase and a phosphatase contribute to revise our view of exit from mitosis. In contrast to the perception

that a global phosphosphorylation to dephosphorylation shift is required for the correct execution of late mitotic events, a model that still holds true for, CDKs and their counteracting phosphatase(s), it suggests that phosphorylation and dephosphorylation kinetics are substrate specific and paves the way for the need of single-molecule studies in parallel to global investigations. In agreement with this view are recent findings from the Uhlmann laboratory where the authors found that mitotic exit is characterized by a global equal number of proteins that gain and loose phosphorylation (REF)

In respect to Cin8 it will be important to test whether our model for its regulation holds true also in other vertebrates.

Last but not least is the question as to why spindle elongation is controlled by two parallel branches, one guided by Cdc5 and the other by Cdc14 or, in other words, one by Cdc5 and the other by a precise threshold between CDKs and their counteracting phosphatase(s). Are the two branches integrating spindle elongation, hence chromosome partitioning, with the correct execution of different cellular processes, or are they simply collaborating by providing the proper conditions for achieving the rapid changes required for a synchronous, robust and high fidelity chromosome separation/segregation process?

We tend to favor the second possibility, building on the knowledge that a similar principle seems to be already at the basis of cohesin cleavage, where efficiency and timing of cohesin removal is promoted by Cdc5-mediated phosphorylation of Scc1 (Yaakov, Thorn and Morgan, 2012), thereby facilitating separase Esp1 cleavage of Scc1 and reversal of CDK1-mediated phosphorylation of securin by the phosphatase Cdc14, and increasing the rate of securin ubiquitination (Holt, Krutchinsky and Morgan, 2008). Both events are conserved in vertebrate cells where, beside the contribution of Cdc5 to cohesin removal Hauf *et al.*, 2005), it was found that an additional level of separase-mediated regulation is accomplished by the inhibitory phosphorylation-dependent binding of Cdk1/cyclin B1 (Stemmann *et al.*, 2001) (Gorr, Boos and Stemmann, 2005).

References

Andersen, S. (1998) 'Licensing centrosome duplication', *Trends in Cell Biology*. Elsevier, 8(6), p. 222. doi: 10.1016/S0962-8924(98)01289-6.

Anton Khmelinskii & Elmar Schiebel (2008) 'Assembling the spindle midzone in the right place at the right time'. doi: 10.4161/cc.7.3.5349.

Anton Khmelinskii, 1 *et al.* (2007) 'Cdc14-regulated midzone assembly controls anaphase B', *The Journal of Cell Biology*, 177(6), pp. 981–993. doi: 10.1083/jcb.200702145.

De Antoni, A. *et al.* (2005) 'The Mad1/Mad2 Complex as a Template for Mad2 Activation in the Spindle Assembly Checkpoint', *Current Biology*, 15(3), pp. 214–225. doi: 10.1016/j.cub.2005.01.038.

Asbury, C. L. *et al.* (2006) 'The Dam1 kinetochore complex harnesses microtubule dynamics to produce force and movement.', *Proceedings of the National Academy of Sciences of the United States of America*. National Academy of Sciences, 103(26), pp. 9873–8. doi: 10.1073/pnas.0602249103.

Asbury, C. L. (2017) 'Anaphase A: Disassembling Microtubules Move Chromosomes toward Spindle Poles.', *Biology*. Multidisciplinary Digital Publishing Institute (MDPI), 6(1). doi: 10.3390/biology6010015.

Avunie-Masala, R. *et al.* (2011) 'Phospho-regulation of kinesin-5 during anaphase spindle elongation.', *Journal of cell science*. Company of Biologists, 124(Pt 6), pp. 873–8. doi: 10.1242/jcs.077396.

Avunie-Masala, R. *et al.* (2011) 'Phospho-regulation of kinesin-5 during anaphase spindle elongation', *Journal of Cell Science*, 124(6), pp. 873–878. doi: 10.1242/jcs.077396.

Barr, F. A., Silljé, H. H. W. and Nigg, E. A. (2004) 'Polo-like kinases and the orchestration of cell division.', *Nature reviews. Molecular cell biology*, 5(6), pp. 429–40. doi: 10.1038/nrm1401.

Baskerville, C., Segal, M. and Reed, S. I. (2008) 'The Protease Activity of Yeast Separase (Esp1) Is Required for Anaphase Spindle Elongation Independently of Its Role In Cleavage of Cohesin', *Genetics*. Genetics, 178(4), pp. 2361–72. doi: 10.1534/genetics.107.085308.

Bäumer, M., Braus, G. H. and Irniger, S. (2000) 'Two different modes of cyclin clb2 proteolysis during mitosis in Saccharomyces cerevisiae.', *FEBS letters*, 468(2–3), pp. 142–8. Available at: http://www.ncbi.nlm.nih.gov/pubmed/10692575 (Accessed: 27 September 2018).

Bell, K. M. *et al.* (2017) 'The yeast kinesin-5 Cin8 interacts with the microtubule in a noncanonical manner', *Journal of Biological Chemistry*, 292(35), pp. 14680–14694. doi: 10.1074/jbc.M117.797662.

Belmont, L. D. *et al.* (1990) 'Real-time visualization of cell cycle-dependent changes in microtubule dynamics in cytoplasmic extracts.', *Cell*, 62(3), pp. 579–89. Available at: http://www.ncbi.nlm.nih.gov/pubmed/2379239 (Accessed: 27 September 2018).

Biggins, S. and Murray, A. W. (2001) 'The budding yeast protein kinase Ipl1/Aurora allows the absence of tension to activate the spindle checkpoint.', *Genes & development*. Cold Spring Harbor Laboratory Press, 15(23), pp. 3118–29. doi: 10.1101/gad.934801.

Black, B. E. and Bassett, E. A. (2008) 'The histone variant CENP-A and centromere specification', *Current Opinion in Cell Biology*, 20(1), pp. 91–100. doi: 10.1016/j.ceb.2007.11.007.

Bouchoux, C. and Uhlmann, F. (2011) 'A quantitative model for ordered Cdk substrate dephosphorylation during mitotic exit', *Cell*, 147(4), pp. 803–814. doi: 10.1016/j.cell.2011.09.047.

Brennan, I. M. *et al.* (2007a) 'Polo-like kinase controls vertebrate spindle elongation and cytokinesis', *PLoS ONE*, 2(5), pp. 1–8. doi: 10.1371/journal.pone.0000409.

Brennan, I. M. *et al.* (2007b) 'Polo-Like Kinase Controls Vertebrate Spindle Elongation and Cytokinesis', *PLoS ONE*. Edited by S. Biggins. Public Library of Science, 2(5), p. e409. doi: 10.1371/journal.pone.0000409.

Bullitt, E. *et al.* (1997) 'The Yeast Spindle Pole Body Is Assembled around a Central Crystal of Spc42p', *Cell*. Cell Press, 89(7), pp. 1077–1086. doi: 10.1016/S0092-8674(00)80295-0.

Burbank, K. S. and Mitchison, T. J. (2006) *Microtubule dynamic instability*. Available at: https://www.cell.com/current-biology/pdf/S0960-9822(06)01771-4.pdf (Accessed: 29 September 2018).

Carmena, M. *et al.* (1998) 'Drosophila polo kinase is required for cytokinesis.', *The Journal of cell biology*, 143(3), pp. 659–71. Available at: http://www.ncbi.nlm.nih.gov/pubmed/9813088

(Accessed: 30 September 2018).
Carvalho, P. *et al.* (2004) 'Cell cycle control of kinesin-mediated transport of Bik1 (CLIP-170) regulates microtubule stability and dynein activation.', *Developmental cell*, 6(6), pp. 815–29. doi: 10.1016/j.devcel.2004.05.001.
Cassimeris, L., Pryer, N. K. and Salmon, E. D. (1988) 'Real-time observations of microtubule dynamic instability in living cells.', *The Journal of cell biology*. The Rockefeller University Press, 107(6 Pt 1), pp. 2223–31. Available at: http://www.ncbi.nlm.nih.gov/pubmed/3198684 (Accessed: 5 November 2018).
Chee, M. K. and Haase, S. B. (2010a) 'B-Cyclin/CDKs regulate mitotic spindle assembly by phosphorylating kinesins-5 in budding yeast', *PLoS Genetics*, 6(5), p. 35. doi: 10.1371/journal.pgen.1000935.
Chee, M. K. and Haase, S. B. (2010b) 'B-Cyclin/CDKs Regulate Mitotic Spindle Assembly by Phosphorylating Kinesins-5 in Budding Yeast', *PLoS Genetics*. Edited by S. Biggins. Public Library of Science, 6(5), p. e1000935. doi: 10.1371/journal.pgen.1000935.
Chen, C. J., Rayment, I. and Gilbert, S. P. (2011) 'Kinesin Kar3Cik1 ATPase Pathway for Microtubule Cross-linking', *Journal of Biological Chemistry*, 286(33), pp. 29261–29272. doi: 10.1074/jbc.M111.255554.
Ciferri, C., Musacchio, A. and Petrovic, A. (2007) 'The Ndc80 complex: Hub of kinetochore activity', *FEBS Letters*. No longer published by Elsevier, 581(15), pp. 2862–2869. doi: 10.1016/J.FEBSLET.2007.05.012.
Corbett, K. D. (2017) 'Molecular Mechanisms of Spindle Assembly Checkpoint Activation and Silencing', in. Springer, Cham, pp. 429–455. doi: 10.1007/978-3-319-58592-5_18.
Cottingham, F. R. and Hoyt, M. A. (1997) 'Mitotic spindle positioning in Saccharomyces cerevisiae is accomplished by antagonistically acting microtubule motor proteins.', *The Journal of cell biology*. The Rockefeller University Press, 138(5), pp. 1041–53. Available at: http://www.ncbi.nlm.nih.gov/pubmed/9281582 (Accessed: 21 August 2018).
Crasta, K. *et al.* (2006a) 'Cdk1 regulates centrosome separation by restraining proteolysis of microtubule-associated proteins', *The EMBO Journal*, 25(11), pp. 2551–2563. doi: 10.1038/sj.emboj.7601136.
Crasta, K. *et al.* (2006b) 'Cdk1 regulates centrosome separation by restraining proteolysis of microtubule-associated proteins', *The EMBO Journal*, 25(11), pp. 2551–2563. doi: 10.1038/sj.emboj.7601136.
Crasta, K. *et al.* (2008) 'Inactivation of Cdh1 by synergistic action of Cdk1 and polo kinase is necessary for proper assembly of the mitotic spindle.', *Nature cell biology*. NIH Public Access, 10(6), pp. 665–75. doi: 10.1038/ncb1729.
deCastro, M. J. *et al.* (2000) 'Working strokes by single molecules of the kinesin-related microtubule motor ncd', *Nature Cell Biology*, 2(10), pp. 724–729. doi: 10.1038/35036357.
DeZwaan, T. M. *et al.* (1997) 'Kinesin-related KIP3 of Saccharomyces cerevisiae is required for a distinct step in nuclear migration.', *The Journal of cell biology*, 138(5), pp. 1023–40. Available at: http://www.ncbi.nlm.nih.gov/pubmed/9281581 (Accessed: 30 September 2018).
Donaldson, M. M. *et al.* (2001) 'Metaphase arrest with centromere separation in polo mutants of Drosophila.', *The Journal of cell biology*. Rockefeller University Press, 153(4), pp. 663–76. doi: 10.1083/JCB.153.4.663.
Du, Y., English, C. A. and Ohi, R. (2010) 'The kinesin-8 Kif18A dampens microtubule plus-end dynamics.', *Current biology : CB*, 20(4), pp. 374–80. doi: 10.1016/j.cub.2009.12.049.
Düselder, A. *et al.* (2015) 'Deletion of the Tail Domain of the Kinesin-5 Cin8 affects its directionality'. JBC Papers in Press. doi: 10.1074/jbc.M114.620799.
Farache, D. *et al.* (2018) 'Assembly and regulation of γ-tubulin complexes.', *Open biology*. Royal Society Journals, 8(3), p. 170266. doi: 10.1098/rsob.170266.
Flemming, W. (1879) 'Beitrage zur Kenntniss der Zelle und ihrer Lebenserscheinungen', *Archiv für Mikroskopische Anatomie*. Springer-Verlag, 16(1), pp. 302–436. doi: 10.1007/BF02956386.
Gardner, M. K. *et al.* (2008) 'Chromosome Congression by Kinesin-5 Motor-Mediated Disassembly of Longer Kinetochore Microtubules', *Cell*, 135(5), pp. 894–906. doi: 10.1016/j.cell.2008.09.046.
Gardner, M. K. *et al.* (2009) 'NIH Public Access', 135(5), pp. 894–906. doi: 10.1016/j.cell.2008.09.046.Chromosome.
Gerson-Gurwitz, A. *et al.* (2009) 'Mid-anaphase arrest in S. cerevisiae cells eliminated for the function of Cin8 and dynein', *Cellular and Molecular Life Sciences*, 66(2), pp. 301–313. doi:

10.1007/s00018-008-8479-2.
Gerson-Gurwitz, A. *et al.* (2011) 'Directionality of individual kinesin-5 Cin8 motors is modulated by loop 8, ionic strength and microtubule geometry', *The EMBO Journal*, 30(24), pp. 4942–4954. doi: 10.1038/emboj.2011.403.
Gheber, L., Kuo, S. C. and Hoyt, M. A. (1999) 'Motile properties of the kinesin-related Cin8p spindle motor extracted from Saccharomyces cerevisiae cells.', *The Journal of biological chemistry*. American Society for Biochemistry and Molecular Biology, 274(14), pp. 9564–72. doi: 10.1074/JBC.274.14.9564.
Goh, P. Y. and Kilmartin, J. V (1993) 'NDC10: a gene involved in chromosome segregation in Saccharomyces cerevisiae.', *The Journal of cell biology*, 121(3), pp. 503–12. Available at: http://www.ncbi.nlm.nih.gov/pubmed/8486732 (Accessed: 29 September 2018).
Goldstein, A. *et al.* (2017) 'Three Cdk1 sites in the kinesin-5 Cin8 catalytic domain coordinate motor localization and activity during anaphase', *Cellular and Molecular Life Sciences*, 74(18), pp. 3395–3412. doi: 10.1007/s00018-017-2523-z.
Gordon, D. J., Resio, B. and Pellman, D. (2012) 'Causes and consequences of aneuploidy in cancer', *Nature Reviews Genetics*, 13(3), pp. 189–203. doi: 10.1038/nrg3123.
Gordon, D. M. and Roof, D. M. (2001) 'Degradation of the kinesin Kip1p at anaphase onset is mediated by the anaphase-promoting complex and Cdc20p.', *Proceedings of the National Academy of Sciences of the United States of America*. National Academy of Sciences, 98(22), pp. 12515–20. doi: 10.1073/pnas.231212498.
Gorr, I. H., Boos, D. and Stemmann, O. (2005) 'Mutual Inhibition of Separase and Cdk1 by Two-Step Complex Formation', *Molecular Cell*, 19(1), pp. 135–141. doi: 10.1016/j.molcel.2005.05.022.
Guacci, V., Koshland, D. and Strunnikov, A. (1997) 'A direct link between sister chromatid cohesion and chromosome condensation revealed through the analysis of MCD1 in S. cerevisiae.', *Cell*. NIH Public Access, 91(1), pp. 47–57. Available at: http://www.ncbi.nlm.nih.gov/pubmed/9335334 (Accessed: 29 September 2018).
Guertin, D. A., Trautmann, S. and McCollum, D. (2002) 'Cytokinesis in eukaryotes.', *Microbiology and molecular biology reviews : MMBR*. American Society for Microbiology (ASM), 66(2), pp. 155–78. doi: 10.1128/MMBR.66.2.155-178.2002.
Gupta, M. L. *et al.* (2006) 'Plus end-specific depolymerase activity of Kip3, a kinesin-8 protein, explains its role in positioning the yeast mitotic spindle.', *Nature cell biology*, 8(9), pp. 913–23. doi: 10.1038/ncb1457.
Haase, S. B., Winey, M. and Reed, S. I. (2001) 'Multi-step control of spindle pole body duplication by cyclin-dependent kinase', *NATURE CELL BIOLOGY*, 3. Available at: http://cellbio.nature.com (Accessed: 31 May 2018).
Hammond, J. W. *et al.* (2010) 'Autoinhibition of the kinesin-2 motor KIF17 via dual intramolecular mechanisms.', *The Journal of cell biology*. The Rockefeller University Press, 189(6), pp. 1013–25. doi: 10.1083/jcb.201001057.
Hartwell, L. H. *et al.* (1974) 'Genetic control of the cell division cycle in yeast.', *Science (New York, N.Y.)*, 183(4120), pp. 46–51. Available at: http://www.ncbi.nlm.nih.gov/pubmed/4587263 (Accessed: 27 September 2018).
He, X. *et al.* (2001) 'Molecular analysis of kinetochore-microtubule attachment in budding yeast.', *Cell*, 106(2), pp. 195–206. Available at: http://www.ncbi.nlm.nih.gov/pubmed/11511347 (Accessed: 29 September 2018).
Heald, R. and Khodjakov, A. (2015) 'Thirty years of search and capture: The complex simplicity of mitotic spindle assembly.', *The Journal of cell biology*. Rockefeller University Press, 211(6), pp. 1103–11. doi: 10.1083/jcb.201510015.
Hegemann, J. H. and Fleig, U. N. (1993) 'The centromere of budding yeast', *BioEssays*, 15(7), pp. 451–460. doi: 10.1002/bies.950150704.
Higuchi, T. and Uhlmann, F. (2005a) 'Stabilization of microtubule dynamics at anaphase onset promotes chromosome segregation', *Nature*, 433(7022), pp. 171–176. doi: 10.1038/nature03240.
Higuchi, T. and Uhlmann, F. (2005b) 'Stabilization of microtubule dynamics at anaphase onset promotes chromosome segregation', *Nature*. Nature Publishing Group, 433(7022), pp. 171–176. doi: 10.1038/nature03240.
Hildebrandt, E. R. and Hoyt, M. A. (2000) 'Mitotic motors in Saccharomyces cerevisiae.', *Biochimica et biophysica acta*, 1496(1), pp. 99–116. Available at: http://www.ncbi.nlm.nih.gov/pubmed/10722880 (Accessed: 30 September 2018).
Hildebrandt, E. R. and Hoyt, M. A. (2001) 'Cell cycle-dependent degradation of the

Saccharomyces cerevisiae spindle motor Cin8p requires APC(Cdh1) and a bipartite destruction sequence.', *Molecular biology of the cell*. American Society for Cell Biology, 12(11), pp. 3402–16. doi: 10.1091/mbc.12.11.3402.
Holt, L. J., Krutchinsky, A. N. and Morgan, D. O. (2008) 'Positive feedback sharpens the anaphase switch', *Nature*, 454(7202), pp. 353–357. doi: 10.1038/nature07050.
van Hooff, J. J. *et al.* (2017) 'Evolutionary dynamics of the kinetochore network in eukaryotes as revealed by comparative genomics.', *EMBO reports*. European Molecular Biology Organization, 18(9), pp. 1559–1571. doi: 10.15252/embr.201744102.
Hotz, M. *et al.* (2012) 'Spindle pole bodies exploit the mitotic exit network in metaphase to drive their age-dependent segregation.', *Cell*. NIH Public Access, 148(5), pp. 958–72. doi: 10.1016/j.cell.2012.01.041.
Hoyt, M. A. *et al.* (1992) 'Kinesin-related Gene Products Required for Mitotic Spindle Assembly', *J. Cell Biol.*, 118(1), pp. 109–120.
Hoyt, M. A. *et al.* (1992a) 'Two Saccharomyces cerevisiae kinesin-related gene products required for mitotic spindle assembly.', *The Journal of cell biology*, 118(1), pp. 109–20. Available at: http://www.ncbi.nlm.nih.gov/pubmed/1618897 (Accessed: 21 August 2018).
Hoyt, M. A. *et al.* (1992b) 'Two Saccharomyces cerevisiae kinesin-related gene products required for mitotic spindle assembly.', *The Journal of cell biology*. Rockefeller University Press, 118(1), pp. 109–20. doi: 10.1083/JCB.118.1.109.
Hoyt, M. A. *et al.* (1993) 'Loss of function of Saccharomyces cerevisiae kinesin-related CIN8 and KIP1 is suppressed by KAR3 motor domain mutations.', *Genetics*, 135(1), pp. 35–44. Available at: http://www.ncbi.nlm.nih.gov/pubmed/8224825 (Accessed: 29 September 2018).
Imanishi, M. *et al.* (2006) 'Autoinhibition regulates the motility of the C. elegans intraflagellar transport motor OSM-3', *Journal of Cell Biology*. doi: 10.1083/jcb.200605179.
Jaspersen, S. L. *et al.* (1998) 'A late mitotic regulatory network controlling cyclin destruction in Saccharomyces cerevisiae.', *Molecular biology of the cell*. American Society for Cell Biology, 9(10), pp. 2803–17. Available at: http://www.ncbi.nlm.nih.gov/pubmed/9763445 (Accessed: 7 August 2018).
Jaspersen, S. L. and Winey, M. (2004) 'THE BUDDING YEAST SPINDLE POLE BODY: Structure, Duplication, and Function', *Annual Review of Cell and Developmental Biology*, 20(1), pp. 1–28. doi: 10.1146/annurev.cellbio.20.022003.114106.
Jensen, S. *et al.* (2001) 'A novel role of the budding yeast separin Esp1 in anaphase spindle elongation: evidence that proper spindle association of Esp1 is regulated by Pds1.', *The Journal of cell biology*. Rockefeller University Press, 152(1), pp. 27–40. doi: 10.1083/JCB.152.1.27.
Juang, Y. L. *et al.* (1997) 'APC-mediated proteolysis of Ase1 and the morphogenesis of the mitotic spindle.', *Science (New York, N.Y.)*. American Association for the Advancement of Science, 275(5304), pp. 1311–4. doi: 10.1126/SCIENCE.275.5304.1311.
Kaan, H. Y. K., Hackney, D. D. and Kozielski, F. (2011) 'The Structure of the Kinesin-1 Motor-Tail Complex Reveals the Mechanism of Autoinhibition', *Science*, 333(6044), pp. 883–885. doi: 10.1126/science.1204824.
Kelley, L. A. *et al.* (2015) 'The Phyre2 web portal for protein modeling, prediction and analysis', *Nature Protocols*, 10(6), pp. 845–858. doi: 10.1038/nprot.2015.053.
Khmelinskii, A. *et al.* (2009) 'Phosphorylation-Dependent Protein Interactions at the Spindle Midzone Mediate Cell Cycle Regulation of Spindle Elongation'. doi: 10.1016/j.devcel.2009.06.011.
Kilmartin, J. V (2014) 'Lessons from yeast: the spindle pole body and the centrosome.', *Philosophical transactions of the Royal Society of London. Series B, Biological sciences*. The Royal Society, 369(1650), p. 20130456. doi: 10.1098/rstb.2013.0456.
Kitamura, E. *et al.* (2007) 'Kinetochore microtubule interaction during S phase in Saccharomyces cerevisiae.', *Genes & development*. Cold Spring Harbor Laboratory Press, 21(24), pp. 3319–30. doi: 10.1101/gad.449407.
Kollman, J. M. *et al.* (2010) 'Microtubule nucleating γ-TuSC assembles structures with 13-fold microtubule-like symmetry', *Nature*, 466(7308), pp. 879–882. doi: 10.1038/nature09207.
Krenn, V. and Musacchio, A. (2015) 'The Aurora B Kinase in Chromosome Bi-Orientation and Spindle Checkpoint Signaling.', *Frontiers in oncology*. Frontiers Media SA, 5, p. 225. doi: 10.3389/fonc.2015.00225.
Lampert, F. and Westermann, S. (2011) 'A blueprint for kinetochores — new insights into the molecular mechanics of cell division', *Nature Reviews Molecular Cell Biology*. Nature Publishing

Group, 12(7), pp. 407–412. doi: 10.1038/nrm3133.
Lampson, M. A. *et al.* (2004) 'Correcting improper chromosome–spindle attachments during cell division', *NATURE CELL BIOLOGY*, 6(3). doi: 10.1038/ncb1102.
Lee, M. S. and Spencer, F. A. (2004) 'Bipolar orientation of chromosomes in Saccharomyces cerevisiae is monitored by Mad1 and Mad2, but not by Mad3.', *Proceedings of the National Academy of Sciences of the United States of America*. National Academy of Sciences, 101(29), pp. 10655–60. doi: 10.1073/pnas.0404102101.
Li, Y. and Elledge, S. J. (2003) 'The DASH complex component Ask1 is a cell cycle-regulated Cdk substrate in Saccharomyces cerevisiae.', *Cell cycle (Georgetown, Tex.)*, 2(2), pp. 143–8. Available at: http://www.ncbi.nlm.nih.gov/pubmed/12695666 (Accessed: 30 September 2018).
Liang, F., Richmond, D. and Wang, Y. (2013) 'Coordination of Chromatid Separation and Spindle Elongation by Antagonistic Activities of Mitotic and S-Phase CDKs', *PLoS Genetics*. Edited by G. P. Copenhaver. Public Library of Science, 9(2), p. e1003319. doi: 10.1371/journal.pgen.1003319.
Lim, H. H., Goh, P. Y. and Surana, U. (1996) 'Spindle pole body separation in Saccharomyces cerevisiae requires dephosphorylation of the tyrosine 19 residue of Cdc28.', *Molecular and cellular biology*, 16(11), pp. 6385–6397. doi: 10.1128/MCB.16.11.6385.
Liu, D. *et al.* (2009) 'Sensing Chromosome Bi-Orientation by Spatial Separation of Aurora B Kinase from Kinetochore Substrates', *Science*, 323(5919), pp. 1350–1353. doi: 10.1126/science.1167000.
Liu, D. *et al.* (2010) 'Regulated targeting of protein phosphatase 1 to the outer kinetochore by KNL1 opposes Aurora B kinase.', *The Journal of cell biology*. Rockefeller University Press, 188(6), pp. 809–20. doi: 10.1083/jcb.201001006.
Lodish, H. *et al.* (2000) 'Microtubule Dynamics and Motor Proteins during Mitosis'. W. H. Freeman. Available at: https://www.ncbi.nlm.nih.gov/books/NBK21537/ (Accessed: 29 September 2018).
London, N. and Biggins, S. (2014) 'Signalling dynamics in the spindle checkpoint response', *Nature Reviews Molecular Cell Biology*, 15(11), pp. 736–748. doi: 10.1038/nrm3888.
Maddox, P. S. *et al.* (2003) 'The minus end-directed motor Kar3 is required for coupling dynamic microtubule plus ends to the cortical shmoo tip in budding yeast.', *Current biology : CB*, 13(16), pp. 1423–8. Available at: http://www.ncbi.nlm.nih.gov/pubmed/12932327 (Accessed: 30 September 2018).
Maddox, P. S., Bloom, K. S. and Salmon, E. D. (2000) 'The polarity and dynamics of microtubule assembly in the budding yeast Saccharomyces cerevisiae.', *Nature cell biology*. NIH Public Access, 2(1), pp. 36–41. doi: 10.1038/71357.
Makrantoni, V. and Marston, A. L. (2018) 'Cohesin and chromosome segregation.', *Current biology : CB*. Elsevier, 28(12), pp. R688–R693. doi: 10.1016/j.cub.2018.05.019.
Mallavarapu, a, Sawin, K. and Mitchison, T. (1999) 'A switch in microtubule dynamics at the onset of anaphase B in the mitotic spindle of Schizosaccharomyces pombe.', *Current biology : CB*, 9(23), pp. 1423–1426. doi: 10.1016/S0960-9822(00)80090-1.
Manatschal, C. *et al.* (2016) 'Molecular basis of Kar9-Bim1 complex function during mating and spindle positioning.', *Molecular biology of the cell*. American Society for Cell Biology, 27(23), p. 3729. doi: 10.1091/mbc.E16-07-0552.
Manning, B. D. *et al.* (1999) 'Differential regulation of the Kar3p kinesin-related protein by two associated proteins, Cik1p and Vik1p.', *The Journal of cell biology*. The Rockefeller University Press, 144(6), pp. 1219–33. Available at: http://www.ncbi.nlm.nih.gov/pubmed/10087265 (Accessed: 30 September 2018).
Mapelli, M. *et al.* (2007) 'The Mad2 Conformational Dimer: Structure and Implications for the Spindle Assembly Checkpoint', *Cell*. Cell Press, 131(4), pp. 730–743. doi: 10.1016/J.CELL.2007.08.049.
Mellone, B. G. *et al.* (2003) 'Centromere silencing and function in fission yeast is governed by the amino terminus of histone H3.', *Current biology : CB*, 13(20), pp. 1748–57. Available at: http://www.ncbi.nlm.nih.gov/pubmed/14561399 (Accessed: 13 June 2018).
Miller, R. K. *et al.* (1998) 'The kinesin-related proteins, Kip2p and Kip3p, function differently in nuclear migration in yeast.', *Molecular biology of the cell*, 9(8), pp. 2051–68. Available at: http://www.ncbi.nlm.nih.gov/pubmed/9693366 (Accessed: 30 September 2018).
Movshovich, N. *et al.* (2008) 'Slk19-dependent mid-anaphase pause in kinesin-5-mutated cells', *Journal of Cell Science*, 121(15), pp. 2529–2539. doi: 10.1242/jcs.022996.
Muller, E. G. D. *et al.* (2005) 'The organization of the core proteins of the yeast spindle pole

body.', *Molecular biology of the cell*. American Society for Cell Biology, 16(7), pp. 3341–52. doi: 10.1091/mbc.e05-03-0214.
Musacchio, A. and Salmon, E. D. (2007) 'The spindle-assembly checkpoint in space and time', *Nature Reviews Molecular Cell Biology*, 8(5), pp. 379–393. doi: 10.1038/nrm2163.
Nakajima, Y. *et al.* (2011) 'Ipl1/Aurora-dependent phosphorylation of Sli15/INCENP regulates CPC–spindle interaction to ensure proper microtubule dynamics', *The Journal of Cell Biology*, 194(1), pp. 137–153. doi: 10.1083/jcb.201009137.
Nakojima, H. *et al.* (2003) 'Identification of a consensus motif for PlK (Polo-like kinase) phosphorylation reveals Myt1 as a Plk1 substrate', *Journal of Biological Chemistry*, 278(28), pp. 25277–25280. doi: 10.1074/jbc.C300126200.
Nasmyth, K. (2001) 'A prize for proliferation.', *Cell*, 107(6), pp. 689–701. Available at: http://www.ncbi.nlm.nih.gov/pubmed/11747804 (Accessed: 29 September 2018).
Nasmyth, K. (2002) 'Segregating Sister Genomes: The Molecular Biology of Chromosome Separation', *Science*, 297(5581), pp. 559–565. doi: 10.1126/science.1074757.
Neef, R. *et al.* (2003) 'Phosphorylation of mitotic kinesin-like protein 2 by polo-like kinase 1 is required for cytokinesis', *The Journal of Cell Biology*, 162(5), pp. 863–876. doi: 10.1083/jcb.200306009.
Oegema, K. *et al.* (2001) 'Functional analysis of kinetochore assembly in Caenorhabditis elegans.', *The Journal of cell biology*. The Rockefeller University Press, 153(6), pp. 1209–26. Available at: http://www.ncbi.nlm.nih.gov/pubmed/11402065 (Accessed: 29 September 2018).
Pagliuca, C. *et al.* (2009) 'Roles for the Conserved Spc105p/Kre28p Complex in Kinetochore-Microtubule Binding and the Spindle Assembly Checkpoint', *PLoS ONE*. Edited by K. G. Hardwick. Public Library of Science, 4(10), p. e7640. doi: 10.1371/journal.pone.0007640.
Palmer, R. E. *et al.* (1992) 'Role of astral microtubules and actin in spindle orientation and migration in the budding yeast, Saccharomyces cerevisiae.', *The Journal of cell biology*, 119(3), pp. 583–93. Available at: http://www.ncbi.nlm.nih.gov/pubmed/1400594 (Accessed: 29 September 2018).
Pearson, C. G. *et al.* (2001) 'Budding Yeast Chromosome Structure and Dynamics during Mitosis', *The Journal of Cell Biology*, 152(6), pp. 1255–1266. Available at: http://www.jcb.org/cgi/content/full/152/6/1255 (Accessed: 20 June 2018).
Pereira, G. and Schiebel, E. (2003) 'Separase Regulates INCENP-Aurora B Anaphase Spindle Function Through Cdc14', *Science*, 302(5653), pp. 2120–2124. doi: 10.1126/science.1091936.
di Pietro, F., Echard, A. and Morin, X. (2016) 'Regulation of mitotic spindle orientation: an integrated view.', *EMBO reports*. European Molecular Biology Organization, 17(8), pp. 1106–30. doi: 10.15252/embr.201642292.
Pinsky, B. A. and Biggins, S. (2005) 'The spindle checkpoint: tension versus attachment'. doi: 10.1016/j.tcb.2005.07.005.
Qiao, X. *et al.* (2010) 'APC/C-Cdh1: from cell cycle to cellular differentiation and genomic integrity.', *Cell cycle (Georgetown, Tex.)*. Taylor & Francis, 9(19), pp. 3904–12. doi: 10.4161/cc.9.19.13585.
Rahal, R. and Amon, A. (2008) 'Mitotic CDKs control the metaphase-anaphase transition and trigger spindle elongation', *Genes & Development*, 22(11), pp. 1534–1548. doi: 10.1101/gad.1638308.
Rees, D. *et al.* (1990) 'Regulation of microtubule dynamics by cdc2 protein kinase in cell-free extracts of Xenopus eggs', *Nature*, 374(18), pp. 685–689. doi: 10.1016/0021-9797(80)90501-9.
Roccuzzo, M. *et al.* (2015) 'FEAR-mediated activation of Cdc14 is the limiting step for spindle elongation and anaphase progression', *Nature Cell Biology*, 17(3), pp. 251–261. doi: 10.1038/ncb3105.
Rodionov, V. I. and Borisy, G. G. (1997) 'Microtubule treadmilling in vivo.', *Science (New York, N.Y.)*, 275(5297), pp. 215–8. Available at: http://www.ncbi.nlm.nih.gov/pubmed/8985015 (Accessed: 5 November 2018).
Roof, D. M., Meluh, P. B. and Rose, M. D. (1992) 'Kinesin-related proteins required for assembly of the mitotic spindle.', *The Journal of cell biology*, 118(1), pp. 95–108. Available at: http://www.ncbi.nlm.nih.gov/pubmed/1618910 (Accessed: 30 September 2018).
Roostalu, J. *et al.* (2011) 'Directional Switching of the Kinesin Cin8 Through Motor Coupling', *Science*, 332(6025), pp. 94–99. doi: 10.1126/science.1199945.
Roostalu, J., Schiebel, E. and Khmelinskii, A. (2010) 'Cell cycle control of spindle elongation', *Cell Cycle*, 9(6), pp. 1084–1090. doi: 10.4161/cc.9.6.11017.

Ruchaud, S., Carmena, M. and Earnshaw, W. C. (2007) 'Chromosomal passengers: conducting cell division', *Nature Reviews Molecular Cell Biology*, 8(10), pp. 798–812. doi: 10.1038/nrm2257.
Rüthnick, D. and Schiebel, E. (2016) 'Duplication of the Yeast Spindle Pole Body Once per Cell Cycle.', *Molecular and cellular biology*. American Society for Microbiology Journals, 36(9), pp. 1324–31. doi: 10.1128/MCB.00048-16.
Rüthnick, D. and Schiebel, E. (2018) 'Duplication and Nuclear Envelope Insertion of the Yeast Microtubule Organizing Centre, the Spindle Pole Body', *Cells*, 7(5), p. 42. doi: 10.3390/cells7050042.
Santamaria, A. *et al.* (2011) 'The Plk1-dependent Phosphoproteome of the Early Mitotic Spindle', *Molecular & Cellular Proteomics*, 10(1), p. M110.004457. doi: 10.1074/mcp.M110.004457.
Saunders, W. *et al.* (1997) 'The Saccharomyces cerevisiae kinesin-related motor Kar3p acts at preanaphase spindle poles to limit the number and length of cytoplasmic microtubules.', *The Journal of cell biology*. The Rockefeller University Press, 137(2), pp. 417–31. Available at: http://www.ncbi.nlm.nih.gov/pubmed/9128252 (Accessed: 30 September 2018).
Saunders, W. S. *et al.* (1995) 'Saccharomyces cerevisiae Kinesin and Dynein related ProteinsRequired for Anaphase Chromosome Segregation', *Jcb*, (March 1995), pp. 1–8. Available at: http://jcb.rupress.org/content/128/4/617.abstract.
Scholey, J. M., Civelekoglu-Scholey, G. and Brust-Mascher, I. (2016) 'Anaphase B.', *Biology*. Multidisciplinary Digital Publishing Institute (MDPI), 5(4). doi: 10.3390/biology5040051.
Schuyler, S. C., Liu, J. Y. and Pellman, D. (2003a) 'The molecular function of Ase1p', *The Journal of Cell Biology*, 160(4), pp. 517–528. doi: 10.1083/jcb.200210021.
Schuyler, S. C., Liu, J. Y. and Pellman, D. (2003b) 'The molecular function of Ase1p', *The Journal of Cell Biology*, 160(4), pp. 517–528. doi: 10.1083/jcb.200210021.
Severin, F. *et al.* (2001) *Stu2 Promotes Mitotic Spindle Elongation in Anaphase*, *The Journal of Cell Biology*. Available at: http://www.jcb.org/cgi/content/full/153/2/435 (Accessed: 26 July 2018).
Severin, F., Hyman, A. A. and Piatti, S. (2001) 'Correct spindle elongation at the metaphase/anaphase transition is an APC-dependent event in budding yeast.', *The Journal of cell biology*. Rockefeller University Press, 155(5), pp. 711–8. doi: 10.1083/jcb.200104096.
Seybold, C. *et al.* (2015) 'Kar1 binding to Sfi1 C-terminal regions anchors the SPB bridge to the nuclear envelope', *Journal of Cell Biology*, 209(6), pp. 843–861. doi: 10.1083/jcb.201412050.
Seybold, C. and Schiebel, E. (2013) *Spindle pole bodies*, *CURBIO*. doi: 10.1016/j.cub.2013.07.024.
Sharp, D. J., Rogers, G. C. and Scholey, J. M. (2000) 'Microtubule motors in mitosis.', *Nature*, 407(6800), pp. 41–7. doi: 10.1038/35024000.
Sharp, D. J., Rogers, G. C. and Scholey, J. M. (2000) 'Microtubule motors in mitosis', *Nature*, 407(6800), pp. 41–47. doi: 10.1038/35024000.
Short, B. (2015) 'Building a bridge to a new spindle pole body', *The Journal of Cell Biology*. Rockefeller University Press, 209(6), p. 777.1-777. doi: 10.1083/jcb.2096iti1.
Smith, E. *et al.* (2011) 'Differential control of Eg5-dependent centrosome separation by Plk1 and Cdk1', *Embo J*, 30(11), pp. 2233–2245. doi: 10.1038/emboj.2011.120.
Snead, J. L. *et al.* (2007) 'A Coupled Chemical-Genetic and Bioinformatic Approach to Polo-like Kinase Pathway Exploration', *Chemistry and Biology*, 14(11), pp. 1261–1272. doi: 10.1016/j.chembiol.2007.09.011.
Sorger, P. K., Severin, E. and Hyman, A. A. (1994) *Factors Required for the Binding of Reassembled Yeast Kinetochores to Microtubules In Vitro*. Available at: http://images.biomedsearch.com/7962081/jc1274995.pdf?AWSAccessKeyId=AKIAIBOKHYOLP4MBMRGQ&Expires=1538352000&Signature=JACCuelZovjztuLNrpBmZ%2B9oXII%3D (Accessed: 29 September 2018).
Sproul, L. R. *et al.* (2005) 'Cik1 targets the minus-end kinesin depolymerase kar3 to microtubule plus ends.', *Current biology : CB*, 15(15), pp. 1420–7. doi: 10.1016/j.cub.2005.06.066.
Stegmeier, F. and Amon, A. (2004) 'Closing Mitosis: The Functions of the Cdc14 Phosphatase and Its Regulation', *Annual Review of Genetics*, 38(1), pp. 203–232. doi: 10.1146/annurev.genet.38.072902.093051.
Stemmann, O. *et al.* (2001) 'Dual inhibition of sister chromatid separation at metaphase.', *Cell*, 107(6), pp. 715–26. Available at: http://www.ncbi.nlm.nih.gov/pubmed/11747808 (Accessed: 27 September 2018).
Straight, A. F., Sedat, J. W. and Murray, A. W. (1998) 'Time-Lapse Microscopy Reveals Unique Roles for Kinesins during Anaphase in Budding Yeast', *The Journal of Cell Biology*, 143(3), pp. 687–694. doi: 10.1083/jcb.143.3.687.

Sullivan, D. S. and Huffaker, T. C. (1992) *Astral Microtubules Are Not Required for Anaphase B in Saccharomyces cer isiae*. Available at: https://www.ncbi.nlm.nih.gov/pmc/articles/PMC2289657/pdf/jc1192379.pdf (Accessed: 3 September 2018).
Sullivan, M. and Uhlmann, F. (2003) 'A non-proteolytic function of separase links the onset of anaphase to mitotic exit', *Nature Cell Biology*, 5(3), pp. 249–254. doi: 10.1038/ncb940.
Sunkel, C. E. and Glover, D. M. (1988) 'polo, a mitotic mutant of Drosophila displaying abnormal spindle poles.', *Journal of cell science*, 89 (Pt 1), pp. 25–38. Available at: http://www.ncbi.nlm.nih.gov/pubmed/3417791 (Accessed: 30 September 2018).
Tanaka, K. *et al.* (2005) 'Molecular mechanisms of kinetochore capture by spindle microtubules', *Nature*, 434(7036), pp. 987–994. doi: 10.1038/nature03483.
Tanaka, K. (2014) 'Centrosome Duplication: Suspending a License by Phosphorylating a Template', *Current Biology*, 24, pp. R651–R653. doi: 10.1016/j.cub.2014.06.020.
Tanaka, T. U. (2010) 'Kinetochore-microtubule interactions: steps towards bi-orientation.', *The EMBO journal*. European Molecular Biology Organization, 29(24), pp. 4070–82. doi: 10.1038/emboj.2010.294.
Tanaka, T. U. and Desai, A. (2008) 'Kinetochore-microtubule interactions: the means to the end.', *Current opinion in cell biology*. NIH Public Access, 20(1), pp. 53–63. doi: 10.1016/j.ceb.2007.11.005.
Tischer, C., Brunner, D. and Dogterom, M. (2009) 'Force- and kinesin-8-dependent effects in the spatial regulation of fission yeast microtubule dynamics.', *Molecular systems biology*, 5, p. 250. doi: 10.1038/msb.2009.5.
Uhlmann, F., Bouchoux, C. and López-Avilés, S. (2011) 'A quantitative model for cyclin-dependent kinase control of the cell cycle: revisited.', *Philosophical transactions of the Royal Society of London. Series B, Biological sciences*. The Royal Society, 366(1584), pp. 3572–83. doi: 10.1098/rstb.2011.0082.
Varga, V. *et al.* (2006) 'Yeast kinesin-8 depolymerizes microtubules in a length-dependent manner.', *Nature cell biology*, 8(9), pp. 957–62. doi: 10.1038/ncb1462.
Varga, V. *et al.* (2009) 'Kinesin-8 motors act cooperatively to mediate length-dependent microtubule depolymerization.', *Cell*, 138(6), pp. 1174–83. doi: 10.1016/j.cell.2009.07.032.
Verhey, K. J. and Hammond, J. W. (2009) 'Traffic control: regulation of kinesin motors', *Nature Reviews Molecular Cell Biology*. Nature Publishing Group, 10(11), pp. 765–777. doi: 10.1038/nrm2782.
Visintin, R. *et al.* (1998) 'The phosphatase Cdc14 triggers mitotic exit by reversal of Cdk-dependent phosphorylation.', *Molecular cell*, 2(6), pp. 709–18. Available at: http://www.ncbi.nlm.nih.gov/pubmed/9885559 (Accessed: 7 August 2018).
Vleugel, M. *et al.* (2012) 'Evolution and Function of the Mitotic Checkpoint', *Developmental Cell*, 23(2), pp. 239–250. doi: 10.1016/j.devcel.2012.06.013.
Wargacki, M. M. *et al.* (2010) 'Kip3, the yeast kinesin-8, is required for clustering of kinetochores at metaphase.', *Cell cycle (Georgetown, Tex.)*, 9(13), pp. 2581–8. doi: 10.4161/cc.9.13.12076.
Waterman-Storer, C. M. and Salmon, E. D. (1997) 'Microtubule dynamics: Treadmilling comes around again', *Current Biology*. Cell Press, 7(6), pp. R369–R372. doi: 10.1016/S0960-9822(06)00177-1.
Winey, M. *et al.* (1995) 'Three-dimensional ultrastructural analysis of the Saccharomyces cerevisiae mitotic spindle.', *The Journal of cell biology*. Rockefeller University Press, 129(6), pp. 1601–15. doi: 10.1083/JCB.129.6.1601.
Winey, M. and Bloom, K. (2012) 'Mitotic spindle form and function', *Genetics*, 190(4), pp. 1197–1224. doi: 10.1534/genetics.111.128710.
Winey, M. and Bloom, K. (2012) 'Mitotic Spindle Form and Function', *Genetics*, 190(4), pp. 1197–1224. doi: 10.1534/genetics.111.128710.
Wittmann, T., Hyman, A. and Desai, A. (2001) *The spindle: a dynamic assembly of microtubules and motors*, *NATURE CELL BIOLOGY*. Available at: http://cellbio.nature.come28 (Accessed: 29 September 2018).
Wloka, C. and Bi, E. (2012) 'Mechanisms of cytokinesis in budding yeast', *Cytoskeleton*, 69(10), pp. 710–726. doi: 10.1002/cm.21046.
Wollman, R. *et al.* (2005) 'Efficient Chromosome Capture Requires a Bias in the "Search-and-Capture" Process during Mitotic-Spindle Assembly', *Current Biology*, 15(9), pp. 828–832. doi: 10.1016/j.cub.2005.03.019.

Woodbury, E. L. and Morgan, D. O. (2007) 'The Role of Self-association in Fin1 Function on the Mitotic Spindle *'. doi: 10.1074/jbc.M705344200.
De Wulf, K., Odekerken-Schröder, G. and Van Kenhove, P. (2003) 'Investments in consumer relationships: a critical reassessment and model extension', *The International Review of Retail, Distribution and Consumer Research*, 13(3), pp. 245–261. doi: 10.1080/0959396032000101354.
Yaakov, G., Thorn, K. and Morgan, D. O. (2012) 'Separase biosensor reveals that cohesin cleavage timing depends on phosphatase PP2A(Cdc55) regulation.', *Developmental cell*. NIH Public Access, 23(1), pp. 124–36. doi: 10.1016/j.devcel.2012.06.007.
Yamagishi, Y. *et al.* (2012) 'MPS1/Mph1 phosphorylates the kinetochore protein KNL1/Spc7 to recruit SAC components', *Nature Cell Biology*, 14(7), pp. 746–752. doi: 10.1038/ncb2515.
Yeh, E. *et al.* (1995) 'Spindle dynamics and cell cycle regulation of dynein in the budding yeast, Saccharomyces cerevisiae.', *The Journal of cell biology*, 130(3), pp. 687–700. doi: 10.1083/jcb.130.3.687.
Yeong, F. M. *et al.* (2000) 'Exit from mitosis in budding yeast: biphasic inactivation of the Cdc28-Clb2 mitotic kinase and the role of Cdc20.', *Molecular cell*, 5(3), pp. 501–11. Available at: http://www.ncbi.nlm.nih.gov/pubmed/10882135 (Accessed: 27 September 2018).
Yin, H. *et al.* (2002) 'Stu1p Is Physically Associated with β-Tubulin and Is Required for Structural Integrity of the Mitotic Spindle', *Molecular Biology of the Cell*. Edited by T. Stearns, 13(6), pp. 1881–1892. doi: 10.1091/mbc.01-09-0458.
Zimniak, T. *et al.* (2009) 'Phosphoregulation of the budding yeast EB1 homologue Bim1p by Aurora/Ipl1p.', *The Journal of cell biology*. Rockefeller University Press, 186(3), pp. 379–91. doi: 10.1083/jcb.200901036.